CIVIL ENGINEERING STUDIES
Illinois Center for Transportation Series No. 07-005
UILU-ENG-2007-2021
ISSN: 0197-9191

HMA DYNAMIC MODULUS PREDICTIVE MODELS– A REVIEW

By

Gabriel Garcia
University of Illinois at Urbana-Champaign

and

Marshall Thompson
University of Illinois at Urbana-Champaign

Research Report FHWA-ICT-07-005

A report of the findings of

ICT-R39
Validation of Extended Life HMA Design Concepts

Illinois Center for Transportation
January 2007

Technical Report Documentation Page

1. Report No.	2. Government Accession No.	3. Recipient's Catalog No.
FHWA-ICT-07-005		

4. Title and Subtitle	5. Report Date
HMA DYNAMIC MODULUS PREDICTIVE MODELS (A REVIEW)	January, 2007
	6. Performing Organization Code
7. Author(s)	8. Performing Organization Report N o.
Gabriel Garcia & Marshall Thompson	FHWA-ICT-07-005 UILU-2007-2021
9. Performing Organization Name and Address	10. Work Unit (TRAIS)
Illinois Center for Transportation Department of Civil and Environmental Engineering University of Illinois 205 North Mathews – MC-250 Urbana, IL 61801	
	11. Contract or Grant No. ICT-R39
	13. Type of Report and Period Covered Project Report 2002-2006
12. Sponsoring Agency Name and Address Illinois Department of Transportation Bureau of Materials and Physical Research 126 East Ash Street Springfield, IL 62704-4766	14. Sponsoring Agency Code

15. Supplementary Notes

Study was conducted in cooperation with the U.S. Department of Transportation, Federal Highway Administration.

16. Abstract

The most important hot-mix asphalt (HMA) property influencing the structural response of a flexible pavement is the HMA modulus (E_{HMA}).

Dynamic modulus concepts are reviewed. The construction of master curves for HMA mixtures is presented. The procedures are based on the fitting of a sigmoidal function.

Two IE*I predictive equations are presented. The Witczak, as proposed in the new AASHTO 2002 Design Guide, and the Hirsch model. In general, both appear to be in good agreement and have similar accuracy.

The Witczak predictive equation requires eight input parameters. This information is normally available from material specifications or volumetric design of the mixture. The master curve for IE*I can be developed directly by using the binder A and VTS parameters in the viscosity components of the equation.

The Hirsch model needs only three input parameters, which are available from the routine Superpave mix design process. To build the IE*I master curve, a master curve for IG*I_{binder} has to be developed to take into account the effect of temperature and frequency. This can be done with data obtained from Dynamic Shear Rheometer tests.

Several studies are presented where the dynamic modulus predictive models are evaluated. The studies used different binders and represent typical mixtures used by different agencies. The results clearly confirm the good agreement and similar accuracy between the Witczak equation and the Hirsch model and between these models and dynamic modulus obtained from laboratory tests.

In general, it is concluded that both predictive models generate sufficiently accurate and reasonable dynamic modulus estimates adequate for use in mechanistic-empirical design, at least for broad range of binders and mixtures studied.

17. Key Words	18. Distribution Statement
HMA modulus, hot mix asphalt, HMA modulus predictive models	No restrictions. This document is available to the public through the National Technical Information Service, Springfield, Virginia 22161.

19. Security Classif. (of this report)	20. Security Classif. (of this page)	21. No. of Pages	22. Price
Unclassified	Unclassified	101	

ACKNOWLEDGMENTS / DISCLAIMER

This report is based on the results of Project IHR-R39 “Extended Life HMA Pavements”. IHR-R39 is sponsored by the Illinois Department of Transportation.

Special thanks are extended to the Technical Review Panel members: Scott Lackey, David Lippert, Rick Mauch, Matt Mueller, Paul Niedernhofer, Dave Piper, LaDonna Rowden, Amy Schutzbach, Jim Trepanier, Hal Wakefield (FHWA), and Tom Winkelman.

TABLE OF CONTENTS

LIST OF TABLES

LIST OF FIGURES

EXECUTIVE SUMMARY

The most important hot-mix asphalt (HMA) property influencing the structural response of a flexible pavement is the HMA modulus (E_{HMA}). Temperature and rate of loading significantly influence E_{HMA}, given a specific HMA, as well as the effect of aging.

Dynamic modulus concepts are reviewed. The construction of master curves for HMA mixtures (per the AASHTO 2002 Design Guide) is presented. The procedure is based on the fitting of a sigmoidal function. A new approach proposed by Bonaquist and Christensen is also presented. The procedure is based on the Hirsch model and the sigmoidal function, and eliminates the need to perform tests at lower temperatures than 40^oF (4.4^oC). Thus, the cost of the equipment, the complexity of the procedure, and the overall time to generate a master curve can be reduced.

Two IE*I predictive equations are presented. The Witczak, as proposed in the new AASHTO 2002 Design Guide, and the Hirsch model proposed by Christensen et al. In general, both appear to be in good agreement and have similar accuracy.

The Witczak predictive equation requires eight input parameters. This information is normally available from material specifications or volumetric design of the mixture. The master curve for IE*I can be developed directly by using the binder A and VTS parameters in the viscosity components of the equation.

The Hirsch model needs only three input parameters, which are available from the routine Superpave mix design process. To build the IE*I master curve, a master curve for IG^*I_{binder} has to be developed to take into account the effect of temperature and frequency. This can be done with data obtained from a Dynamic Shear Rheometer test.

Perhaps the main disadvantage of the Witczak predictive equation when compared to the Hirsch model is that viscosity is used in the predictive equation to describe the temperature effects and to express the shift factors. Consequently, it uses the VTS method (to determine A and VTS parameters) which is a linear relationship considered only applicable for conventional (non-modified) type “S” (Shell Oil / Heukelom category) asphalt cements. It should be noted that it is not clear that the log-log viscosity – log temperature relationship for modified asphalt binders is linear. Thus, the estimate viscosity may not be accurate. The Hirsch model only needs the master curve for IG^*I_{binder}, which is applicable for neat and modified asphalts.

Several studies are presented where the dynamic modulus predictive models are evaluated. The studies used different binders and represent typical mixtures used by different agencies. The results clearly confirm the good agreement and similar accuracy between the Witczak equation and the Hirsch model and between these models and dynamic modulus obtained from laboratory tests.

In general, it is concluded that both predictive models generate sufficiently accurate and reasonable dynamic modulus estimates adequate for use in mechanistic-empirical design, at least for the broad range of binders and mixtures studied.

However, to develop increased confidence in the models, it is recommended that an agency compare these models with results obtained from laboratory tests of typical mixtures.

1. INTRODUCTION

The most important hot-mix asphalt (HMA) property influencing the structural response of a flexible pavement is the HMA modulus (E_{HMA}). Temperature and rate of loading significantly influence E_{HMA}, given a specific HMA, as well as the effect of aging.

NCHRP Project 1-37A has developed the new 2002 Design Guide for New and Rehabilitated Pavements. During this project, dynamic modulus (E*) was selected as the required parameter to compute stresses and strains in HMA pavements. The selection was based on a study which compared E* to an Indirect Diametral Test (Resilient Modulus, M_R) [Dougan et al., 2003]. Using the dynamic modulus for mix design has the advantage that it can also be used in models to determine the rutting and fatigue cracking performance properties of a mix [Dongré et al., 2005]. On the other hand, E* is one of the tests currently under consideration for addition to the Superpave mix design system as a simple performance test [Harman, 2001].

The present report contains an updated literature review about the main concepts related to the dynamic modulus and the use of some predictive equations to estimate E* when laboratory test results are not available.

2. DYNAMIC MODULUS

The complex dynamic modulus (E*), is a complex number that relates stress to strain for linear viscoelastic materials subjected to continuously applied sinusoidal loading in the frequency domain. The absolute value of the complex modulus, IE*I, is commonly referred to as the dynamic modulus [Yoder and Witczak, 1975] [Witczak et al., 2002b].

HMA mixtures can be considered as a linear viscoelastic material under small strain levels (<~100με, [Schwartz, 2005]). Thus, the HMA stress-strain relationship under continuous sinusoidal loading in the linear viscoelastic region can be defined by the complex dynamic modulus.

The complex modulus is defined as the ratio of the amplitude of the sinusoidal stress (at any given time and load frequency) and sinusoidal strain (at the same time and frequency) that results in a steady state response [Dougan et al., 2003] (Figure 1):

$$E^* = \frac{\sigma}{\varepsilon} = \frac{\sigma_o \cdot e^{i\omega t}}{\varepsilon_o \cdot e^{i(\omega t - \delta)}} = \frac{\sigma_o \cdot sin(\omega t)}{\varepsilon_o \cdot sin(\omega t - \delta)} \quad (1)$$

where

- E* = complex modulus
- σ_o = peak (maximum) stress
- ε_o = peak (maximum) strain
- δ = phase angle, degrees
- ω = angular velocity
- t = time, seconds

e = exponential
i = imaginary component of the complex modulus

Thus, the dynamic modulus is defined:

$$|E^*| = \frac{\sigma_o}{\varepsilon_o} \tag{2}$$

For pure elastic materials, $\delta = 0$ and for pure viscous materials, $\delta = 90^o$.

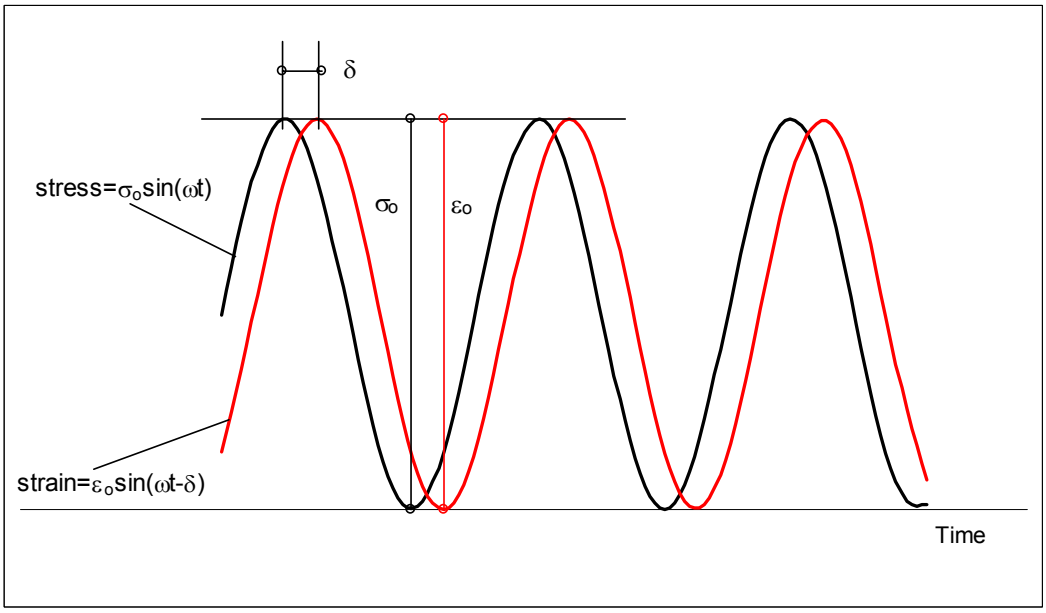

Figure 1. Stress and Strain in Dynamic Loading

The dynamic modulus IE*I is used as an overall measure of asphalt stiffness for quasi-static flexible pavement analyses. This means, analyses where time is not considered explicitly but as nominal loading rates to determine the appropriate asphalt stiffness [Schwartz, 2005].

3. MASTER CURVES AND SHIFT FACTORS

To account for the influence of temperature and rate of loading, the E_{HMA} can be determined from a master curve developed at an arbitrarily selected reference temperature (normally 70°F (21.1°C)).

A master curve represents the response of an asphalt mix at the selected reference temperature over a wide range of frequency or time [Christensen and Anderson, 1992]. It allows comparisons of linear viscoelastic materials when testing has been conducted using different loading times (frequencies) and test temperatures. In addition, this makes possible comparing the results obtained by two laboratories with different sets of tests conditions, such as frequencies and temperatures [Pellinen et al., 2002].

A master curve can be constructed utilizing the time temperature superposition principle, which describes viscoelastic behavior of asphalt binders and mixtures [Pellinen and Witczak, 2002].

However, in interpreting the results of viscoelastic tests in terms of potential pavement performance, isochronal representations should be used. An isochronal plot is simply a plot of some viscoelastic functions, such as complex modulus, versus temperature at a constant loading time or frequency [Christensen and Anderson, 1992].

Once the reference temperature has been selected, test data collected at different temperatures can be "shifted" with respect to the time of loading or frequency, so that the different curves can be aligned to form a single smooth master curve [Pellinen et al., 2002]. The shift needed at each temperature is called the shift factor, a(T), which is a constant for a given temperature. Thus, the actual frequency must be divided by this shift factor to obtain a reduced frequency, f_r, for the master curve:

$$f_r = \frac{f}{a(T)} \quad => \quad \log(f_r) = \log(f) - \log(a(T)) \tag{3}$$

where

f_r = reduced frequency (loading frequency at the reference temperature)
f = loading frequency
a(T) = shift factor

or, in terms of time of loading:

$$t_r = \frac{t}{a(T)} \quad => \quad \log(t_r) = \log(t) - \log(a(T)) \tag{4}$$

where

t_r = reduced time (loading time at the reference temperature)
t = loading time
a(T) = shift factor

At the reference temperature, the shift factor, $a(T_r) = 1$.

In summary, the master curve of modulus developed in the manner explained, describes the time dependency of the material. The amount of shifting at each temperature required to form the master curve describes the temperature dependency of the material.

Figure 2 shows an example of a master curve developed shifting moduli obtained at four different temperatures (T1, T2, T4 and T5). Figure 3 shows isochronal plots of complex modulus for two different mixes (M1 and M2), where the effect of the mix composition or frequency can be compared over a range of temperatures.

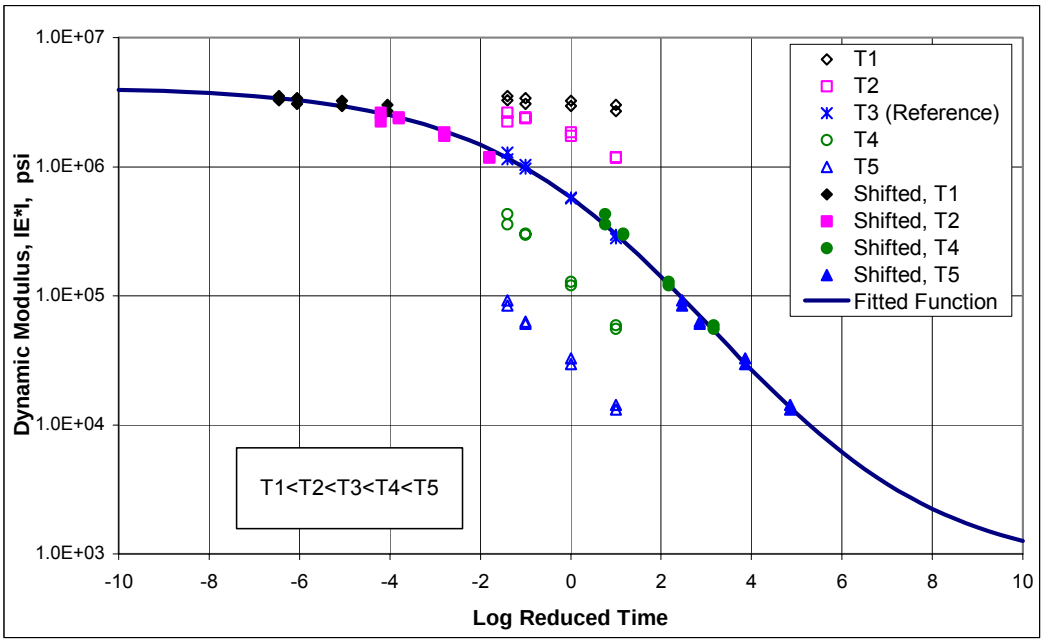

Figure 2. Example of a Complex Modulus Master Curve

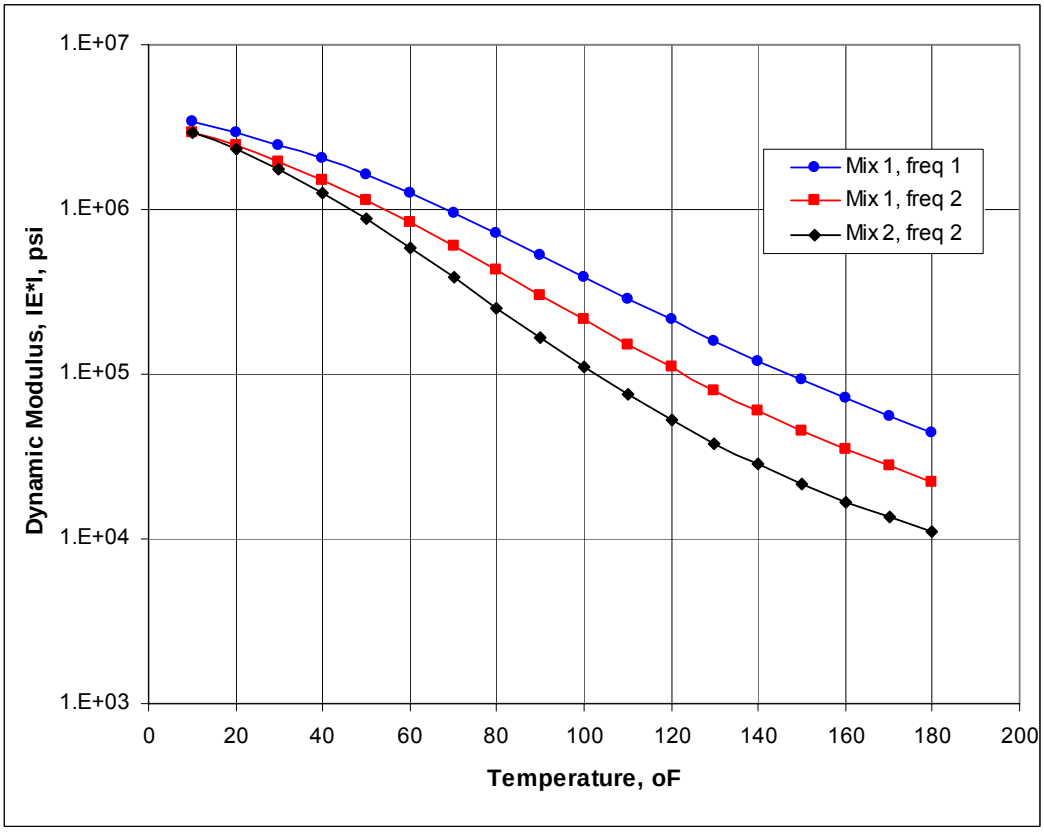

Figure 3. Example of Isochronal Plots of Complex Modulus

There are several models that have been used to represent the time temperature superposition relationship to obtain shift factors of viscoelastic materials. The Arrhenius and Williams-Landel-Ferry (WLF) equations have been used for asphalt binders, and the Arrhenius and Log-linear equations have been used for asphalt mixtures.

On the other hand, to develop the master curve for frequency or time dependency, the generalized power law has been the most widely accepted mathematical model for bituminous material response at low and intermediate temperatures. As higher temperatures are considered, polynomial fitting functions also have been used [Pellinen and Witczak, 2002]. However, a single polynomial model is not appropriate for fitting the entire master curve because its swing at low and high temperatures produces irrational modulus predictions when used to extrapolate outside the range of data [Pellinen et al., 2002].

To avoid the problem presented by the polynomial model, research developed at the University of Maryland showed that the modulus master curve for asphalt mixtures can be represented by a sigmoidal function [2002 Design Guide, (2004)] defined by equation (5). This research proposes to construct the master curves fitting a sigmoidal function to the measured compressive dynamic (complex) modulus test data using non-linear least squares regression, which can be done using the Solver Function in the Excel spreadsheet. The shifting could be done by solving shift factors simultaneously with the coefficients of the sigmoidal function, using any available shifting function to solve reduced frequency (f_r), or time (t_r), as a function of temperature [Pellinen and Witczak, 2002].

$$\log(|E^*|) = \delta + \frac{\alpha}{1 + e^{\beta + \gamma \log(t_r)}} \quad (5)$$

where

IE*I = dynamic modulus
t_r = time of loading at the reference temperature (reduced time)
δ = minimum modulus value
$\delta + \alpha$ = maximum modulus value
β, γ = parameters describing the shape of the sigmoidal function

In this equation, parameter γ influences the steepness of the function (rate of change between minimum and maximum) and β, the horizontal position of the turning point (Figure 4). In addition, δ and α depend on aggregate gradation, binder content, and air void content. Parameters β and γ, on the other hand, depend on the characteristics of the asphalt binder and the magnitude of δ and α [2002 Design Guide, (2004)].

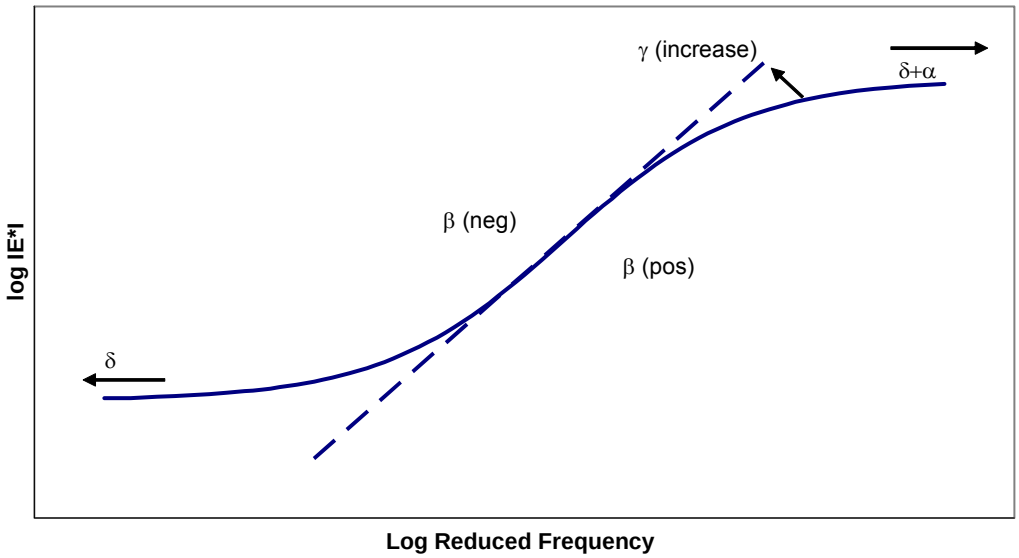

Figure 4. Sigmoidal Function [Pellinen and Witczak, 2002]

The justification of using a sigmoidal function for fitting the compressive dynamic modulus data is based on the physical observations of the mix behavior. The upper range of the sigmoidal function approaches asymptotically to the maximum stiffness of the mix, which depends on the limiting binder stiffness at cold temperatures. At high temperatures, the compressive loading causes aggregate influence to be more dominant than the viscous binder influence. The modulus starts to approach a limiting equilibrium value, which is dependent on the aggregate gradation. Thus, the sigmoidal function captures the physical behavior of the asphalt mixtures observed in the mechanical testing using compressive cyclic loading through the entire temperature range [Pellinen and Witczak, 2002].

It has been demonstrated [2002 Design Guide, 2000] that :

$$\log(t_r) = \log(t) - c(\log(\eta) - \log(\eta_{Tr})) \quad (6)$$

where

t_r = time of loading at the reference temperature (reduced time)
t = time of loading
c = fitting parameter
η = viscosity at temperature of interest
η_{Tr} = viscosity at reference temperature

Then, from equations (4) and (6):

$$\log(a(T)) = c(\log(\eta) - \log(\eta_{Tr})) \quad (7)$$

Thus, the shift factors from experimentally derived master curves can be expressed using equation (7), as a function of viscosity, after shifting the experimental data using nonlinear optimization. The resulting shift factors can be plotted as a function of viscosity and the constant c in equation (7) will be the slope of the best-fit line through the origin. Expressing shift factors as a function of binder viscosity is a key element because it allows the consideration of binder aging using the Global Aging System (GAS) developed by Mirza and Witczak [2002 Design Guide, 2000].

As an alternative, equation (6) can be included directly in equation (5) resulting in equation (8):

$$\log(|E^*|) = \delta + \frac{\alpha}{1 + e^{\beta+\gamma[\log(t)-c(\log(\eta)-\log(\eta_{Tr}))]}} \quad (8)$$

where

IE*I = dynamic modulus
t = time of loading
η = viscosity at temperature of interest
η_{Tr} = viscosity at reference temperature
α, β, δ, γ, c = fitting parameters

In this case, through the nonlinear optimization, parameters α, β, γ, δ, and c can be obtained.

In a recently completed Federal Highway Administration (FHWA) study [Dougan et al., 2003] several issues have been identified related to the dynamic modulus test protocol, concluding that the overall time to perform the testing must be reduced if highway agencies are going to use the IE*I test for routine testing. The minimum testing required to develop master curves has been studied in NCHRP Project 9-29. It was concluded that reasonable master curves can be developed using tests at three temperatures (14 (-10), 70 (21.1) and 130^{o}F (54.4^{o}C)) and loading frequencies of 33, 2.22, 0.15, and 0.01 Hz. This reduced set still requires testing at 14^{o}F (-10^{o}C), which is difficult due to moisture condensation and ice formation. In addition, low temperature testing increases the cost of the environmental chamber and increases the loading capacity and cost of the test equipment [Bonaquist and Christensen, 2005]. By eliminating this low temperature test, the cost of the equipment, the complexity of the procedure, and the overall time required to generate a master curve can be reduced [Bonaquist and Christensen, 2005].

On the other hand, as it is known, for engineering purposes all asphalt binders reach approximately the same glassy modulus at very low temperatures (145,000 psi or 1 GPa) [Christensen and Anderson, 1992]. Using this fact and the recently developed Hirsch model (equations (33) and (34) presented later) to predict mixture dynamic modulus from binder IG*I, VMA and VFA, an estimate of the limiting maximum modulus of the mixture can be made and used in the generation of IE*I master curves. Bonaquist and Christensen (2005) have proposed this modification which for a known limiting

maximum modulus, the master curve given in equation (8) can be reduced into equation (9) as follows:

$$\log(|E^*|) = \delta + \frac{(Max - \delta)}{1 + e^{\beta + \gamma[\log(t) - c(\log(\eta) - \log(\eta_{Tr}))]}} \quad (9)$$

where

IE*I = dynamic modulus
t = time of loading
η = viscosity at temperature of interest
η_{Tr} = viscosity at reference temperature
Max = limiting maximum dynamic modulus
β, δ, γ, c = fitting parameters

The four unknown fitting parameters are still estimated using numerical optimization of the test data, but since the limiting maximum modulus is now known, data at low temperatures are no longer needed.

4. DYNAMIC MODULUS CALCULATED FROM PREDICTIVE EQUATIONS

There are several models to predict dynamic modulus of asphalt concrete. The most of them are empirical or semi-empirical and based on volumetric mixture properties and binder characteristics. Two of them will be presented in this report because of their simplicity and promise: the Witczak predictive equation, which is proposed in the new AASHTO 2002 Design Guide, and the Hirsch model, proposed by Christensen et al. (2003).

4.1. Witczak Predictive Equation Model

Depending on what material properties are available, the 2002 Design Guide uses different hierarchical levels (1, 2, and 3) for determining the material parameters needed in the performance models. For the highest level of accuracy (Level 1), the dynamic modulus is obtained from laboratory testing and requires nonlinear optimization using equations (3) or (4) and (5), as explained above. For the lower hierarchical levels (Level 2 and 3), different combinations of existing predictive material models are used. One of these models is the Witczak dynamic modulus predictive equation, equation (10), which is one of the most comprehensive mixture stiffness models available today. This model is capable of predicting mixture stiffness over a range of temperatures, rate of loading, and aging conditions from information that is readily available from material specifications or volumetric design of the mixture.

$$\log|E^*| = 3.750063 + 0.02932\rho_{200} - 0.001767(\rho_{200})^2 - 0.002841\rho_4 - 0.058097V_a$$
$$- 0.802208\left(\frac{V_{beff}}{V_{beff} + V_a}\right) + \frac{3.871977 - 0.0021\rho_4 + 0.003958\rho_{38} - 0.000017(\rho_{38})^2 + 0.00547\rho_{34}}{1 + e^{(-0.603313 - 0.313351\log(f) - 0.393532\log(\eta))}} \quad (10)$$

where

IE*I = dynamic modulus, psi
η= bitumen viscosity, 10^6 Poise
f = loading frequency, Hz
V_a = air void content, %
V_{beff} = effective bitumen content, % by volume
ρ_{34} = cumulative % retained on the 19-mm (3/4) sieve
ρ_{38} = cumulative % retained on the 9.5-mm (3/8) sieve
ρ_4 = cumulative % retained on the 4.76-mm (No. 4) sieve
ρ_{200} = % passing the 0.075-mm (No. 200) sieve

Equation (10) represents the current form of the Witczak predictive equation. It is based on a database of 2750 dynamic modulus measurements from 205 different asphalt mixtures tested over the last 30 years in the laboratories of the Asphalt Institute, the University of Maryland, and the Federal Highway Administration [2002 Design Guide, 2000]. This model can predict the dynamic modulus of mixtures using both modified and conventional asphalt cements [2002 Design Guide, 1999]. Table 1 shows summary statistics for this equation.

Table 1. Summary Statistics for the Witczak Dynamic Modulus Predictive Equation

Statistic	Value
Goodness of fit	R^2 = 0.96 Se/Sy = 0.24
Data points	2750
Temperature range	0 to 130 ^oF
Loading rates	0.1 to 25 Hz
Mixtures	205 Total 171 With unmodified asphalt binders 34 With modified binders
Binders	23 Total 9 Unmodified 14 Modified
Aggregates	39
Compaction methods	Kneading and gyratory
Specimen sizes	Cylindrical 4 in by 8 in or 2.75 in by 5.5 in

[Note 1: It must be noted that there are discrepancies between equation (10), which is published in the TRB web site <http://www.trb.org/mepdg/guide.htm> in Chapter 2

"Design Inputs" dated March 2004 and that appearing in the same web site but in Appendix CC-4 "Development of a Revised Predictive Model for the Dynamic (Complex) Modulus of Asphalt Mixtures" dated March 1999. The first equation gives IE*I directly in psi and the second one in 10^5 psi. The units of psi can be demonstrated to be correct because it only affects the first constant of the equation (3.750063 when psi are used and -1.249937 when 10^5 psi). However, the second constant of the equation (0.02932 ρ_{200}) is different than that in Appendix CC-4 (0.029232 ρ_{200}). Appendix CC-4, although published 5 years earlier, presents the development of the model that should be contained in the final report of the Design Guide dated March 2004. The draft issued on October 2000 presents the equation with the same constant as in the final report. On the other hand, because of the "Log" term in the equation, that small difference produces a larger difference in the estimated IE*I that should be taken into account in some situations. So far, there is not an explanation for that discrepancy, except that it probably may be only a "typing error". It is thought that the Witczak equation should be used as it appears in the final draft of the 2002 Design Guide (equation 9) until a definite correction be made.]

[Note 2: There is an issue related with the development of the Witczak model, contained in Appendix CC-4 "Development of a Revised Predictive Model for the Dynamic (Complex) Modulus of Asphalt Mixtures" dated March 1999, which is thought appropriate to explain at this point.
One of the conclusions of that Appendix is: "The resulting model can accurately predict the dynamic modulus of mixtures using both modified and conventional asphalt cements…." On the other hand, in the chapter related to the new database the authors mention that 34 of the 56 additional mixes used modified asphalt cements and that in order to apply the model (Witczak) to the new data, bitumen viscosity values were needed for each mix at the temperatures at which the tests were actually performed. They also explain that those viscosity values were obtained by using the linear relationship between log-log viscosity (in centipoises) and log temperature (in degrees Rankine), also known as the A and VTS relationship.
In the paper related to the development of the Global Aging System [Mirza and Witczak, 1995], the authors concluded: "The fundamental basis of the aging models developed is the ASTM log-log viscosity – log temperature linear relationship. This relationship has been justified over a broad range (39°F (3.9°C) - 300°F (148.9°C)) for the original, mix/laydown and the field aged conditions. However, this linearity is considered only applicable for conventional (non-modified) type "S" asphalt cements. As a result, the aging system developed should not be used for modified asphalt, type "W" (waxy) or type "B" (blown) asphalt". This conclusion is reasonable since it is not clear that the log-log viscosity – log temperature relationship for modified asphalt binders is linear, in which case determining A and VTS will not be practical and the estimated viscosity will not be so accurate.
Justification was not provided for the authors' assumption that the linear relationship is valid for the modified asphalts used in their study. One explanation could be that the modified binders were tested in a broad range of temperatures and within that range, the relationship showed to be linear.]

Comparing equations (5) and (10), note that equation (10) also has the form of a sigmoidal function. Thus, it can be used directly to develop a master curve. In this case, viscosity is used to describe the temperature effects.

A simplification of equation (10) as a sigmoidal function would be:

$$\log(|E^*|) = d + \frac{a}{1 + e^{b + g_1 \log(f) + g_2 \log(\eta)}} \tag{11}$$

where

d = minimum modulus
d + a = maximum modulus
g_1, g_2, and b = fitting parameters

Thus, to transform equation (11) into the form of the master curve in equation (5), it has to be shown that:

$$\delta + \frac{\alpha}{1 + e^{\beta + \gamma \log(t_r)}} = d + \frac{a}{1 + e^{b + g_1 \log(f) + g_2 \log(\eta)}} \tag{12}$$

In equation (12), for definition, δ and d are equal and α and a are also equal. Then, equation (12) requires that the exponents in both denominators be equal at the reference temperature:

$$\beta + \gamma \log(t_r) = b + g_1 \log(f_r) + g_2 \log(\eta_{Tr}) \tag{13}$$

where

η_{Tr} = viscosity at the reference temperature
β, γ, t_r, b, g_1, g_2, and f_r = as previously defined

Considering that frequency is equal to 1/t [2002 Design Guide, 2000]:

$$\gamma = -g_1 \tag{14}$$

$$\beta = b + g_2 \log(\eta_{Tr}) \tag{15}$$

Therefore:

$$\log(|E^*|) = \delta + \frac{\alpha}{1 + e^{\beta + \gamma \log(t_r)}} \tag{16}$$

where

$$\log(t_r) = \log(t) - c(\log(\eta) - \log(\eta_{Tr}))$$

$$\delta = 3.750063 + 0.02932\rho_{200} - 0.001767(\rho_{200})^2 - 0.002841\rho_4 - 0.058097V_a - 0.802208\left(\frac{V_{beff}}{V_{beff} + V_a}\right)$$

$$\alpha = 3.871977 - 0.0021\,\rho_4 + 0.003958\,\rho_{38} - 0.000017\,(\rho_{38})^2 + 0.00547\,(\rho_{34})$$

$$\beta = -0.603313 - 0.393532\log(\eta_{Tr})$$

$$\gamma = 0.313351$$

$$c = 1.255882$$

[Note 3: In the comparison between Equations (10) and (5), it is assumed that frequency, f (Hz), is equal to 1/t (1/s), based on the draft of the Design Guide [2002 Design Guide, 2000]. Dongré et al. (2005) have pointed out that this relationship is an error. They mention that the correct approach is to first convert the cyclic frequency, f (Hz), to angular frequency, ω (rad/s), and then take the inverse of ω to determine loading time (t, seconds). It is not clear in the Final Report of the Design Guide [2002 Design Guide, 2004] if this situation was taken into account.]

Using the predictive equation model, is possible to express the shift factors as a function of binder viscosity. This can be done solving equation (7) with the constant value of "c" as determined above (1.255882). Then, the GAS also can be used to take into account the binder aging.

Viscosity Temperature Susceptibility Method (VTS)

As mentioned earlier, viscosity is used in the predictive equation model to describe the temperature effects and to express the shift factors.

On the other hand, for unaged binders, the viscosity at the temperature of interest can be determined from the ASTM viscosity temperature relationship, equation (17):

$$\log(\log\eta) = A + VTS[\log(T_R)] \qquad (17)$$

where

η = viscosity, centiPoise
T_R = temperature, ^{o}Rankine
A = regression intercept
VTS = regression slope of viscosity temperature susceptibility

This linear relationship is characterized by its unique A and VTS parameters for the original asphalt cement condition. It allows a continuous binder viscosity characterization over a wide range of temperature. However, this linearity is considered only applicable for conventional (non-modified) type "S" (Shell Oil / Heukelom category) asphalt cements [Mirza and Witczak, 1995].

[Note 4: Note 2 explained the situation about the linear relationship for modified asphalts. It must be noted in addition, that neither in the reference [2002 Design Guide,

2000] nor in [2002 Design Guide, 2004] there is a mention about the use of the linear relationship for modified asphalt.]

Because equation (17) is in terms of viscosity units, it is necessary to incorporate the entire range of temperature-consistency data into the common fundamental form of bitumen viscosity. For example, Brookfield viscosity measurements between 140°F (60°C) and 347°F (175°C) can be used to get the regression coefficients as well as absolute and kinematic viscosities. The equation can also be extended to lower temperatures using ring and ball softening point, in which case the binder viscosity corresponds to 13,000 Poise. In addition, penetration data (100 g, 5 sec loading), between test temperatures of about 41 (5) to 95°F (35°C), can be transformed to viscosity using equation (18) [Mirza and Witczak, 1995]:

$$\log \eta = 10.5012 - 2.2601 \log(Pen) + 0.00389 \ (\log(Pen))^2 \qquad (18)$$

where

η = viscosity, Poise
Pen = penetration for 100g, 5 sec loading, 0.10 mm

Equation (18) was developed for penetration values between 3 and 269 and it is not recommended for use beyond a penetration value of 300 [Mirza and Witczak, 1995]. The summary statistics for this equation are shown in Table 2.

Table 2. Summary Statistics for the Penetration-Viscosity Relationship

Model	Equation No.	No. of Test Roads	No. of Test Sections	No. of Data Points	R^2	
					Normal	Log
Penetration-Viscosity	18	17	-	766	0.377	0.927

With the adoption of the Superpave Performance Grading system, traditional consistency testing (viscosity, softening point, and penetration) data are no longer collected routinely. Another model has been developed to obtain the corresponding viscosity at any temperature, equation (19), based on different binder types and various aging conditions [2002 Design Guide, 2000] [2002 Design Guide, 2004]:

$$\eta = \frac{|G^*|}{10}\left(\frac{1}{\sin\delta}\right)^{4.8628} \qquad (19)$$

where

η = viscosity, Pa·sec
IG*I = binder complex shear modulus (using ω = 10 rad/sec), Pa
δ = phase angle

[Note 5: A discrepancy has been found in equation (19) as it appears in both of the references cited above. In the first one, Design Guide (Draft) dated October 2000, there are no units for the variables η, IG*I and δ. Nevertheless, from the example in Table 2.20 in the same reference, it can be inferred that the units are: η(Pa·sec), IG*I(Pa) and δ(degrees). On the other hand, in the second reference, Design Guide (Final Report) dated March 2004, the units are as follows: η(cP), IG*I(Pa) and δ(degrees). It is thought that units should be as in equation (19). Since 1 Pa·sec = 1000 cP, to get viscosity in units of cP, multiply the right side of equation (19) by 1000. When using equation (19) in a spreadsheet, the phase angle (δ) must be in radians.]

After obtaining the viscosity data (at least two points) in any of the ways explained above, the A and VTS parameters can be determined by least squares regression as shown in Figure 5, which was developed with data from Table 3.

Table 3. Consistency Data (original) [Mirza and Witczak, 1995]

	Pen	Temp. ^{o}F (^{o}C)	Temp. ^{o}R	η cP	log(log(η))	log(T_R)
Pen	5.9	39 (4)	499	5.8E+10	1.0319	2.6980
	8	39 (4)	499	2.9E+10	1.0197	2.6980
	15.3	50 (10)	510	6.8E+09	0.9925	2.7073
	15	50 (10)	510	7.1E+09	0.9934	2.7073
	29.8	60 (16)	520	1.5E+09	0.9628	2.7164
	33	60 (16)	520	1.2E+09	0.9580	2.7164
	77.9	77 (25)	537	1.7E+08	0.9160	2.7297
	78	77 (25)	537	1.7E+08	0.9158	2.7297
	187.8	90 (32)	549	2.4E+07	0.8684	2.7398
	164	90 (32)	549	3.3E+07	0.8759	2.7398
R&B		121 (49)	580	1.3E+06	0.7863	2.7633
		121 (49)	580	1.3E+06	0.7863	2.7633
Ab. Visc.		140 (60)	600	2.0E+05	0.7238	2.7779
Ki. Visc.		275 (135)	735	3.8E+02	0.4122	2.8661
Brook. Visc.		140 (60)	600	1.7E+05	0.7185	2.7779
		275 (135)	735	3.6E+02	0.4072	2.8661
		350 (177)	810	6.6E+01	0.2600	2.9086

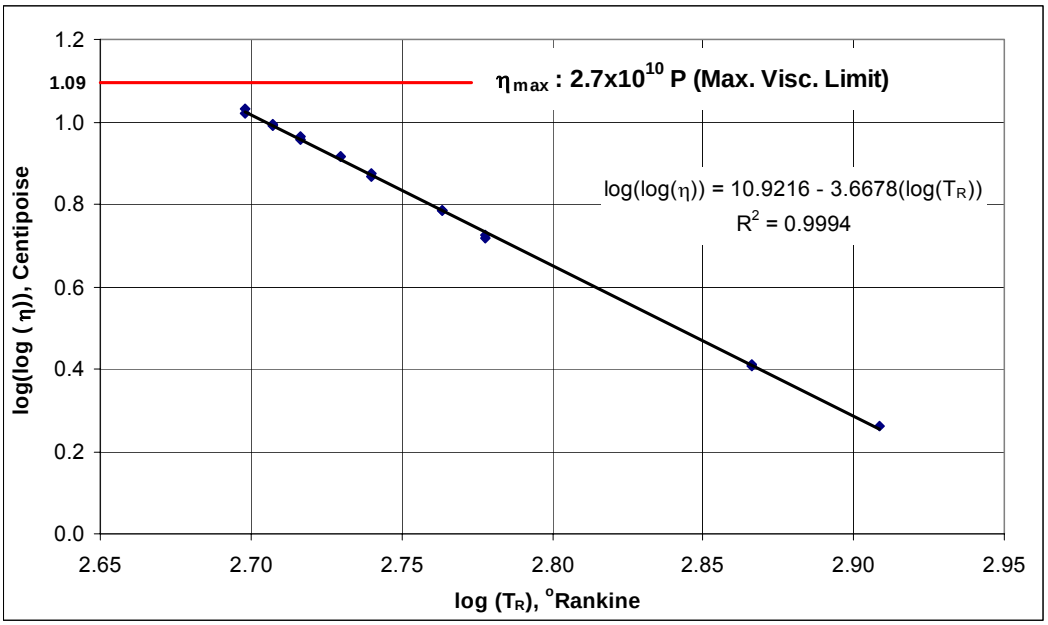

Figure 5. Viscosity-Temperature Relationship [Modified, Mirza and Witczak, 1995]

To obtain shift factors directly from the A and VTS parameters (determined as described above), note that the viscosity, η, obtained from any of the ways explained, can be related to the relaxation time, τ_t, and shift factor, a(T), through the following equations [Painter and Coleman, 1997]:

$$\tau_t = \frac{\eta}{E} \tag{20}$$

where

τ_t = relaxation time

η = viscosity

and:

$$a(T) = \frac{\tau_{t,1}}{\tau_{t,0}} \approx \frac{\eta_1}{\eta_0} \tag{21}$$

where

a(T) = shift factor

$\tau_{t,1}$ = relaxation time at temperature T_1

η_1 = viscosity at temperature T_1

Then:

$$\log(a(T)) \approx \log(\eta_1) - \log(\eta_0) \tag{22}$$

On the other hand, from equation (17):

$$\log(\eta) = 10^{A+VTS[\log(T_R)]} \tag{23}$$

Thus, substituting equation (23) in equation (22), shift factors can be obtained as a function of A and VTS parameters with equation (24) [Pellinen et al., 2002]:

$$\log(a(T)) = c\left(10^{A+VTS[\log(T_R)]} - 10^{A+VTS[\log(T_R)_0]}\right) \quad (24)$$

where

c = constant
T_R = temperature of interest, °Rankine
$(T_R)_o$ = reference temperature, °Rankine
A = regression intercept
VTS = regression slope of viscosity temperature susceptibility

Equation (24) is equivalent to equation (7). Equation (24) uses A and VTS parameters and Equation (7) uses viscosity directly.

Global Aging System (GAS)

The effect of aging influences the HMA modulus. This effect can be taken into account by determining the change in viscosity that occurs in a mixture during mixing and compaction, as well as in the long-term in-situ. The effect of aging in the Witczak model is incorporated using the GAS.

The GAS provides a series of sequential analytical models to predict aging (in terms of viscosity increase) characteristics of conventional "S" type asphalt cements due to both short (mixing and compaction) and long term (in-situ aging) effects [Mirza and Witczak, 1995]. It comprises four different models: original to mix/laydown model, surface aging model, air voids adjustment and viscosity-depth model.

1. Original (orig) to Mix/Laydown (t=0) Model

The original to mix/laydown model, equation (25), takes into account the short-term aging that occurs during mixing and compaction. The code value is defined by the ratio of log-log mix/laydown viscosity (Rolling Thin Film Oven Test, RTFO) to the log-log original viscosity (hardening ratio, HR). Table 4 summarizes the code values recommended. Local experience with individual asphalt cement types is the recommended best approach to select an appropriate code value [Mirza and Witczak, 1995].

$$\begin{aligned} \log(\log(\eta_{t=0})) &= a_0 + a_1 \log(\log(\eta_{orig})) \\ a_0 &= 0.054405 + 0.004082 \cdot code \\ a_1 &= 0.972035 + 0.010886 \cdot code \end{aligned} \quad (25)$$

where

$\eta_{t=0}$ = mix/laydown viscosity, cP at temperature T_R in °Rankine
η_{orig} = original viscosity, cP at temperature T_R in °Rankine
code = hardening resistance (0 for average)

Table 4. Typical Hardening Resistance and Code Values Recommended

Mix/Laydown Hardening Resistance	Expected Hardening Resistance Values	Code Value
Excellent to Good	HR ≤ 1.03	-1
Average	1.03 < HR ≤ 1.075	0
Fair	1.075 < HR ≤ 1.1	1
Poor to Very Poor	HR > 1.1	2

A minimum of two, and preferably four to five temperatures (i.e., viscosity values at original condition at the temperature selected, η_{orig}) can be used to predict the mix/laydown viscosity ($\eta_{t=0}$) using equation (25). These predicted viscosities at t=0 are then used to estimate the linear regression coefficients, $A_{t=0}$ and $VTS_{t=0}$, using equation (17) [Mirza and Witczak, 1995].

It must be noted that when viscosity data are directly obtained after RTFO aging or from actual measurement of mix/laydown viscosities after extraction, the original to mix/laydown model does not need to be applied. In that case, the viscosity values after RTFO or actual measured mix/laydown viscosities, are directly used to estimate the $A_{t=0}$ and $VTS_{t=0}$ parameters using equation (17). On the other hand, the 2002 Design Guide recommends some typical $A_{t=0}$ and $VTS_{t=0}$ values established for all binder grades (Table 5), to be used in the level 3 analysis. Level 3 does not require laboratory test data.

Table 5. Recommended RTFO A and VTS Parameters by AASHTO [2002 Design Guide, (2000)]

High Temp.	Low Temperature Grade													
	-10		-16		-22		-28		-34		-40		-46	
Grade	$A_{t=0}$	$VTS_{t=0}$	$A_{t=0}$	$VTS_{t=0}$	$A_{t=0}$	$VTS_{t=0}$	$A_{t=0}$	$VTS_{t=0}$	$A_{t=0}$	$VTS_{t=0}$	$A_{t=0}$	$VTS_{t=0}$	$A_{t=0}$	$VTS_{t=0}$
46									11.504	-3.901	10.101	-3.393	8.755	-2.905
52	13.386	-4.570	13.305	-4.541	12.755	-4.342	11.840	-4.012	10.707	-3.602	9.496	-3.164	8.310	-2.736
58	12.316	-4.172	12.248	-4.147	11.787	-3.981	11.010	-3.701	10.035	-3.350	8.976	-2.968		
64	11.432	-3.842	11.375	-3.822	10.980	-3.680	10.312	-3.440	9.461	-3.134	8.524	-2.798		
70	10.690	-3.566	10.641	-3.548	10.299	-3.426	9.715	-3.217	8.965	-2.948	8.129	-2.648		
76	10.059	-3.331	10.015	-3.315	9.715	-3.208	9.200	-3.024	8.532	-2.785				
82	9.514	-3.128	9.475	-3.114	9.209	-3.019	8.750	-2.856	8.151	-2.642				

2. Mix/Laydown (t=0) to Surface Aging (t>0, z=0.25") Model

This model, equation (26), predicts the viscosity of the binder ($\eta_{t>0}$) at the surface of the pavement after any period of time (t>0) using mix/laydown viscosity ($\eta_{t=0}$) as input. Under the GAS frame, "surface" viscosity really means that corresponding to a depth of approximately 0.25 in. (z=0.25 in.). The environmental effect on the long-term aging is considered through the use of the mean annual air temperature.

$$\log(\log(\eta_{t>0})) = \frac{\log(\log(\eta_{t=0})) + A \cdot t}{1 + B \cdot t} \tag{26}$$

where

A = -0.004166+1.41213·C+C·log(Maat)+D·log(log($\eta_{t=0}$))
B = 0.197725+0.068384·log(C)
C = $10^{274.4946-193.831\cdot\log(T_R)+33.9366\cdot\log(T_R)2}$
D = -14.5521+10.47662·log(T_R)-1.88161·log(T_R)^2
$\eta_{t>0}$ = aged viscosity at time t, cP
$\eta_{t=0}$ = viscosity at mix/laydown, cP
Maat = mean annual air temperature, ^{o}F
T_R = temperature, ^{o}Rankine
t = time in months

Analogous to the original to mix/laydown model, a minimum of two, and preferably four to five temperatures (i.e., viscosity values at t=0 condition at the temperature selected, $\eta_{t=0}$) can be selected between a range of 77^{o}F (25^{o}C) and 275^{o}F (135^{o}C) to predict the aged viscosities at any given time and climatic environment ($\eta_{t>0}$) using equation (26). These estimated viscosities at t>0 are then used to determine the linear regression coefficients, $A_{t>0}$ and $VTS_{t>0}$, using equation (17) [Mirza and Witczak, 1995].

3. Air Voids Adjustment

During the development of the GAS the air voids variable could not be included directly in the mix/laydown to surface aging model, equation (26), because of the limited amount of information available. To overcome this shortcoming, an adjustment factor based on the limited available air voids information was developed, equation (27). This adjustment is considered to be an optional factor. If no adjustment for the air voids is used, the adjustment factor takes a value of one in equation (27) [Mirza and Witczak, 1995].

$$F_v = \frac{1 + 1.0367 \cdot 10^{-4} \cdot VA \cdot t}{1 + 6.1798 \cdot 10^{-4} \cdot t} \tag{27}$$

where

F_v = adjustment factor
VA = air voids at time t, %
t = time, months

The mix/laydown to surface aging model may be modified for the air voids effect by applying:

$$\log(\log(\eta_{t>0}))' = F_v \log(\log(\eta_{t>0})) \tag{28}$$

The prediction of air voids at any time can be obtained by equation (29):

$$VA = \frac{VA_{orig} + 0.0111 \cdot t - 2}{1 + 4.24 \cdot 10^{-4} \cdot t \cdot Maat + 1.169 \cdot 10^{-3}\left(\frac{t}{\eta_{orig,77}}\right)} + 2 \quad (29)$$

where

VA = air voids at time t, %
VA_{orig} = original (initial) air voids, %
t = time, months
Maat = mean annual air temperature, ^{o}F
$\eta_{orig,77}$ = original binder viscosity at 77^{o}F (25^{o}C), MPoise

4. Viscosity-Depth Model

The following equation represents the field aged viscosity at any time, t, and depth, z, within the pavement layer:

$$\eta_{t,z} = \frac{\eta_t \cdot (4 + E) - E \cdot \eta_{t=0} \cdot (1 - 4 \cdot z)}{4 \cdot (1 + E \cdot z)} \quad (30)$$

where

$\eta_{t,z}$ = aged viscosity at time t, and depth z, MPoise
η_t = aged surface viscosity, MPoise
z = depth, inches
$E = 23.82 \cdot e^{-0.0308\ Maat}$
Maat = mean annual air temperature, ^{o}F

In this model, η_t represents the surface (z=0.25 in.) aged viscosity determined from equation (26) or (28).

The summary statistics for the models of the GAS are shown in Table 6.

As seen in equations (6) and (7), the binder viscosity is a direct input in the reduced time and shift factor equations for the master curve. Thus, a combined shift factor that accounts for aging, temperature, and rate of loading is developed directly in those equations, after applying the GAS models to determine the appropriate aged viscosity.

From GAS it can be inferred that the aged viscosity increases as the binder ages (at a constant temperature). However, in equation (6), as the aged viscosity increases, the reduced time for that temperature decreases. This effect is equivalent to a shift to the left on the master curve, as shown in Figure 6 below. Accordingly, the new 2002 Design Guide suggests using the same master curve for all aging conditions, changing only the reduced time for computing the dynamic modulus, and this change will be determined using equation (6) and the viscosity from the GAS models [2002 Design Guide, (2000)].

Table 6. Summary Statistics for the Predictive Models of the GAS [Mirza and Witczak, 1995]

Model	Equation No.	No. of Test Roads	No. of Test Sections	No. of Data Points	R^2	
					Normal	Log [1)]
Original to Mix/Laydown Without HR (code=0)	25	21	-	740	0.775	0.992
Original to Mix/Laydown With HR	25	21	-	740	0.853	0.995
Mix/Laydown to Surface Aging	26	16	149	1382	0.549	0.993
Air Voids Adjustment	29	9	50	193	0.96	-
Viscosity- Depth	30	3	43	134	0.91	-

1) Statistical parameters in log-log space

According to the data in Table 7, equation (31) represents the dynamic modulus master curve for the mixture in the example (E* in psi). The corresponding reduced time equation is shown in equation (32). The dynamic modulus for the pavement design analysis can be obtained applying these equations after adjusting the binder viscosity for age.

$$\log|E^*| = 2.844176 + \frac{3.833025}{1 + e^{(-1.0084 + 0.313351 \cdot \log(t_r))}} \tag{31}$$

$$\log(t_r) = \log(t) - 1.255882 \cdot (\log(\eta) - \log(10.7)) \tag{32}$$

In this example, the original to mix/laydown model is not needed since the master curve was developed using the recommended parameters ($A_{t=0}$ and $VTS_{t=0}$) that account for the initial aging (values taken directly from the 2002 Design Guide) . On the other hand, the air voids adjustment was not used (F_V=1 in equation (28)) because it was assumed that the air voids in the pavement will be the same as average air voids from the pavement used to develop the GAS model.

Note in Figure 7, the greatest change in dynamic modulus occurs only at approximately the top 1 to 1.5 inches, with a relatively smaller change at greater depths within the pavement. At t=0, the dynamic modulus is considered the same no matter the depth. This is because at the mix/laydown condition (t=0), the viscosity is represented by a constant viscosity with depth. In terms of time, according to this example, the greatest change in dynamic modulus occurs during the first two to four years, with almost no change after this time.

Figures 6 and 7 show the master curve and the dynamic modulus as a function of time and depth, respectively.

Table 7. Parameters Used in the Master Curve and Dynamic Modulus/Time Plot

Mix design parameters	
Mix type	12.5 mm
Binder type	PG 64-22
Air voids content, Va, %	7.0
Effective binder content, Vb_{eff}, %	11.5
ρ_{34}, %	0
ρ_{38}, %	12.0
ρ_{4}, %	40.0
ρ_{200}, %	6.1
Master curve parameters	
A	10.98
VTS	-3.68
Reference temperature, ^{o}F	70
η, 70 ^{o}F, 10^{6} Poise	10.70
α	3.833025
β	-1.0084
γ	0.313351
δ	2.844176
c	1.255882
Loading time, sec.	0.1
Aging model parameters	
η, 100 ^{o}F, cPoise	23573342
A	0.061698
B	0.069155
C	0.013179
D	0.028657
E	5.106558
Maat, ^{o}F	50

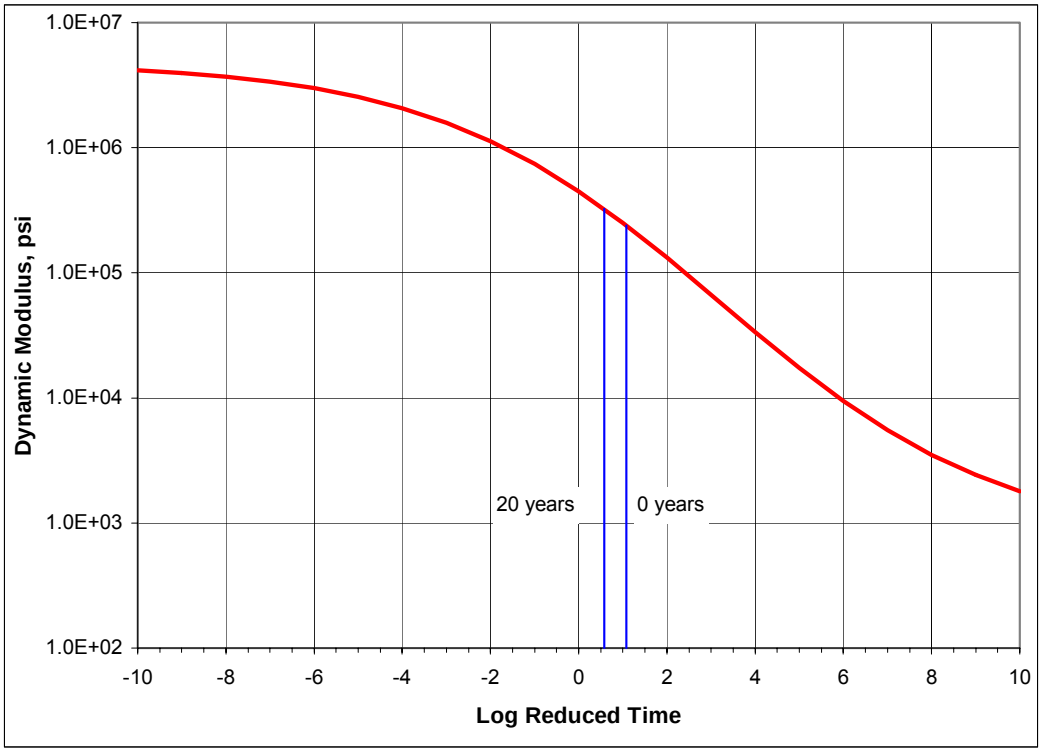

Figure 6. Master Curve with the Range of Reduced Time from Aging Analysis

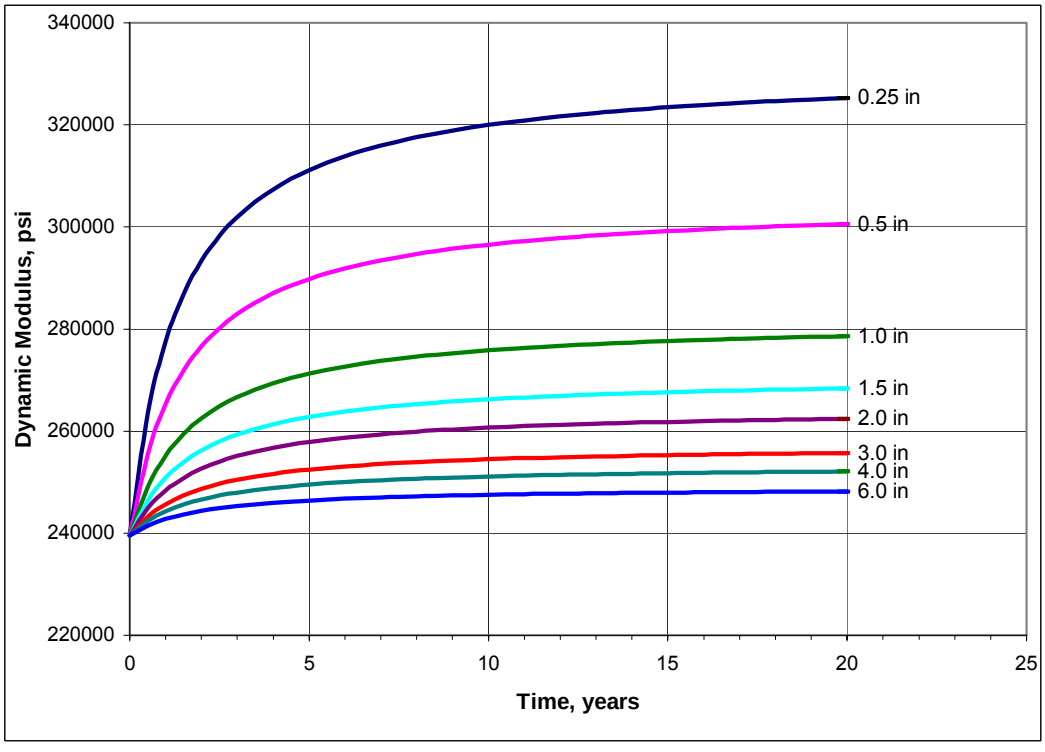

Figure 7. Dynamic Modulus vs. Time at Different Depths

[Note 6: In spite of the conclusion cited in Note 2 related to the application of the GAS system only for conventional (non-modified) asphalt cements, it must be noted that in the 2002 Design Guide (2004) there is no mention about the use of this system for a specific type of asphalt binder. This is an issue that should be clarified.]

4.2. Hirsch Model for HMA

The Hirsch model is a rational, though semi-empirical method of predicting asphalt concrete modulus. It is based on an existing version of the law of mixtures, called the Hirsch model, which combines series and parallel elements of the phases, Figure 8.

Asphalt concrete tends to behave like a series composite at high temperatures, but more like a parallel composite at low temperatures, and so the Hirsch model should be appropriate for estimating the modulus of asphalt concrete. However, for this modulus to be useful in modeling the modulus of asphalt concrete, the relative proportions of the series and parallel phases must be time and temperature dependent.

Christensen et al. (2003) presented the application of the Hirsch model to asphalt concrete based on an alternate version of the modified Hirsch model shown in Figure 9, in which the relative proportion of material in parallel arrangement, called the contact volume, is not constant but varies with time and temperature. In Figures 8 and 9, the subscripts *p* and *s* denote parallel and series phases, respectively. In Figure 9, *Va* refers to the aggregate volume exclusive of the contact volume, *Vm* refers to the binder volume, and *Vv* is the air void volume.

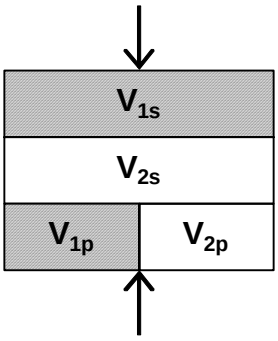

Figure 8. Hirsch Model

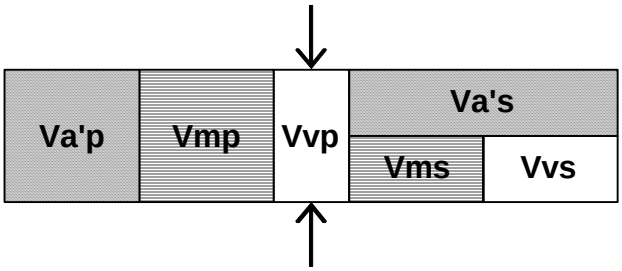

Figure 9. Alternate Version of the Modified Hirsch Model

Although the authors evaluated several alternate versions of the modified Hirsch model, the most effective was the simplest, in which the dynamic modulus of the asphalt concrete (IE*I) is directly estimated from binder modulus (G*), voids in the mineral aggregate (VMA), and voids filled with asphalt (VFA), equations (33) and (34) [Christensen et al., 2003]:

$$|E^*| = Pc\left[4{,}200{,}000\left(1-\frac{VMA}{100}\right)+3|G^*|_{binder}\left(\frac{VFA\cdot VMA}{10{,}000}\right)\right]+(1-Pc)\left[\frac{1-\frac{VMA}{100}}{4{,}200{,}000}+\frac{VMA}{VFA\cdot 3|G^*|_{binder}}\right]^{-1} \quad (33)$$

$$Pc = \frac{\left(20+\frac{VFA\cdot 3|G^*|_{binder}}{VMA}\right)^{0.58}}{650+\left(\frac{VFA\cdot 3|G^*|_{binder}}{VMA}\right)^{0.58}} \quad (34)$$

where

IE*I = dynamic modulus, psi
IG*I$_{binder}$ = binder dynamic modulus, psi
VMA= voids in the mineral aggregate, %
VFA = voids filled with asphalt, %
Pc = aggregate contact factor

In these equations, the binder modulus can be determined experimentally using the dynamic shear rheometer (DSR) or a similar device or can be estimated from one of several mathematical models. It should be at the same temperature and loading time selected for the mixture modulus, and in consistent units [Christensen et al., 2003].

Table 8 shows a summary of the database used in the development of equations (33) and (34).

The database in Table 8 was used in the initial calibration of the model. However, a subsequent evaluation of the model showed that results at extreme high and low temperatures were not always accurate. Therefore, an expanded data set was created including additional data at -9 and 129.2^{o}F (54^{o}C).

An R^2 value of 98.2 % was obtained for this model. Figure 10 shows the relationship between the predicted and measured values for IE*I.

Table 8. Summary of the Database of Mixture Modulus Data

Factor	ALF	MN/ROAD	WesTrack	Total
Design Method	Marshall	Marshall	Superpave	2
Binders	AC-5, 10, 20	AC-20	PG 64-22	8
	SBS-modified	120/150-Pen		
	PE-modified			
Aggregate Sizes and Gradations	19-mm dense	9.5-mm fine	19-mm fine	5
	37.5-mm fine		19-mm coarse	
Mixtures	7	5	6	18
Total data Points	78	59	69	206
For Complete Database				
Voids, Vol. %	5.6 to 11.2			
VMA, Vol. %	13.7 to 21.6			
VFA, Vol. %	38.7 to 68.0			
Temperature, ^{o}C	4, 21, 38			
Frequencies	0.1 and 5			
IE*I, MPa	183 to 20,900			

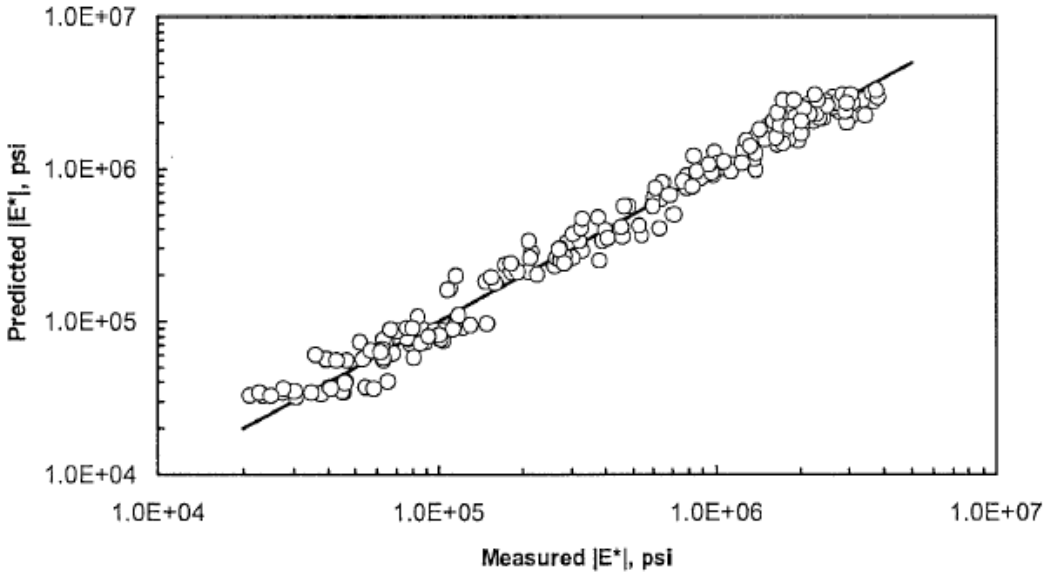

Figure 10. Predicted and Measured Values for Dynamic Modulus [Christensen et al., 2003]

5. EVALUATION OF THE DYNAMIC MODULUS PREDICTIVE EQUATIONS

Several studies have been performed in which at least part of them is dedicated to evaluating how well the equations considered in this report predict the dynamic modulus. The following is a summary containing the main findings of these studies.

5.1. University of Minnesota Study [Clyne et al., 2003]

Asphalt mixtures corresponding to four cells (21, 33, 34, and 35) at Mn/ROAD were analyzed in a study performed by the University of Minnesota [Clyne et al., 2003]. Three cells had identical mix designs except for the asphalt type (PG 58-28, PG 58-34, and PG 58-40, respectively). Cell 21 had a different design and asphalt type (Pen 120/150). Specimens were prepared in the laboratory according to NCHRP Project 9-29 from the mixtures in cells 33, 34, and 35. For the mixture from cell 21, cores were directly taken at Mn/ROAD. In addition, two different procedures were used for the mixture from cell 35; the procedure mentioned above (cored in Figure 14) and using a special device (Testquip 100-mm diameter mold) to prepare the samples where coring is not needed (compacted in Figure 14).

Table 9 shows a summary of the material properties and Table 10 the gradation for each mixture.

The dynamic modulus for each mixture was measured through laboratory tests at temperatures of -4 (-20), 14 (-10), 39.2 (4), 68 (20), 104 (40), and 129.2^{o}F (54^{o}C) and frequencies of 25, 10, 1, 0.1, and 0.01 Hz.

Dynamic modulus master curves were built for each mixture using nonlinear regression techniques to fit experimental data to a sigmoidal function, as earlier explained, solving the shift factors simultaneously with the coefficients of that function.

The dynamic modulus for each mixture was estimated using the Witczak predictive equation (see Note 7 later). Then, the predictive values were compared to the laboratory test results.

Table 9. Material Properties [Clyne et al., 2003]

Cell	21	33	34	35
Binder Type	120/150	PG 58-28	PG 58-34	PG 58-40
Polymer Modified	No	No	Yes	Yes
Sample Type	Core	Loose Mix	Loose Mix	Loose Mix
Paving Date	Jul-93	Aug-99	Aug-99	Aug-99

Table 10. Mixture Gradation [Clyne et al., 2003]

		Percent Passing			
Sieve Size, mm	Sieve Size, in.	Cell 21	Cell 33	Cell 34	Cell 35
19	3/4	100	100	100	100
16	5/8	99			
12.5	1/2	96	94	94	94
9.0	3/8	88	86	86	86
4.75	#4	70	66	66	66
2.36	#8		54	54	54
2.0	#10	58			
1.0	#20	44			
0.45	#40	26			
0.25	#80	9			
0.075	#200	4.3	4.7	4.7	4.7

Figures 11, 12, 13, and 14 show the master curve comparison between data obtained from laboratory test and the values calculated from the Witczak predictive equation for mixtures from cells 21, 33, 34, and 35 respectively. In those figures, the master curve called “Witczak 1995”, corresponds to that applying the predictive equation developed by Witczak in 1995, which is not included in this report. The master curve named “Witczak 2000” is that corresponding to equation (10) in this report (see Note 7 later).

As a result of this comparison, some observations were made [Clyne et al., 2003]:

- The predictive equation fit the data relatively well at intermediate and low temperatures for mixtures from cells 21 and 35. At high temperatures, the predictive equation tends to drift away from the test data.

- The predictive equation does not fit the test data very well for mixtures from cells 33 and 34.

- For all the mixtures, the test data are generally larger than the predictive value of dynamic modulus.

Finally, the study recommends that the Witczak predictive equation included in the 2002 Design Guide should be used with caution.

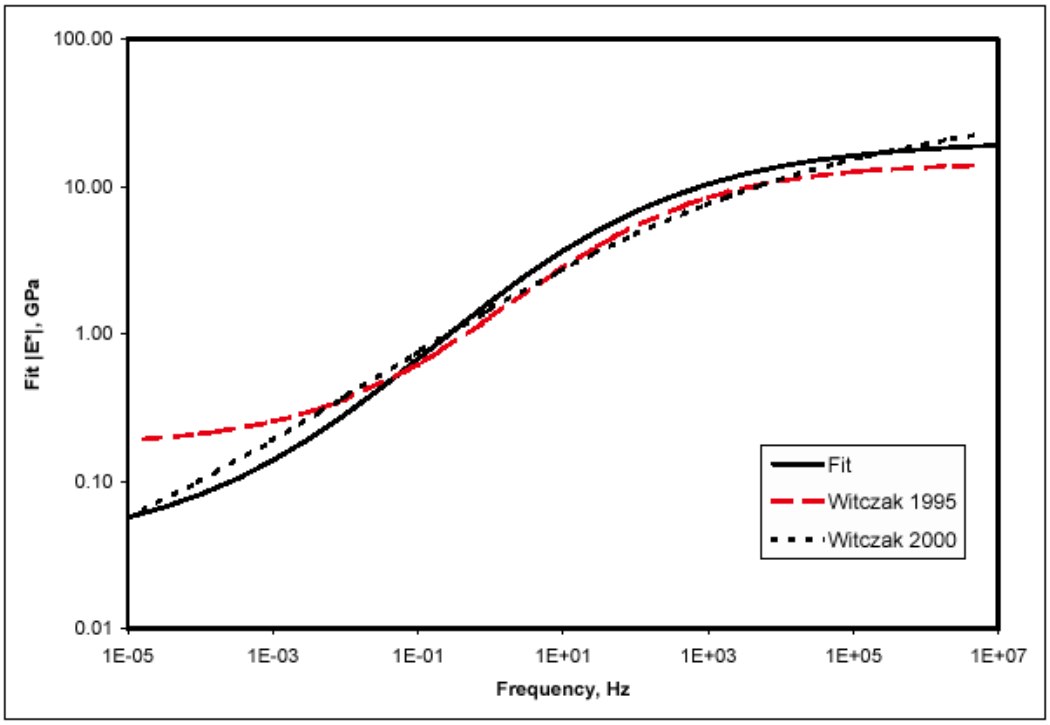

Figure 11. Master Curve Comparison (Cell 21) [Clyne et al., 2003]

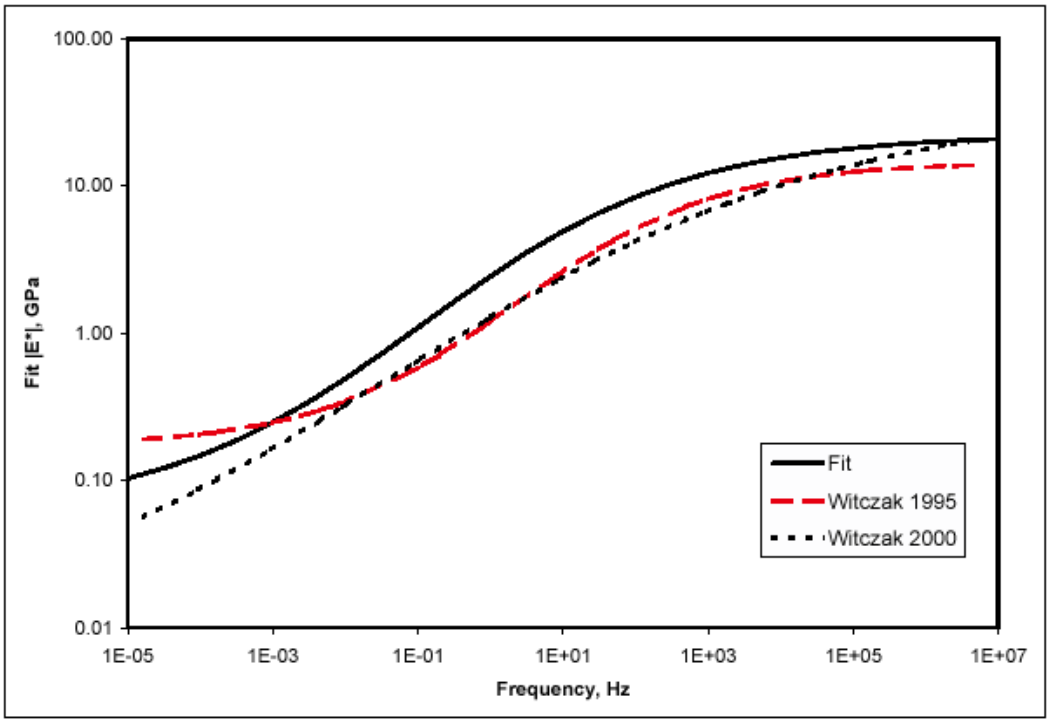

Figure 12. Master Curve Comparison (Cell 33) [Clyne et al., 2003]

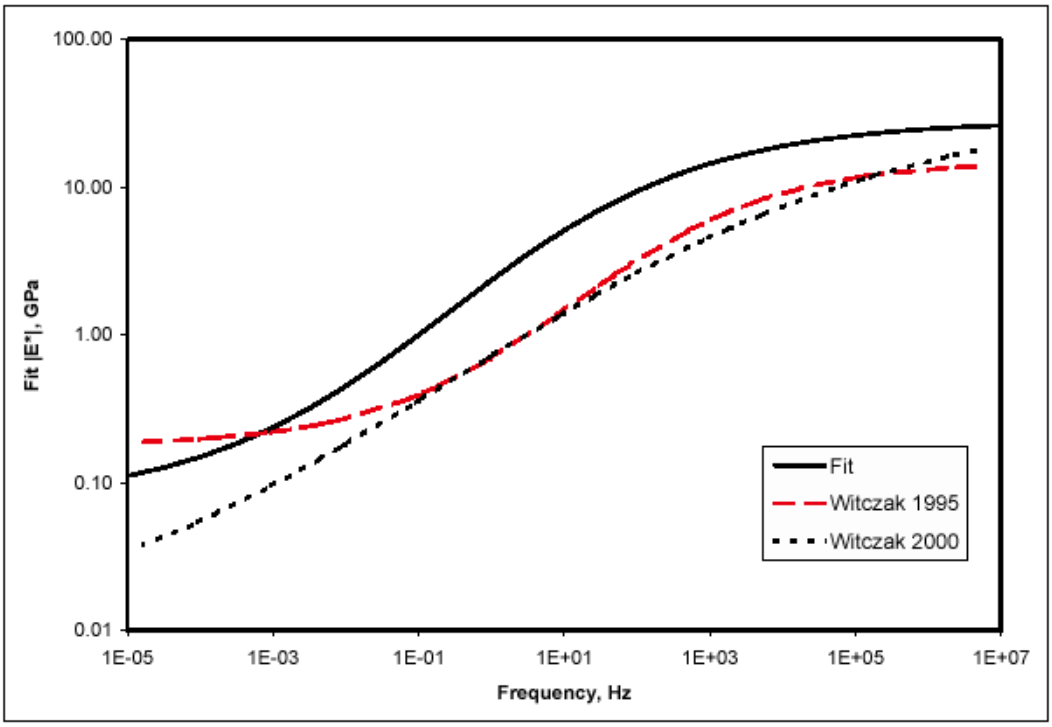

Figure 13. Master Curve Comparison (Cell 34) [Clyne et al., 2003]

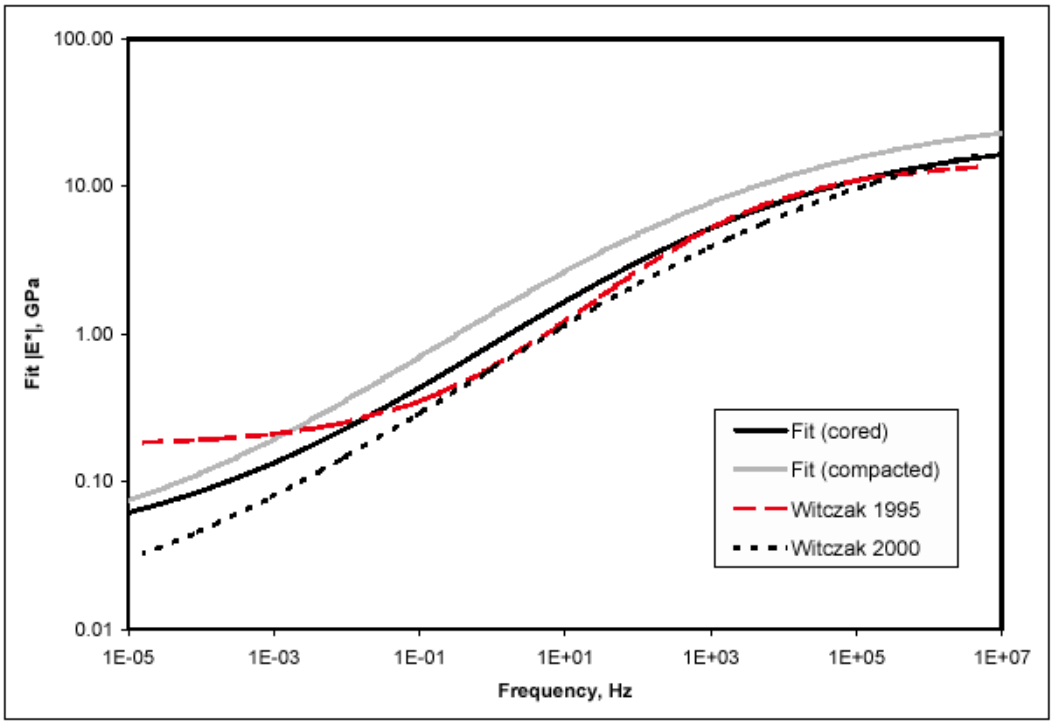

Figure 14. Master Curve Comparison (Cell 35) [Clyne et al., 2003]

[Note 7: In the reference of this study [Clyne et al., 2003], the Witczak equation (equation 2.13 in that report) was written as in Appendix CC-4 "Development of a Revised Predictive Model for the Dynamic (Complex) Modulus of Asphalt Mixtures" dated on March 1999 [2002 Design Guide, (1999)], except that the first term involving ρ_4 ($0.002841 \cdot \rho_4$) is positive in the University of Minnesota study and negative in Appendix CC-4. It is not known if that is only a typing error in the report or if the equation was really used in that form in the calculations. The effect of this error has not been quantified.]

5.2. Christensen, Pellinen and Bonaquist Study [Christensen et al., 2003]

The authors of this study, where they actually propose the Hirsch model for HMA, performed several verifications to quantify the goodness of fit of the model. Figure 15 shows a comparison of master curves built for mixture V0W1 from the Alavi and Monismith study [Alavi et al., 1994], which is useful to verify the Hirsch model. There, predicted and measured values for IE*I and phase angle as a function of reduced frequency at 104°F (40°C) are shown. It can be noted that the frequency dependence and general shape of the function for dynamic modulus as predicted by the Hirsch model is reasonable and in good agreement with experimental values.

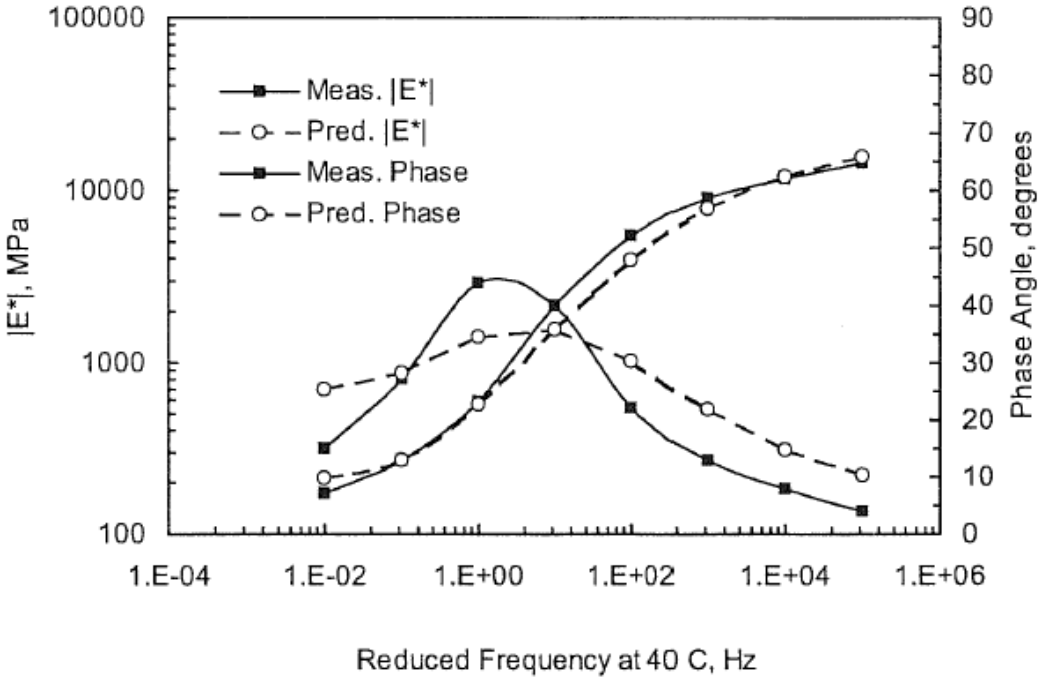

Figure 15. Master Curve for Mixture V0W1 as Reported by Alavi and Monismith, and as Predicted Using the Hirsch Model [Christensen et al., 2003]

In another verification, they predicted dynamic modulus using both the Hirsch model and the Witczak predictive equation, and compared both to the measured values reported by Alavi and Monismith [Alavi et al., 1994]. Figure 16 shows this comparison.

The values obtained with the Hirsch model are in excellent agreement, whereas those obtained with the Witczak predictive equation slightly under-predicts at higher modulus values. Although this comparison is too limited to make broad generalizations, it suggests that the Hirsch model is in general agreement with the Witczak predictive equation, and at least as accurate [Christensen et al., 2003].

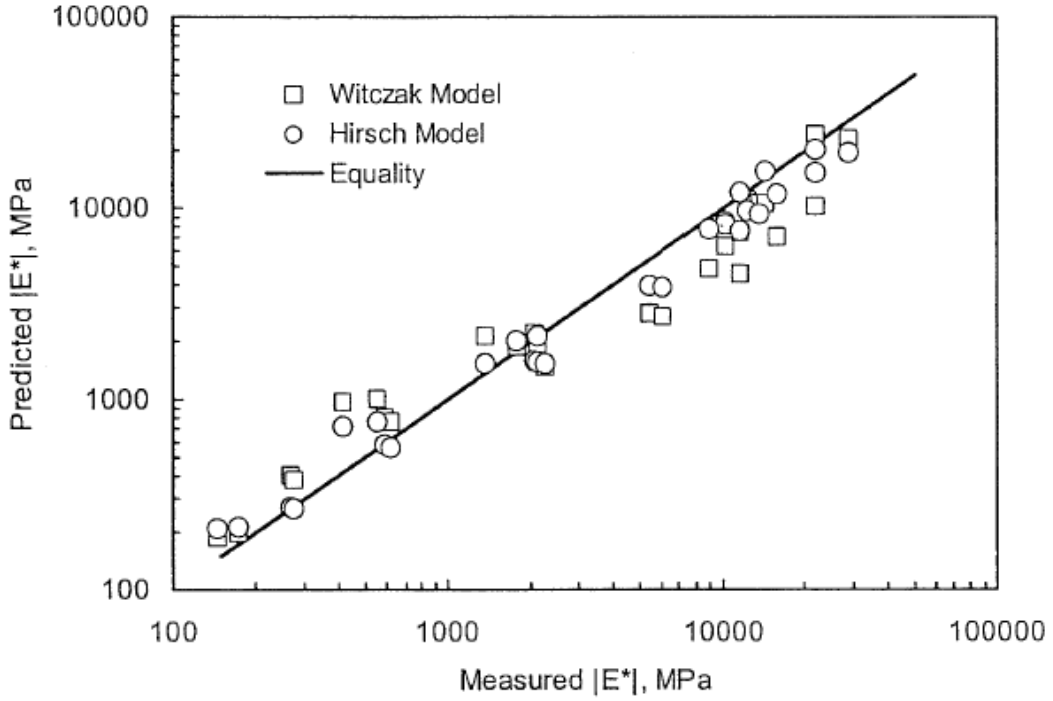

Figure 16. Predicted and Measured IE*I Values [Christensen et al., 2003]

They also used data from the NCHRP 9-19 study by Witczak and his associates to perform another comparison between the two models. The cited study included IE*I measurements on a range of mix variations based on an Arizona Department of Transportation mixture. Table 11 shows the main properties and variation of the mixture used.

Table 11. Properties of the Mixture Used in the Witczak Study

Binder	PG 64-22
Aggregate Size	25 mm
Voids, %	1.5 - 4 - 7 - 10
Binder Content, %	3.9 - 4.55 - 5.2 - 5.9

In addition to measured IE*I values, moduli were also predicted using Witczak's equation and the Hirsch model. Figure 17 shows IE*I values predicted with the Hirsch

model versus the measured values reported by Witczak and his team. According to these researchers, the standard error in this case was 41%, which is slightly better than the standard error for Witczak's equation (45%), but about the double that for the experimental error for these data (20%).

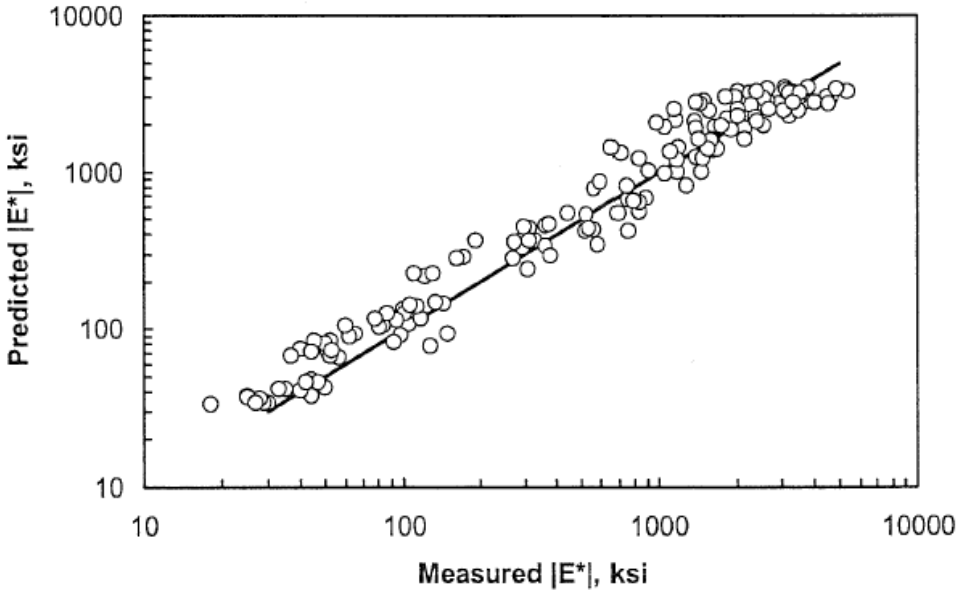

Figure 17. Predicted and Measured IE*I Values Using Data from NCHRP 9-19 Study [Christensen et al., 2003]

Figure 18 shows IE*I values predicted using the Hirsch model versus values determined with Witczak's equation.

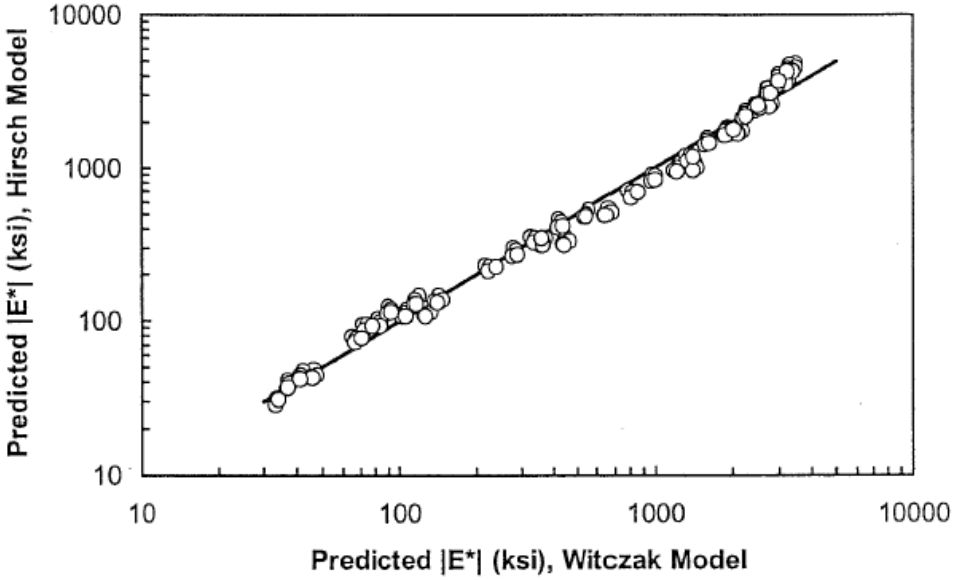

Figure 18. IE*I Values Predicted with the Hirsch Model and with Witczak's Equation Using Data from NCHRP 9-19 Study [Christensen et al., 2003]

As seen in Figure 18, the agreement between the two models is extremely close. However, such close agreement will not always occur. In this case, it is probably fortuitous and brought about by close agreement between the SHRP binder data used to develop the Hirsch model and the routine data used in Witczak's equation. Based upon the close agreement between the models and the similar standard errors compared to the measured |E*| values, it is thought that both models are of similar accuracy and in reasonably close agreement [Christensen et al., 2003].

[Note 8: In the reference of this study [Christensen et al., 2003], the Witczak equation used, although not explicitly written, is based on [2002 Design Guide, 1999].]

5.3. University of Florida Study [Birgisson et al., 2005]

This study focuses on the evaluation of the Witczak predictive equation for mixtures typical to Florida and identifying appropriate viscosity-temperature relationships to predict dynamic modulus. Dynamic modulus testing was conducted for 28 different mixtures, 22 laboratory-based mixtures (Limestone, granite and FAA) and 6 mixtures with proven field performance (SuperPave^{TM} and Heavy Vehicle Simulator (HVS) mixtures). Tables 12 and 13 list the gradations and volumetric properties for all the mixtures used, respectively. For all the mixtures, only one type of binder was used, namely PG 67-22 (AC-30), which is commonly used in Florida.

The dynamic modulus for each mixture was obtained from the average of three 102-mm diameter and 150-mm tall test specimens, prepared in a gyratory compactor mold with an inner diameter of 102-mm. This means that coring was not necessary. However, in the case of mixture WR-C1, dynamic moduli were obtained using 102-mm diameter gyratory compacted specimens as well as specimens cored out of 150-mm diameter gyratory compacted samples, in order to compare the differences in dynamic modulus for the two procedures. The tests were run on each specimen at temperatures of 50 (10), 77 (25), 86 (30), and 104^{o}F (40^{o}C) and frequencies of 16, 10, 4, and 1 Hz. Four on-specimen vertical LVDT's were used to measured the vertical deformation of each specimen.

Figure 19 shows the comparison of dynamic modulus obtained at 104^{o}F (40^{o}C) using both procedures of specimen preparation for mixture WR-C1. The differences in dynamic modulus ranged from 0.6 to 1.9 percent. In addition, the trends of the two lines cross, which implies that there is no bias due to sampling procedure, according to the authors.

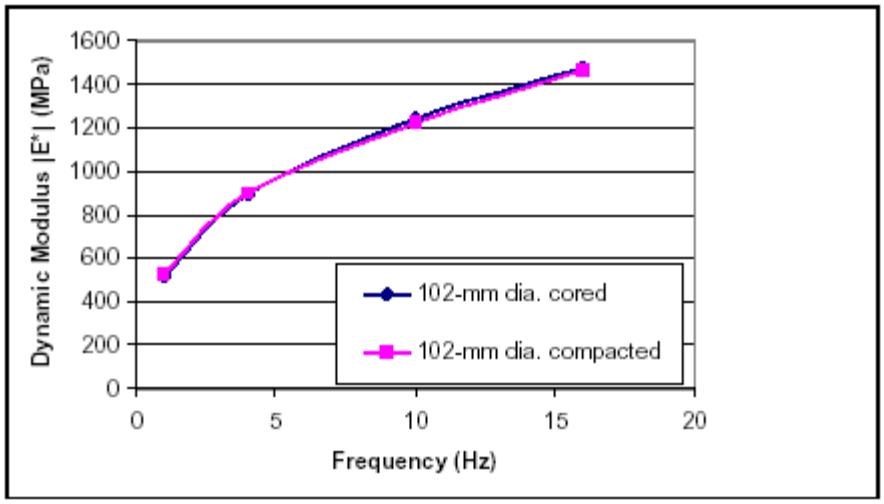

Figure 19. Comparison of IE*I for Mixture WR-C1 Using 102-mm Diameter Specimens from Cored 150-mm Diameter Gyratory Pills vs. Compacted 102-mm Gyratory Pills. (Test Temp.: 104°F (40°C)) [Birgisson et al., 2005]

Table 12. Gradation and N_{design} for Study Mixtures [Modified, Birgisson et al., 2005]

Mixtures		Sieve Size, mm											N_{design}
		25 (1")	19 (3/4")	12.5 (1/2")	9.5 (3/8")	4.75 (#4)	2.36 (#8)	1.18 (#16)	0.6 (#30)	0.3 (#50)	0.15 (#100)	0.075 (#200)	
Coarse FAA	CG	100	100	97.4	88.8	54.8	30.4	20.5	14.8	11.0	7.2	5.5	109
	RB	100	100	97.5	89.5	57.6	31.6	21.1	15.1	11.0	7.0	5.2	109
	CH	100	100	97.5	89.4	56.9	31.3	20.9	15.0	11.0	7.1	5.2	109
	CAL	100	100	97.5	89.3	56.5	31.2	20.9	15.0	11.0	7.1	5.3	109
Fine FAA	CG	100	100	97.4	83.8	66.0	49.4	33.3	21.9	13.9	7.0	4.5	109
	RB	100	100	95.1	85.0	68.5	51.2	34.2	22.4	14.0	6.9	4.3	109
	CAL	100	100	94.9	84.6	67.6	50.6	33.9	22.2	14.0	6.9	4.3	109
	CH	100	100	95.0	84.7	67.9	50.8	34.0	22.2	14.0	6.9	4.3	109
SuperPave™ Field Monitoring	P1	100	100	100.0	99.0	64.0	40.0	29.0	21.0	14.0	8.0	5.1	96
	P2	100	100	98.0	89.0	45.0	28.0	22.0	17.0	12.0	7.0	4.9	96
	P3	100	100	94.0	90.0	67.0	34.0	25.0	18.0	13.0	7.0	4.4	96
	P7	100	100	95.0	88.0	70.0	57.0	41.0	30.0	19.0	9.0	4.2	84
	P8	100	100	94.0	90.0	59.0	32.0	25.0	18.0	12.0	7.0	4.5	96
Limestone	WR-C1	100	100	97.4	90.0	60.2	33.1	20.3	14.7	10.8	7.6	4.8	109
	WR-C2	100	100	91.1	73.5	47.1	29.6	20.2	14.4	10.4	6.7	4.8	109
	WR-C3	100	100	97.6	89.3	57.4	36.4	24.0	17.7	12.9	9.0	6.3	109
	WR-F1	100	100	95.5	85.1	69.3	52.7	34.0	22.9	15.3	9.6	4.8	109
	WR-F2	100	100	90.8	78.0	61.3	44.1	34.7	23.6	15.7	8.9	6.3	109
	WR-F4	100	100	95.5	85.1	69.3	52.7	40.0	29.0	20.0	12.0	6.3	109
	WR-F5	100	100	95.5	85.1	61.3	52.7	34.0	22.9	15.3	9.6	4.8	109
	WR-F6	100	100	95.5	85.1	69.3	44.4	34.7	23.6	15.7	9.1	6.3	109
Granite	GA-C1	100	100	97.4	89.0	55.4	29.6	19.2	13.2	9.2	5.3	3.4	109
	GA-C2	100	100	90.9	72.9	45.9	28.1	18.9	13.2	9.2	5.6	3.9	109
	GA-C3	100	100	97.3	89.5	55.4	33.9	23.0	16.0	11.2	6.8	4.7	109
	GA-F1	100	100	94.7	84.0	66.4	49.2	32.7	21.0	12.9	5.9	3.3	109
	GA-F2	100	100	90.5	77.4	60.3	43.2	34.0	23.0	15.3	8.7	5.4	109
	GA-C4	100	100	94.6	85.1	65.1	34.8	26.0	18.1	12.5	7.7	5.8	109
HVS	67-22	100	100	97.4	95.7	76.3	54.2	44.1	37.8	23.7	8.9	4.2	100

Table 13. Volumetric Properties for Study Mixtures [Modified, Birgisson et al., 2005]

Mixtures		Volumetric Properties											
		G_{mm}	G_b	G_{mb}	P_b	G_{sb}	G_{se}	P_{ba}	P_{be}	VMA (%)	Va (%)	VFA (%)	D/A
Coarse FAA	CG	2.386	1.035	2.295	6.50	2.418	2.625	1.20	3.30	11.2	3.8	66.5	1.7
	RB	2.393	1.035	2.300	6.25	2.576	2.622	1.20	5.60	16.1	3.9	77.3	0.9
	CH	2.394	1.035	2.289	5.70	2.535	2.601	1.00	4.70	14.8	4.4	70.6	1.1
	CAL	2.454	1.035	2.353	5.80	2.540	2.680	1.20	3.70	12.6	4.1	67.4	1.4
Fine FAA	CG	2.381	1.035	2.288	6.70	2.403	2.630	1.20	3.20	11.2	3.9	65.2	1.4
	RB	2.416	1.035	2.327	5.90	2.599	2.637	1.20	5.70	16.0	3.7	76.8	0.7
	CAL	2.480	1.035	2.396	5.30	2.524	2.691	1.20	3.40	10.5	3.8	63.8	1.3
	CH	2.407	1.035	2.315	5.50	2.549	2.608	1.00	4.80	14.1	3.7	73.7	0.9
SuperPave™ Field Monitoring	P1	2.509	1.035	2.407	5.50	2.691	2.736	0.60	4.90	15.5	4.1	73.7	1.2
	P2	2.523	1.035	2.445	5.00	2.694	2.725	0.40	4.50	14.8	4.4	70.6	0.6
	P3	2.216	1.035	2.122	8.30	2.325	2.475	2.70	5.70	16.4	4.2	74.1	0.6
	P7	2.334	1.035	2.229	6.10	2.470	2.573	1.70	5.20	16.0	4.5	71.9	0.6
	P8	2.382	1.035	2.284	6.00	2.503	2.598	1.40	4.50	14.0	3.9	72.4	1.0
Limestone	WR-C1	2.328	1.035	2.235	6.50	2.469	2.549	1.10	5.30	15.4	4.0	74.0	1.0
	WR-C2	2.347	1.035	2.255	5.80	2.465	2.545	1.30	4.60	13.8	3.9	71.6	0.8
	WR-C3	2.349	1.035	2.254	5.30	2.474	2.528	0.90	4.50	13.6	4.0	70.2	1.2
	WR-F1	2.338	1.035	2.244	6.30	2.488	2.554	1.10	5.30	15.6	4.0	74.2	0.8
	WR-F2	2.375	1.035	2.281	5.40	2.489	2.565	1.20	4.20	13.2	3.9	70.1	1.4
	WR-F4	2.368	1.035	2.272	5.70	2.491	2.568	1.20	4.50	14.0	4.0	71.2	1.3
	WR-F5	2.326	1.035	2.233	6.70	2.485	2.555	1.20	5.60	16.2	4.0	75.0	0.8
	WR-F6	2.341	1.035	2.244	6.10	2.489	2.559	1.00	5.20	15.4	4.2	72.8	1.1
Granite	GA-C1	2.442	1.035	2.442	6.63	2.687	2.710	0.37	6.32	18.5	4.0	78.5	0.6
	GA-C2	2.500	1.035	2.399	5.26	2.687	2.719	0.43	4.85	15.4	4.0	73.9	0.8
	GA-C3	2.492	1.035	2.391	5.25	2.686	2.709	0.31	4.96	15.7	4.1	74.2	0.9
	GA-F1	2.473	1.035	2.473	5.68	2.686	2.706	0.28	5.42	16.6	4.0	75.9	0.6
	GA-F2	2.532	1.035	2.433	4.56	2.687	2.725	0.53	4.06	13.6	3.9	71.2	1.2
	GA-C4	2.505	1.035	2.404	5.14	2.687	2.720	0.46	4.70	15.1	4.0	73.3	1.2
HVS	67-22	2.267	1.035	2.202	7.90	2.346	2.525	3.10	5.04	13.6	3.1	78.9	0.8

Viscosity is the input that represents the binder properties in the Witczak predictive equation. Three procedures to obtain binder viscosity, and consequently A and VTS parameters, were used in this study: 1) Brookfield rotational viscometer at 140.9 (60.5), 159.3 (70.7), and 177.3°F (80.7°C) (after Rolling Thin Film Oven, RTFO), by which viscosity is obtained directly; 2) Dynamic Shear Rheometer (DSR) tests at 86 (30) and 104°F (40°C) (after RTFO) and frequency of 10 radians per second and applying equation (19) presented earlier; and 3) recommended viscosity values by Witczak and Fonseca for "mixture/laydown" conditions [Witczak and Fonseca, 1996].

Table 14 presents A and VTS parameters obtained from the three procedures mentioned above. Using these parameters and equation (17), viscosity at 50 (10), 77 (25), 86 (30) and 104°F (40°C) were calculated to use as inputs in the Witczak predictive equation.

Figures 20, 21 and 22 show the comparisons between measured and predicted dynamic moduli obtained at the different temperatures and frequencies studied for the three A-VTS procedures used. The relative quality of the predictions was evaluated performing a linear regression with zero intercept, which is also shown in each plot. The closer the slope of the regression to unity, the less of a bias is represented in the prediction. A high R^2 indicates a good fit, whereas a low R^2 represents a poor fit.

Table 14. A and VTS Parameters for RTFO Aged PG 67-22 (AC-30) Asphalt and Mix/Laydown Conditions Suggested by Witczak and Fonseca [Modified, Birgisson et al., 2005]

Parameter	From Brookfield Results	From DSR Results	From Mix/Laydown Condition Suggested by Witczak and Fonseca
A	10.407	9.0824	10.6768
VTS	-3.4655	-3.0165	-3.56455

From the analysis of Figures 20 through 22, it is concluded that the predictions based on the Brookfield measurements presented the lowest bias and the highest R^2, although similar results were obtained using the mix/laydown values suggested by Witczak and Fonseca. The case using DSR measurements resulted in a slope clearly higher than unity and also showed the lowest R^2. It was also noted that the modulus predictions at higher temperatures (lower modulus values) generally were closer to the measured values for all the three cases studied than the predictions at lower temperatures. According to the authors, two reasons may explain this bias: 1) the database used to develop the predictive equation was biased toward mixtures tested at higher temperatures, or 2) the underlying sigmoidal function used in the Witczak equation may produce slightly biased dynamic modulus values at lower temperatures for the mixtures included in this study.

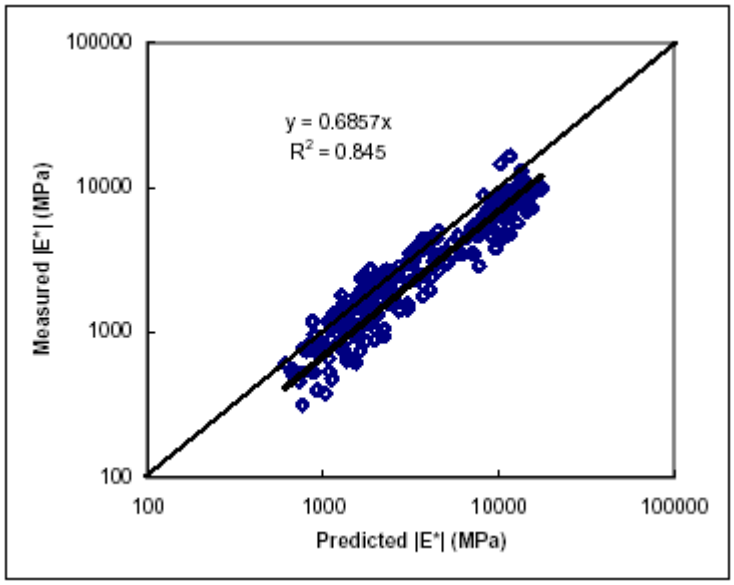

Figure 20. Measured Values vs. Predicted Values of IE*I on log-log Scale (RTFO Condition, Viscosity from Brookfield Test) [Birgisson et al., 2005]

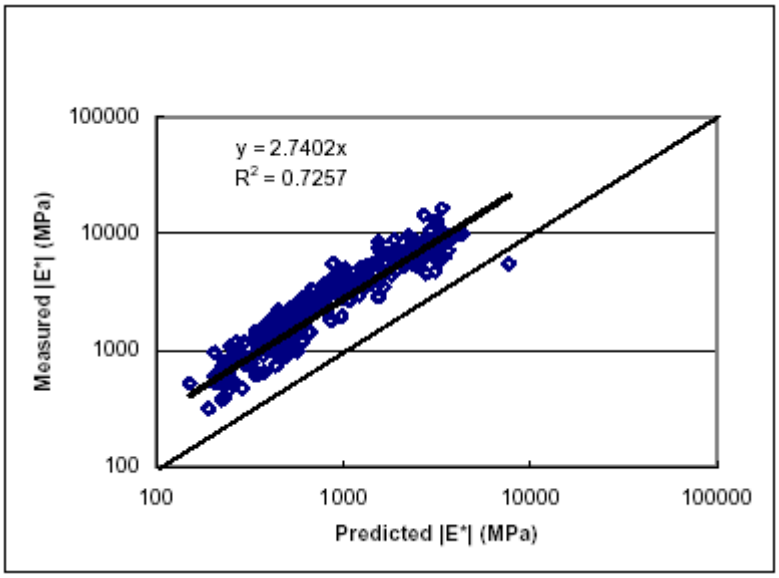

Figure 21. Measured Values vs. Predicted Values of IE*I on log-log Scale (RTFO Condition, Viscosity from DSR Test) [Birgisson et al., 2005]

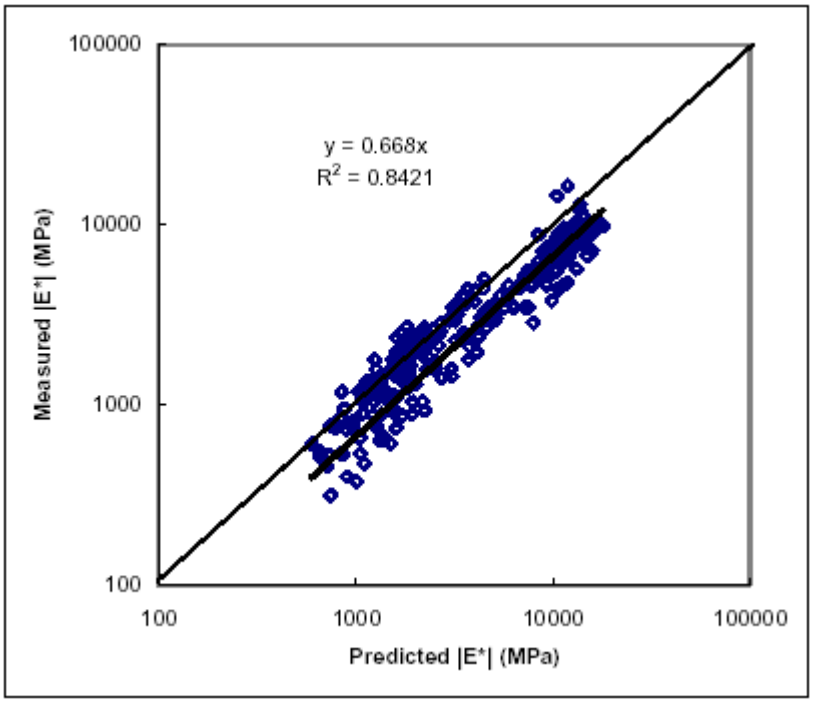

Figure 22. Measured Values vs. Predicted Values of IE*I on log-log Scale (Mix/Laydown condition) [Birgisson et al., 2005]

The authors show that the relationships presented in Figures 20 through 22 can be useful to correct the bias in the dynamic modulus predictions for typical mixtures used in

Florida. As an example based on Figure 20, the predictive dynamic modulus can be corrected using equation (35):

$$IE^*I_{measured} = 0.6857 \cdot IE^*I_{predicted} \quad (35)$$

Equation (35) means that by multiplying the predictive value by 0.6857, the observed bias in the predictive dynamic modulus can be adjusted.

Finally, they conclude that when testing results are not available, reliable first order dynamic modulus estimates for mixtures typical to Florida can be obtained using the Witczak predictive equation, along with a correction factor obtained from the testing of local mixtures.

[Note 9: In the reference of this study [Birgisson et al., 2005], the Witczak equation used is based on [2002 Design Guide, 1999]]

5.4. North Carolina State University Study [Kim et al., 2005]

The prediction accuracies of the Witczak equation and the Hirsch model were determined comparing the measured and predictive dynamic modulus values in 41 mixtures and 7 asphalt binders commonly used by the North Carolina Department of Transportation (NCDOT). Information about the mixtures tested in this study are presented in Table 15 where they are classified based on factors such as traffic level and gradation which allow grouping of similar mixtures.

To determine the binder-related input for the Hirsch model, IG*I values of RTFO aged binder were obtained from DSR tests performed at five different temperatures (60.8, 71.6, 82.4, 104, and 129.2^{o}F (16, 22, 28, 40, and 54^{o}C)) and eight different frequencies (15, 10, 5, 1, 0.5, 0.1, 0.05, and 0.01 Hz). The Witczak predictive equation, in turn, needs viscosity input values to take into account the binder effect. Then, rotational viscometer tests, on RTFO aged binder, were performed at four different temperatures (176, 212, 275, and 347^{o}F (80, 100, 135, and 175^{o}C)) and penetration tests at 59 and 77^{o}F (15 and 25^{o}C). The Penetration values were converted into viscosity using equation (18) presented earlier. Viscosity data were used later to determine A and VTS parameters using equation (17).

The dynamic moduli were obtained averaging three 100-mm diameter and 150-mm tall test specimens, cored and cut from gyratory specimens (150-mm diameter 178-mm tall), for each of the 41 mixtures. Eight different frequencies were used on each specimen (25, 10, 5, 1, 0.5, 0.1, 0.05, and 0.01 Hz). Approximately half of the mixtures were tested at 14, 50, and 95^{o}F (-10, 10, and 35^{o}C) using a reduced test protocol. The remaining mixtures were also tested at the additional temperature of 129.2^{o}F (54^{o}C), because the authors deemed it necessary as the testing progressed. Each test was performed applying a load level such that the obtained strain was between 50 and 75 μstrain. Four loose-core type LDVT's were used to measure the vertical deformation of each specimen.

Table 15. Information of All the Mixtures Tested [Kim et al., 2005]

Mix ID	Aggregate	Aggregate Source	Asphalt Source	Asphalt	% AC
S[a]9.5[b]A[c]-Fine[d]	Granite	Charlotte, NC	Citgo – Wilmington, NC	PG 64-22	6.4
S9.5A-Fine	Limestone	Castle Hayne, NC	Citgo – Wilmington, NC	PG 64-22	6.7
S9.5A-Coarse	Granite	Morganton, NC	AA* – Inman, SC	PG 64-22	5.8
S9.5B-Fine 0	Granite	Morganton, NC	AA* – Inman, SC	PG 64-22	6.3
S9.5B-Fine 1	Granite	Charlotte, NC	Citgo – Wilmington, NC	PG 64-22	5.8
S9.5B-Fine 2	Granite	Garner, NC	Citgo – Wilmington, NC	PG 64-22	5.5
S9.5B-Fine 3	Granite	Garner, NC	Citgo – Wilmington, NC	PG 64-22	5.6
S9.5B-Fine 4	Granite	Garner, NC	Citgo – Wilmington, NC	PG 64-22	5.7
S9.5B-Fine	Limestone	Castle Hayne, NC	Citgo – Wilmington, NC	PG 64-22	6.2
S9.5B-Coarse	Granite	Haw River, NC	Citgo – Wilmington, NC	PG 64-22	5.9
S9.5C-Fine 0	Granite	Garner, NC	Citgo – Wilmington, NC	PG 70-22	5.0
S9.5C-Fine 1	Granite	Garner, NC	Citgo – Wilmington, NC	PG 70-22	5.0
S9.5C-Fine 2	Granite	Garner, NC	Citgo – Wilmington, NC	PG 70-22	5.2
S9.5C-Fine 3	Granite	Garner, NC	Citgo – Wilmington, NC	PG 64-22	5.9
S9.5C-Fine	Limestone	Castle Hayne, NC	Citgo – Wilmington, NC	PG 70-22	6.7
S9.5C-Coarse	Granite	Holly Springs, NC	Citgo – Wilmington, NC	PG 70-22	5.3
S12.5B-Fine	Granite	Holly Springs, NC	Citgo – Wilmington, NC	PG 64-22	5.3
S12.5B-Coarse	Granite	Haw River, NC	Citgo – Wilmington, NC	PG 64-22	5.5
S12.5C-Fine	Granite	Concord, NC	Citgo – Wilmington, NC	PG 70-22	5.0
S12.5C-Fine	Limestone	Castle Hayne, NC	Citgo – Wilmington, NC	PG 70-22	6.7
S12.5D-Fine	Granite	Concord, NC	AA* – Salisbury, NC	PG 76-22	4.7
S12.5D-Coarse	Granite	Concord, NC	Citgo – Wilmington, NC	PG 70-22	5.0
I19.0B-Fine 0	Granite	Garner, NC	Citgo – Wilmington, NC	PG 64-22	5.4
I19.0B-Fine 1	Granite	Charlotte, NC	Citgo – Wilmington, NC	PG 64-22	4.3
I19.0B-Fine 2	Granite	Garner, NC	Citgo – Wilmington, NC	PG 64-22	4.4
I19.0B-Fine 3	Granite	Garner, NC	Citgo – Wilmington, NC	PG 64-22	4.5
I19.0B-Fine	Limestone	Castle Hayne, NC	Citgo – Wilmington, NC	PG 64-22	5.1
I19.0B-Coarse	Granite	Haw River, NC	El Paso – Apex, NC	PG 64-22	5.0
I19.0B-Coarse	Limestone	Castle Hayne, NC	Citgo – Wilmington, NC	PG 64-22	5.2
I19.0C-Fine	Granite	Concord, NC	El Paso – Charlotte, NC	PG 64-22	4.8
I19.0C-Fine	Limestone	Castle Hayne, NC	Citgo – Wilmington, NC	PG 64-22	4.9
I19.0C-Coarse	Granite	Garner, NC	Citgo – Wilmington, NC	PG 64-22	4.7
I19.0D-Fine	Granite	Concord, NC	AA* – Salisbury, NC	PG 70-22	4.1
I19.0D-Coarse	Granite	Charlotte, NC	Citgo – Wilmington, NC	PG 70-22	4.3
B25.0B-Fine	Granite	Garner, NC	Citgo – Wilmington, NC	PG 64-22	4.2
B25.0B-Fine	Limestone	Castle Hayne, NC	Citgo – Wilmington, NC	PG 64-22	5.0
B25.0B-Coarse	Granite	Holly Springs, NC	Citgo – Wilmington, NC	PG 64-22	4.5
B25.0B-Coarse	Limestone	Castle Hayne, NC	Citgo – Wilmington, NC	PG 64-22	4.2
B25.0C-Fine	Granite	Concord, NC	El Paso – Charlotte, NC	PG 64-22	4.4
B25.0C-Fine	Limestone	Castle Hayne, NC	Citgo – Wilmington, NC	PG 64-22	5.1
B25.0C-Coarse	Granite	Haw River, NC	Citgo – Wilmington, NC	PG 64-22	4.0

[a]S: Surface mix; I: Intermediate mix; B: Base mix
[b]Superpave mix designation (Nominal Maximum Aggregate Size)
[c]Traffic volume indicator (million ESALS): A: less than 0.3; B: less than 3; C: 3 to 10; D: over 30
[d]Gradation: Fine or Coarse
*AA: Associated Asphalt

To make conclusions about aggregate source, PG grade and asphalt source, three different groups of mixtures were selected from Table 15: S9.5B-Fine (five mixtures,

from 0 to 4), S9.5C-Fine (four mixtures, from 0 to 3), and I19.0B-Fine (four mixtures, from 0 to 3).

Master curves for S9.5B-Fine mixtures in Figures 23 and 24 may indicate that the aggregate source has less impact on IE*I and that the binder source has a greater impact on IE*I. However, the binder source effect is considered not significant when compared to other binder variables.

Figures 25 and 26 show the master curves for S9.5C-Fine mixtures. Taking into account the properties of those mixtures in Table 15, the authors infer that the observed differences in the master curves, could be attributed to the binder grade or asphalt content, but is likely a combination of both.

Master curves for I19.0B-Fine mixtures in Figures 27 and 28, seem to show that a significantly higher asphalt content in replicate “0” (5.4%) than in the other mixtures (4.3 to 4.5%), is the principal reason for the lower modulus exhibited at low reduced frequencies.

Although the authors found meaningful observations on the effect of some mixture variables, using the graphical method presented above, they acknowledge the need for a comprehensive statistical analysis, which is not included in their report.

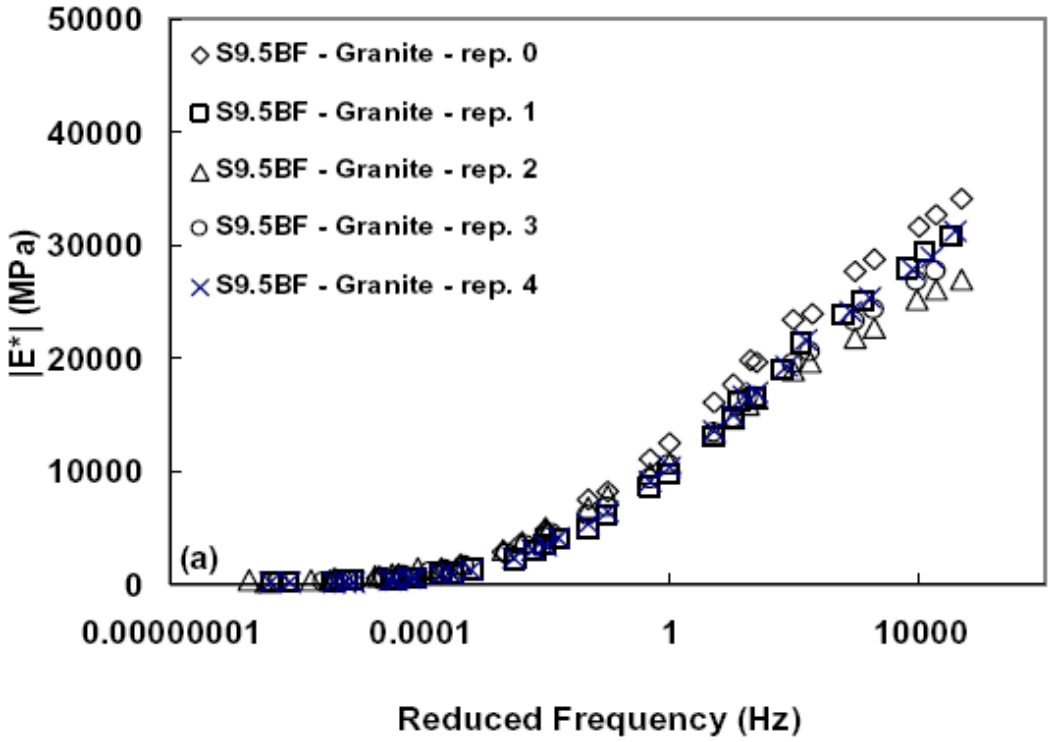

Figure 23. Master Curves for S9.5B-Fine Mixtures: Semi-log Scale [Kim et al., 2005]

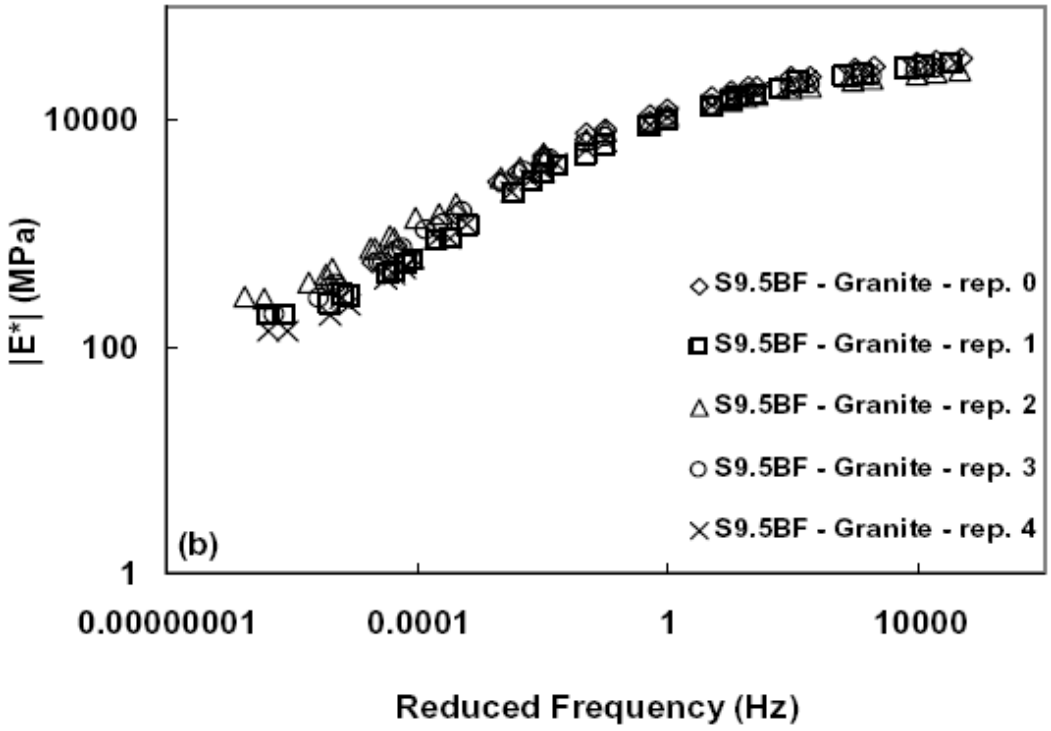

Figure 24. Master Curves for S9.5B-Fine Mixtures: log-log Scale [Kim et al., 2005]

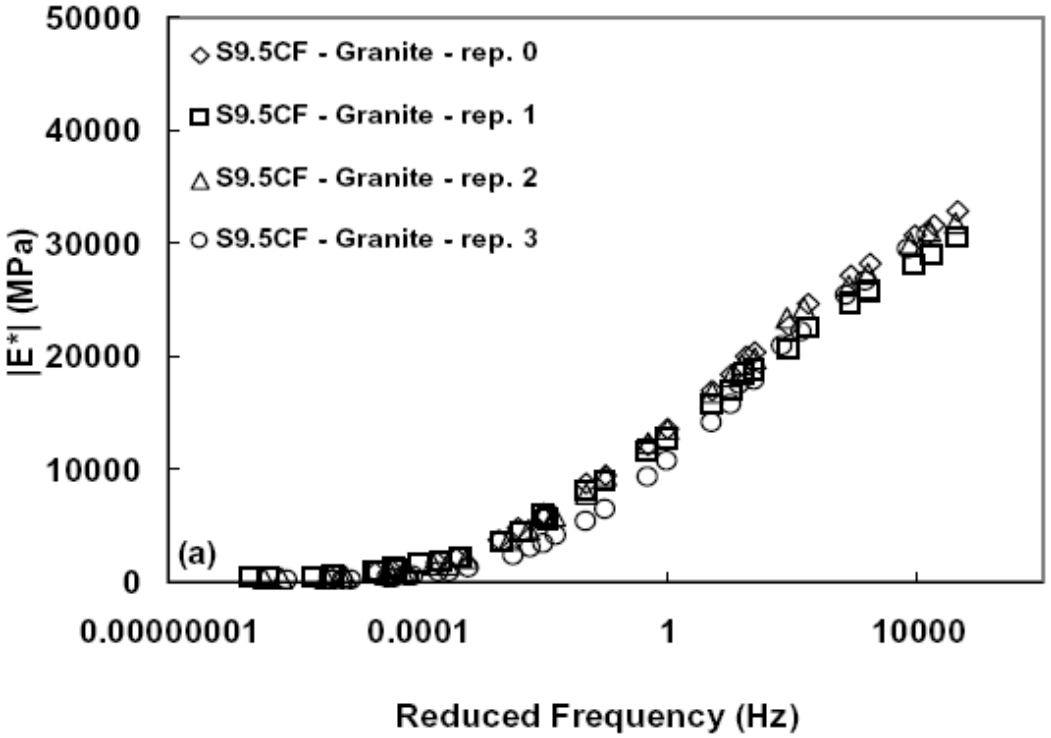

Figure 25. Master Curves for S9.5C-Fine Mixtures: Semi-log Scale [Kim et al., 2005]

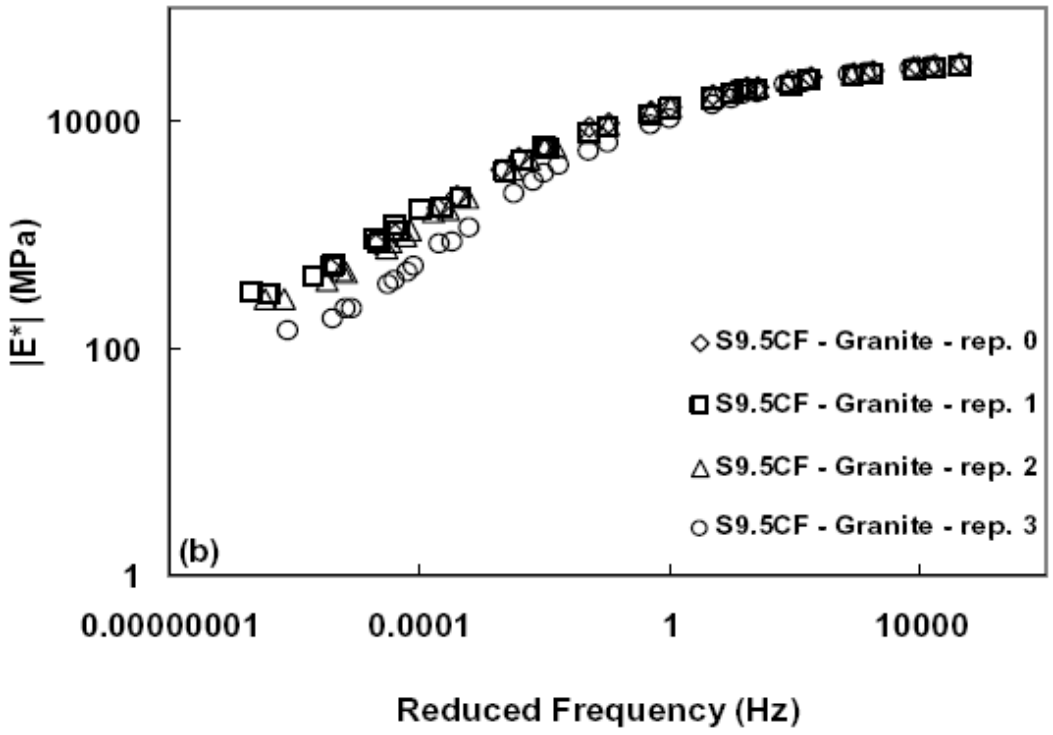

Figure 26. Master Curves for S9.5C-Fine Mixtures: log-log Scale [Kim et al., 2005]

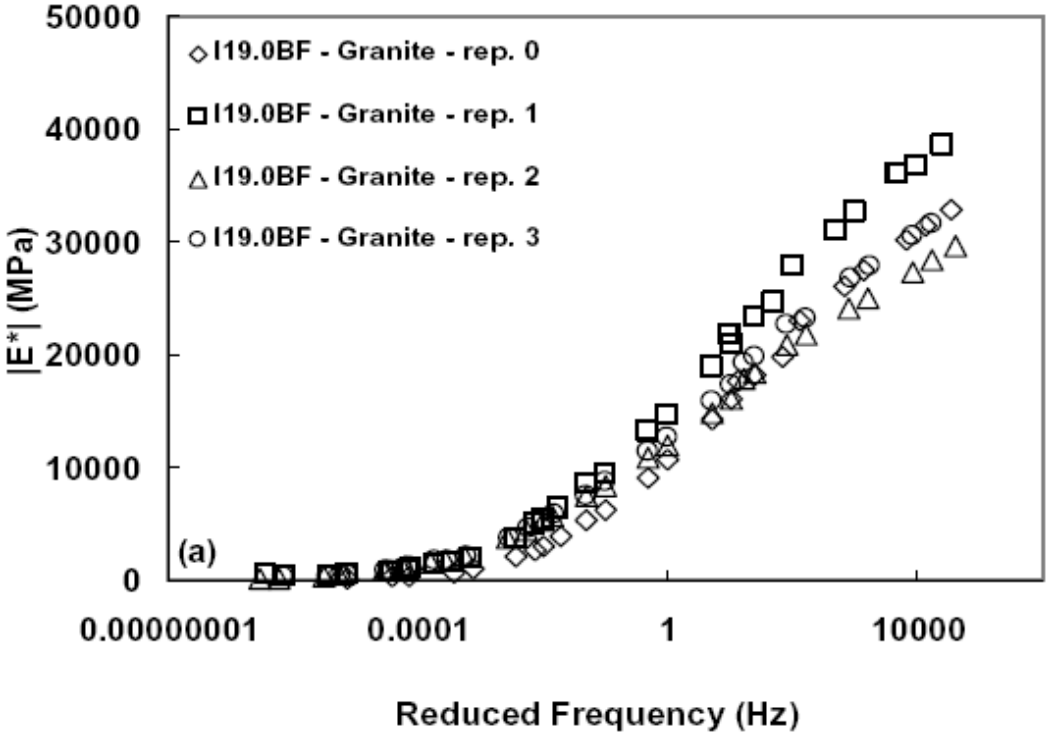

Figure 27. Master Curves for I19.0B-Fine Mixtures: Semi-log Scale [Kim et al., 2005]

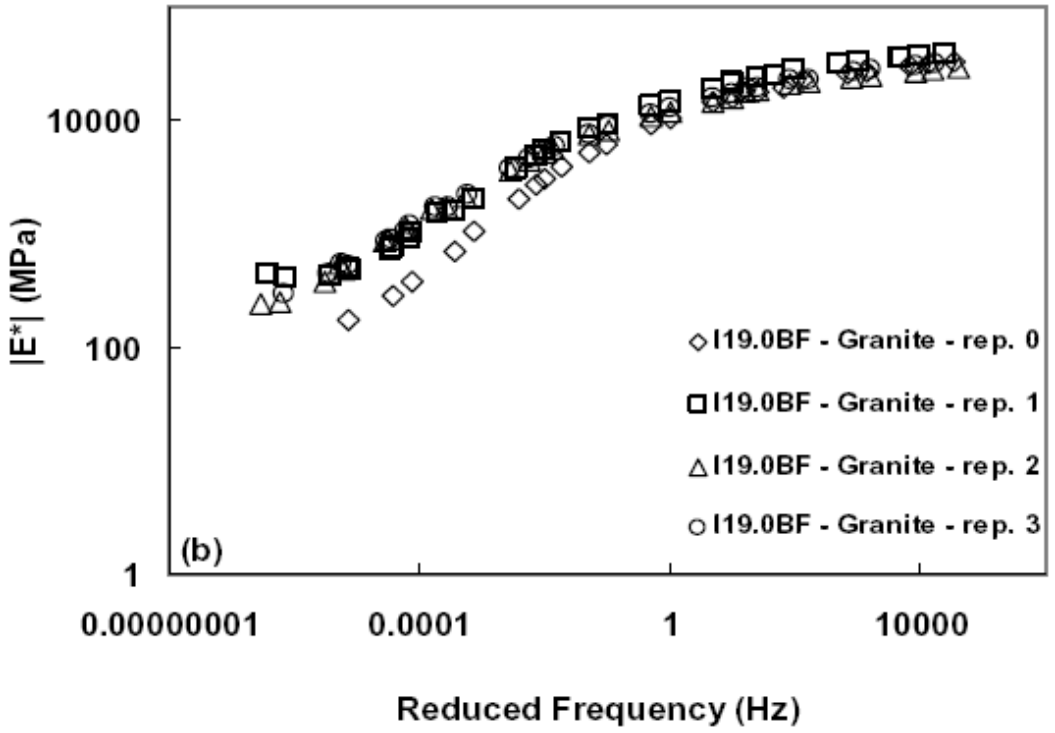

Figure 28. Master Curves for I19.0B-Fine Mixtures: log-log Scale [Kim et al., 2005]

The accuracy of the Witczak and Hirsch predictive models was determined by calculating the percent of error (the difference between the measured and predicted IE*I divided by the measured IE*I) at each frequency and temperature combination and then averaging for different frequencies at the same temperature for each mixture. The resulting percent of error values were then grouped in the following six ranges: 1) %e<5, 2) 5<%e<15, 3) 15<%e<25, 4) 25<%e<35, 5) 35<%e<45, and 6) %e>45 % of error. Figures 29 and 30 show the summary of the percent of error found for the Witczak and Hirsch models, respectively.

As seen in Figure 30, the Hirsch model was evaluated only at three temperatures compared with the four used with the Witczak equation in Figure 29. The reason explained by the authors is that the Hirsch model was developed within the range from 39.2 to 100.4^{o}F (4 to 38^{o}C). Thus, measured data at 14 and 130^{o}F (-10 and 54.4^{o}C) were outside the temperature range in which the model is applicable. On the other hand, the lowest temperature the DSR could handle during the study was 60.8^{o}F (16^{o}C), so they extrapolated the binder data for the model at 50^{o}F (10^{o}C). Consequently, values for 50, 95, and 130^{o}F (10, 35 and 54.4^{o}C) are presented for the Hirsch model, but only 95^{o}F (35^{o}C) accomplishes the requirements of the model. They also remark that the Hirsch model was developed with air voids data in the range from 5.6 to 11.2%, whereas all the data used in this study have air voids of 4±0.5%.

From Figure 29, the authors infer that the Witczak equation predicts better at cooler temperatures than at warmer temperatures. The Hirsch model, in Figure 30, showed a

similar behavior as the Witczak equation at 95 and 130°F (35 and 54.4°C), but at 50°F (10°C) its performance was very poor. The authors attribute this poorer prediction of the Hirsch model to the fact that binder data at 50°F (10°C) were extrapolated instead of directly measured.

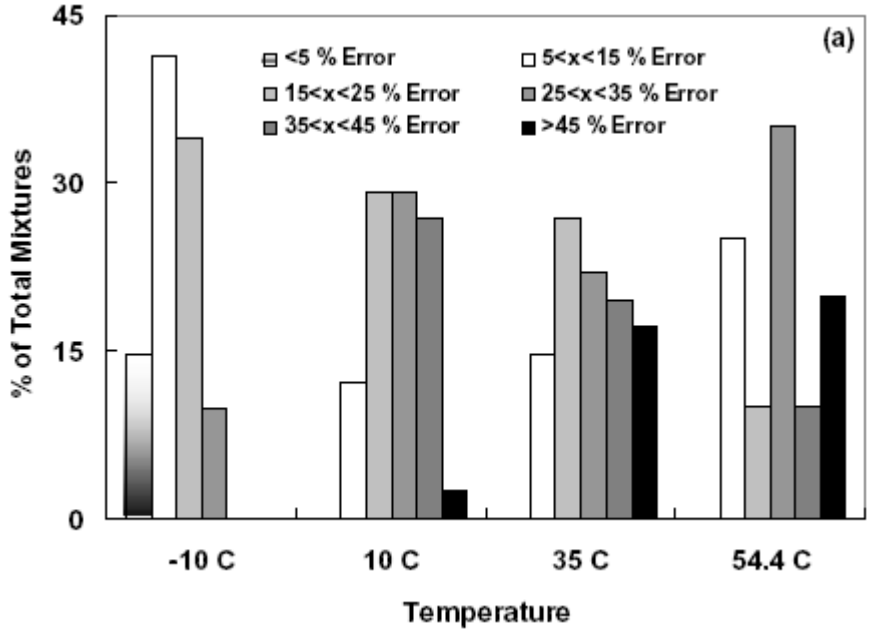

Figure 29. Summary of % of Error in IE*I for Witczak Equation [Kim et al., 2005]

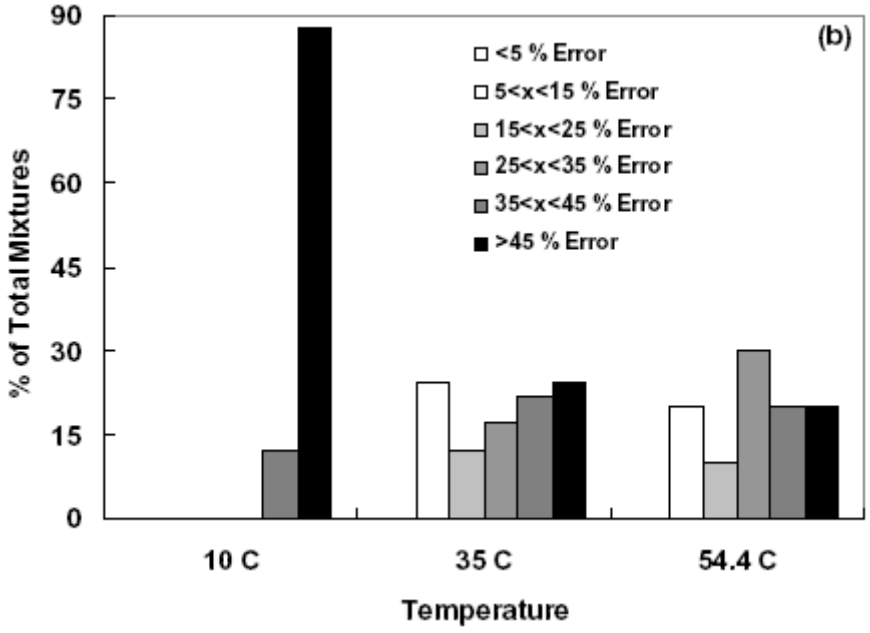

Figure 30. Summary of % of Error in IE*I for Hirsch Model [Kim et al., 2005]

Finally, in Figures 31 and 32 they illustrate a relatively good prediction, graph (a) and (b) for S9.5B-Fine replicate 3 and a relatively poor prediction, graph (c) and (d) for I19.0B-Fine replicate 1, when using the Witczak predictive equation. In those figures is also seen the poorer prediction of the Hirsch model at 50^{o}F (10^{o}C) (clearly under-predicts).

[Note 10: In this study, equation (18) is used to convert penetration into viscosity. They defined "η" as the viscosity in centipoises. However, in the original source of the equation [Mirza and Witczak, 1995], "η" is defined as the viscosity in Poises. At this time, it is not known if that is only a typographical error.]

[Note 11: In the reference of this study [Kim et al., 2005], the Witczak equation used is based on [2002 Design Guide, 1999].]

[Note 12: The authors mention that the Hirsch model was developed using temperature data in the range from 39.2 to 100.4^{o}F (4 to 38^{o}C). It is thought, however, that the temperature range is 15.8 to 129.2^{o}F (-9 to 54^{o}C), according to Christensen et al. (2003).]

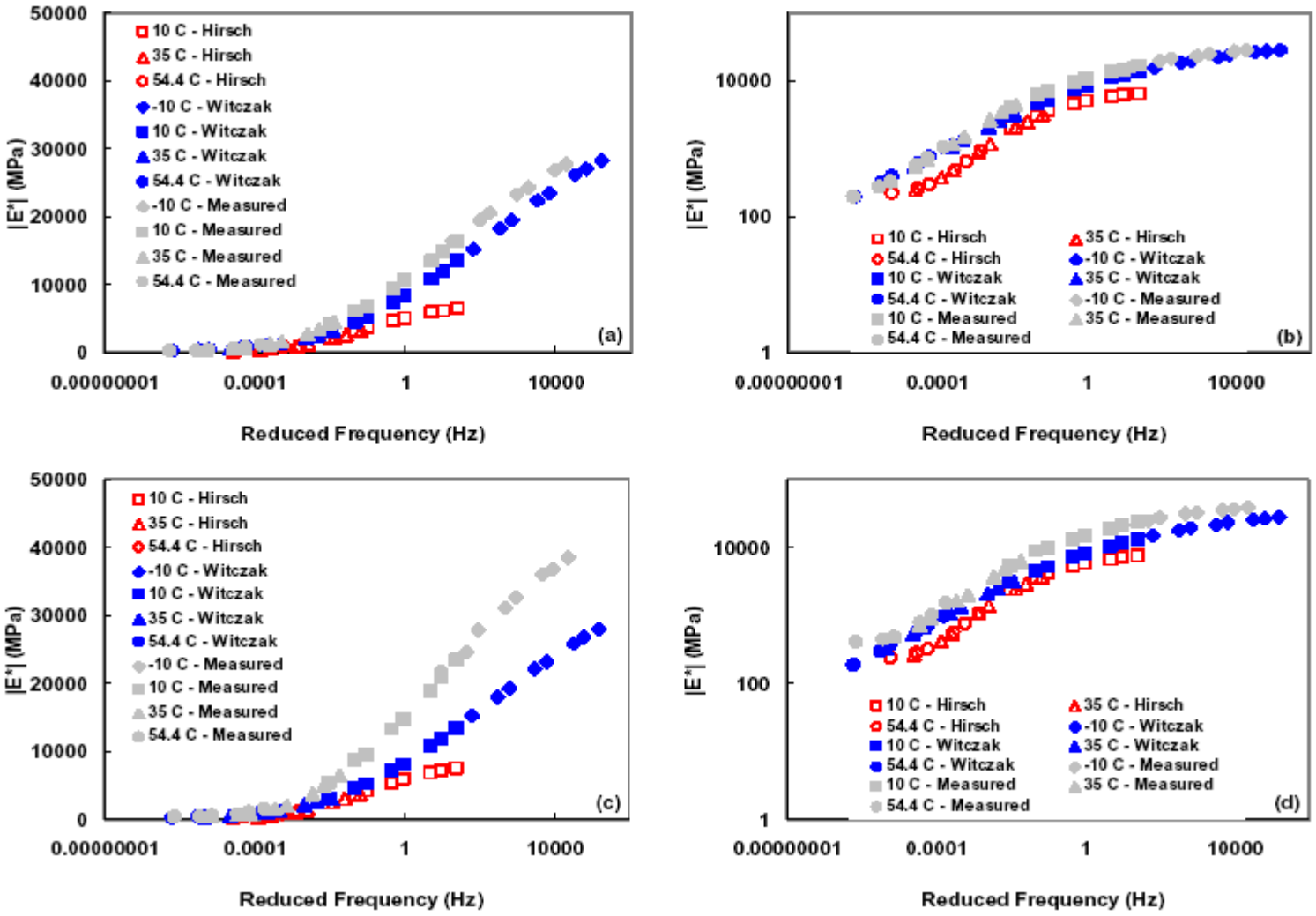

Figure 31. Master Curves of Measured and Predicted Moduli Yielding a Relatively Good Prediction for S9.5B-Fine Replicate 3 in Figures (a) and (b) and a Relatively Poor Prediction for I19.0B- Fine Replicate 1 in Figures (c) and (d) [Kim et al., 2005]

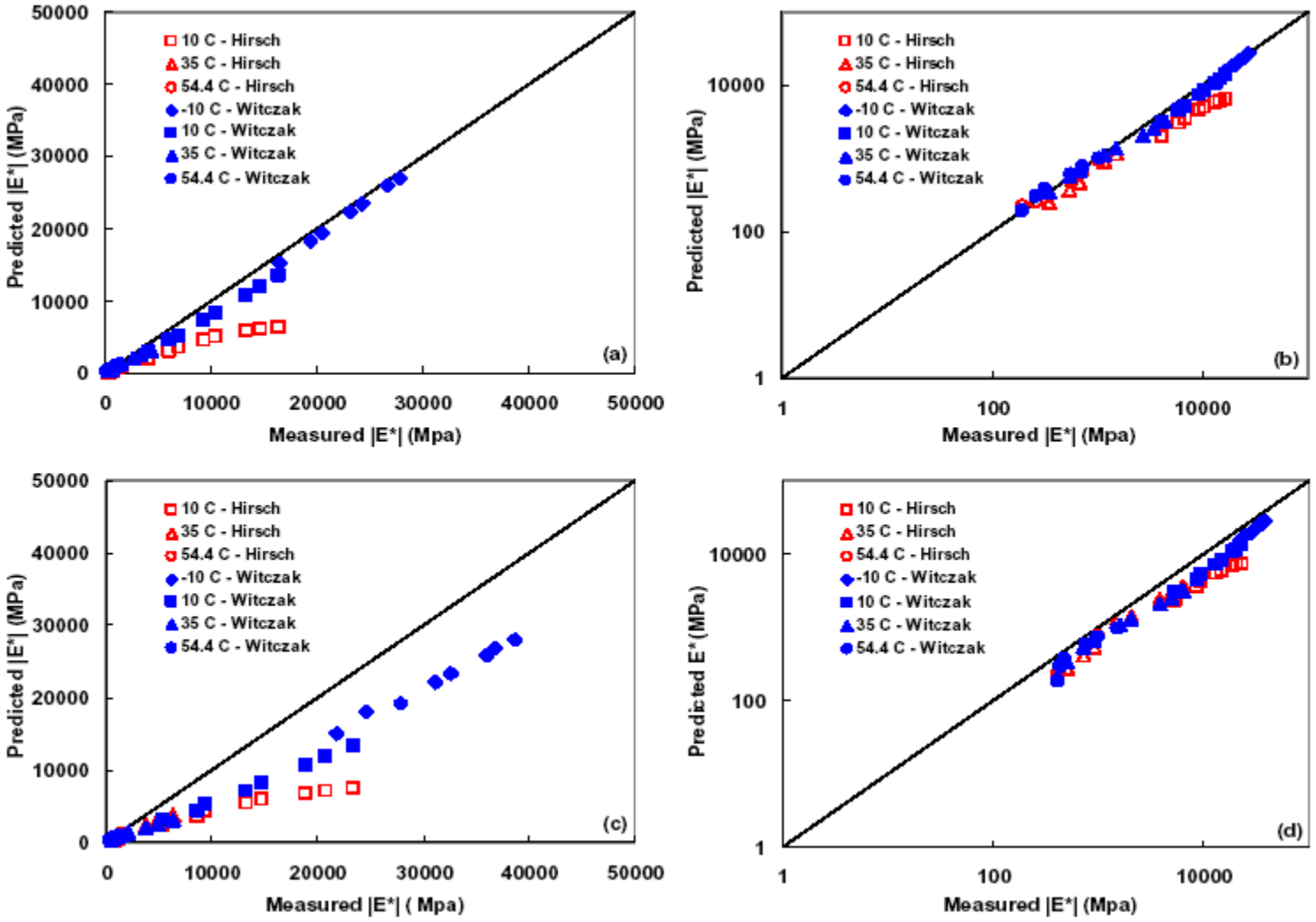

Figure 32. Line of Equality of Measured vs. Predicted Moduli Yielding a Relatively Good Prediction for S9.5B-Fine Replicate 3 in Figures (a) and (b) and a Relatively Poor Prediction for I19.0B- Fine Replicate 1 in Figures (c) and (d) [Kim et al., 2005]

5.5. University of Maryland Study [Schwartz, 2005]

The objective of this study was to evaluate the accuracy and robustness of the Witczak predictive equation for IE*I through a series of sensitivity and validation analyses.

The database used to develop and calibrate the Witczak equation was the same one used as the basis for this sensitivity study of the model. Table 16 presents a summary of some descriptive statistics calculated from the database, for all the input parameters in the Witczak equation except frequency and temperature. Frequency and temperature are exogenous inputs that are not related to mix characteristics.

Table 16. Descriptive Statistics for IE*I Predictive Model Calibration Data [Schwartz, 2005]

	Values in Database				
	Minimum	Maximum	Mean	Std. Dev.	COV
Va (%)	1.6	11.3	5.9	1.7	28.7%
Vbeff (%)	6.5	13.6	9.6	1.5	15.7%
P34 (%)	0.0	22.0	6.1	8.8	144.6%
P38 (%)	0.0	45.0	24.8	12.8	51.5%
P4 (%)	9.0	73.0	52.2	14.6	27.9%
P200 (%)	3.0	7.1	4.7	1.3	27.8%
A	8.8325	11.1165	10.2719	0.6019	5.9%
VTS	-2.8989	-3.7237	-3.4240	0.2208	6.4%

[1] Statistics based upon a version of the database earlier than that used for the final calibration. Statistics for final version of the calibration database are not expected to differ significantly.

From the database analysis was observed that the ratio A/VTS is nearly constant and equal to -3.0, with a small standard deviation of 0.022.

To compare the input parameters of the Witczak equation within similar orders of magnitude, a normalized variation of IE*I (NVE) was used, according to equation (36):

$$NVE = \frac{\left(\frac{\Delta|E^*|}{\overline{|E^*|}}\right)}{\left(\frac{\Delta P_i}{\overline{P}_i}\right)} \tag{36}$$

where

NVE = normalized variation of IE*I

ΔIE*I = change in IE*I caused by change ΔP_i of input parameter i about its mean value $\overline{P}_i$

$\overline{|E^*|}$ = value of IE*I computed using mean values for all input parameters

NVE can be interpreted as the percentage change in IE*I (in arithmetic space) caused by a given percentage change in the input parameter i.

Although frequency and temperature are exogenous variables not related to mixture characteristics, both are very important in the predictive model. Frequency is a direct input parameter in Witczak equation, while temperature is indirectly considered in the determination of viscosity through equation (17). According to Schwartz, frequency can be approximately related to vehicle speed as the inverse of the load pulse duration (The 2002 Design Guide uses a similar approach [2002 Design Guide, 2003]).

Figure 33 illustrates the influence of vehicle speed on predicted IE*I at three different temperatures. Figure 34 presents the corresponding normalized sensitivity of IE*I with respect to vehicle speed at the same temperatures. Figure 35 shows the influence of temperature on IE*I and the corresponding NVE to temperature. The volumetric properties, gradation and A-VTS parameters for these analyses were fixed at the mean values in Table 16. The corresponding viscosity at each temperature was determined applying the A-VTS values in equation (17).

Comparing Figures 34 and 35, the dominating effect of temperature on IE*I is clearly seen. According to Schwartz (2005), a 10% change in vehicle speed will cause only a 0.5% (10°F (-12.2°C)) to 3% (130°F (54.4°C)) change in IE*I while a 10% change in temperature will cause up to a 120% change in IE*I.

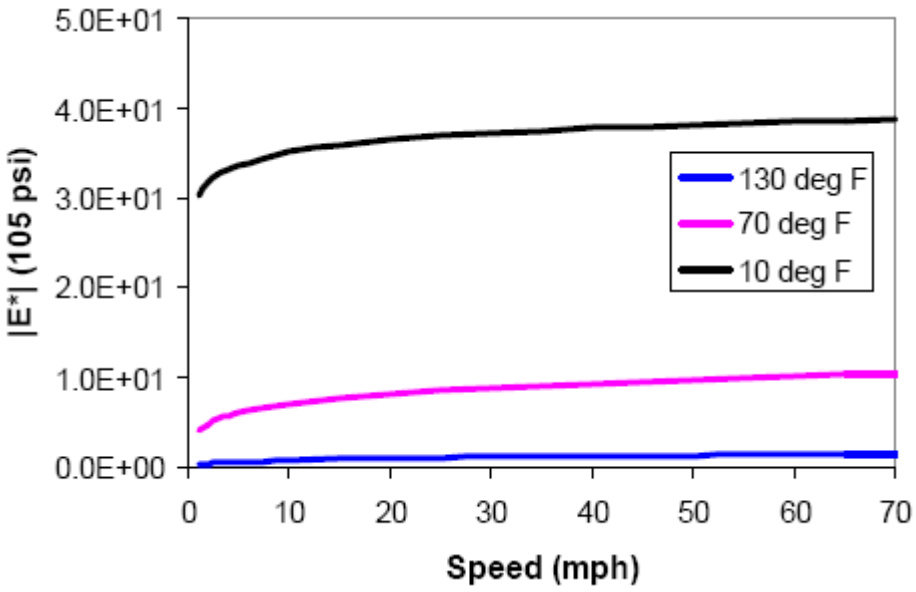

Figure 33. Influence of Vehicle Speed on IE*I [Schwartz, 2005]

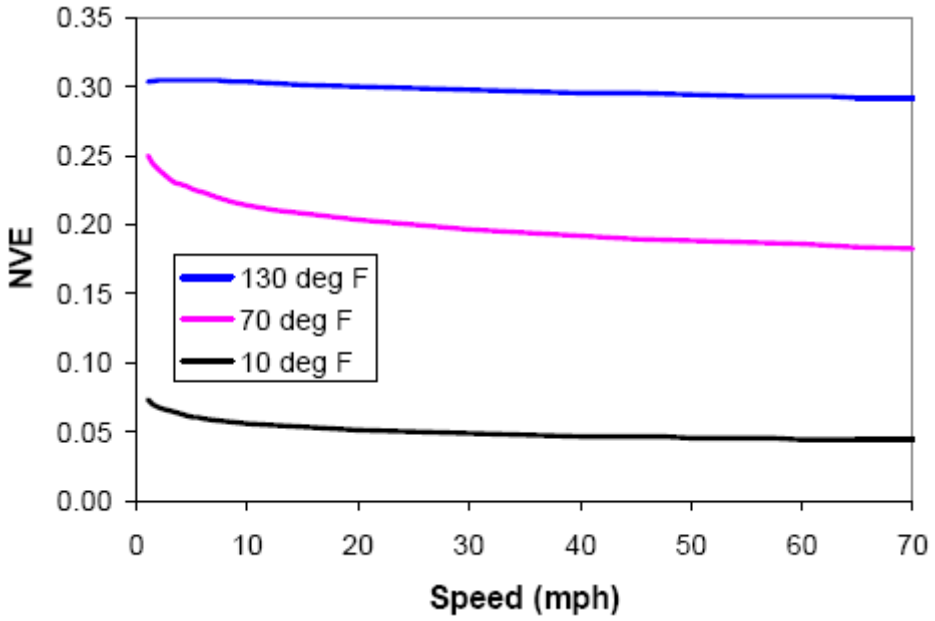

Figure 34. Sensitivity of Predictive IE*I to Vehicle Speed [Schwartz, 2005]

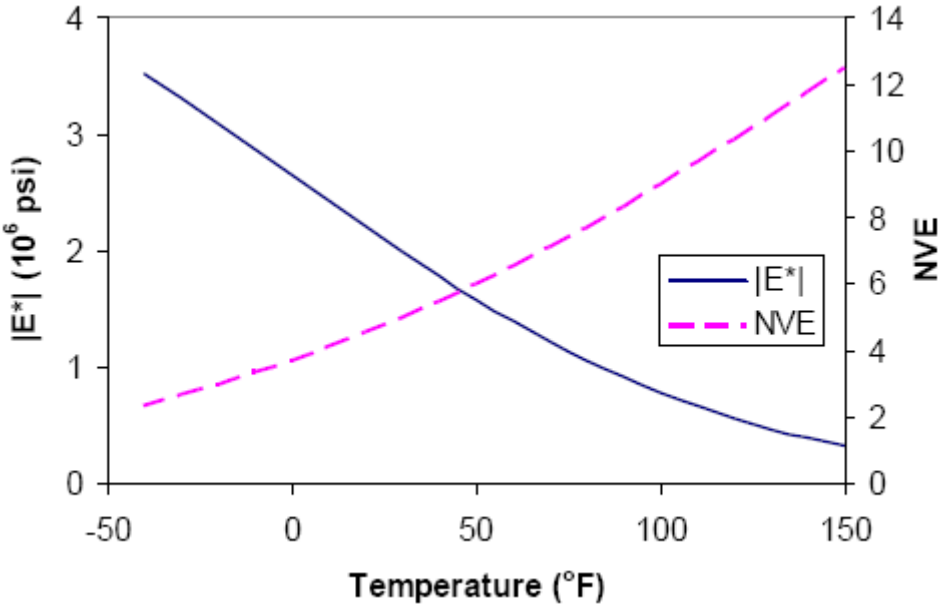

Figure 35. Influence of Temperature on Predictive IE*I [Schwartz, 2005]

To investigate the influence of the mixture-related inputs (endogenous) in the Witczak equation, all the inputs were set at their mean value according to Table 16 and then each input varied independently by one half or one standard deviation. Sensitivity was evaluated at 10 (-12.2), 70 (21.1), and 130^{o}F (54.4^{o}C) and the frequency was fixed at 10 Hz. Mean and standard deviation values for viscosity at each temperature were obtained taking the mean and standard deviation for A from Table 16, computing VTS=-3A and then using equation (17).

Figure 36 shows the actual variation of IE*I obtained for 70°F (21.1°C). The author also developed these relationships for 10 (-12.2) and 130°F (54.4°C), and although there is some variation of the trends with temperature, the following observations are applied for the three cases:

- Variations (in terms of standard deviation) of A and VTS showed the largest influence in predicted IE*I.

- Increasing V_a or V_{beff} produces a decrease in predicted IE*I. Although the influence of V_a is as expected, the influence of V_{beff} is not so clear. There is probably an optimum V_{beff} that maximizes stiffness. The author also thinks that it is possible that the relatively small range of V_{beff} in the calibration dataset makes it difficult to see this trend in the data.

- Predicted IE*I increases for coarser mixtures (larger ρ_{34} and ρ_{38} values).

- Predicted IE*I increases slightly with larger ρ_{200}. This is probably due to mastic stiffness mechanism.

It should be noted, however, that the percent passing or retained on different sieves will be correlated. This study did not consider this effect. It was assumed that each input can be varied independently.

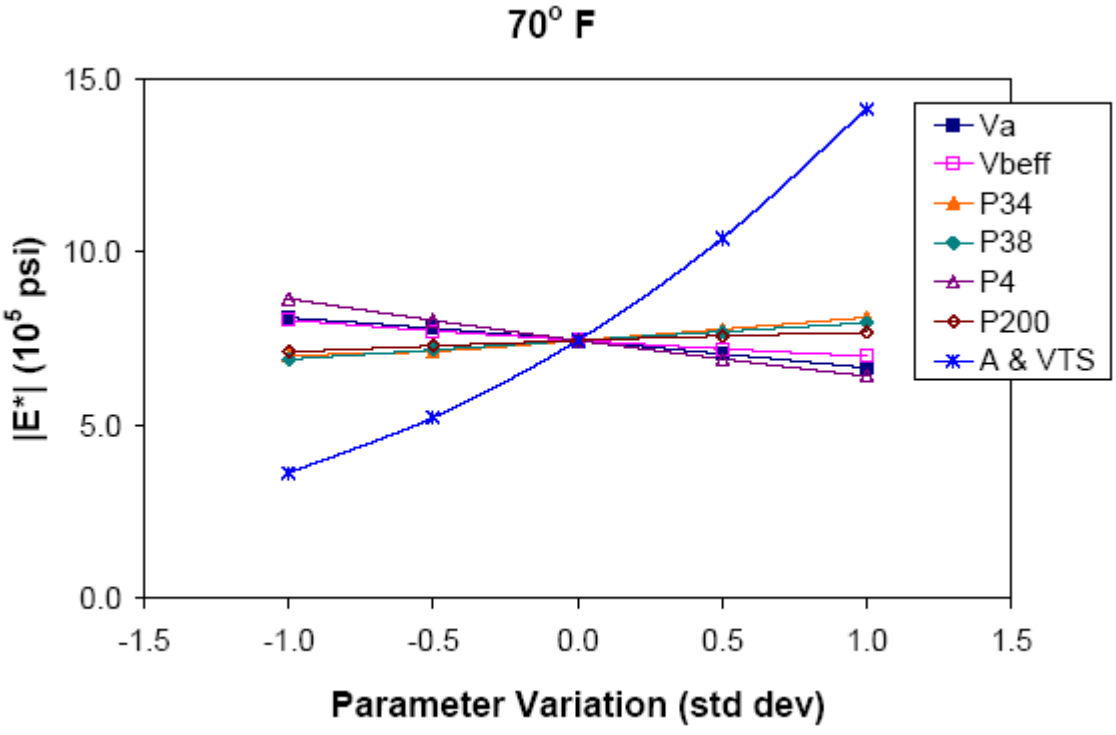

Figure 36. Variation of Predictive IE*I with Mixture Inputs at 158°F (70°C) [Schwartz, 2005]

Figure 37 shows a summary of the sensitivity of IE*I to the mixture inputs in terms of NVE. The following are the main observations by the author:

- As a group, volumetric properties V_a and V_{beff} have the strongest consistent influence on predicted IE*I. NVE ranged from about 0.35 to 0.45 at all three temperatures. This can be translated as a 10% change in either V_a or V_{beff} causes about a 4% change in predicted IE*I.

- The gradation parameters (ρ_{34}, ρ_{38}, ρ_4, and ρ_{200}) have different influence on predicted IE*I. The gradation parameter ρ_4 has the greatest influence on predicted IE*I (NVE between 0.45 and 0.6) not only among the gradation parameters but also among all of the input parameters (at a given temperature). On the other hand, ρ_{34}, ρ_{38}, and ρ_{200} have only a small influence on predictive IE*I (NVE between about 0.05 and 0.15).

- Actual viscosity has a varying influence on predictive IE*I. The effect is low at cold temperatures (NVE < 0.05 at 10°F (-12.2°C)) but is higher at warmer temperatures (NVE about 0.2 at 70°F (21.1°C) and 0.35 at 130°F (54.4°C)).

The author remarks that the relatively low NVE for viscosity should not be interpreted as that viscosity is a relatively unimportant input in the equation. The reason is that the typical ranges of each input parameter vary importantly and is the combination of NVE and the expected variation in the input parameter that must be taken into account.

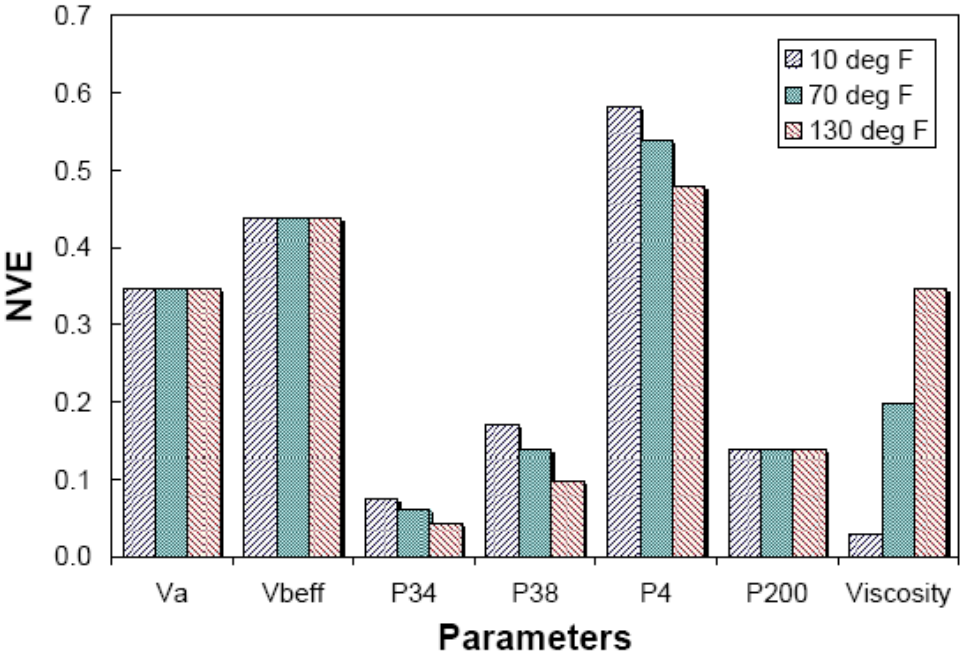

Figure 37. Sensitivity of Predicted IE*I to Mixture Inputs [Schwartz, 2005]

A set of data independent from that used for the calibration of the Witczak predictive equation was used to validate the accuracy of the model. The new set of data was taken from the Terhi Pellinen's Ph.D. dissertation. A total of 26 mixtures (11 from the FHWA ALF, 5 from MnRoad, and 10 from WesTrack) tested at six frequencies and five temperatures were obtained for the new dataset.

From the analysis of the results for the new dataset, Schwartz concludes that overall, the Witczak model provides quite a reasonable estimate for IE*I. Figures 38 and 39 present an example of the best (RMS error=15% in arithmetic IE*I space) and the worst agreement (RME error=177% in arithmetic IE*I space) between measured and predicted IE*I, respectively. Figure 40 shows the good agreement (R^2 of 0.97 in log IE*I and 0.88 in arithmetic IE*I space) between measured and predicted IE*I for all the laboratory test data points. Figures 41 and 42 illustrate the distribution of errors in the prediction of logIE*I (with a mean error of +3.2%) and IE*I (with a mean error of +59.4%), respectively. The skewness observed in Figure 42 is attributed to the transformation of residuals from a regression performed in log space.

To determine any bias in the predicted IE*I values, the errors in predicted IE*I vs. measured IE*I were compared for each group of mixtures. The MnRoad mixtures showed IE*I prediction errors ranging from -50% to +300%, the ALF mixtures showed a similar range, while the WesTrack mixtures ranged from -50% to 200%. All three groups showed an overall positive bias to the error, which is in agreement with the +59.4% mean error in predicted IE*I presented in Figure 42. The MnRoad and ALF mixtures showed consistently larger errors in predicted IE*I at lower stiffness (higher temperature), whereas the WesTrack data showed a nearly uniform error distribution across the entire stiffness (temperature) range.

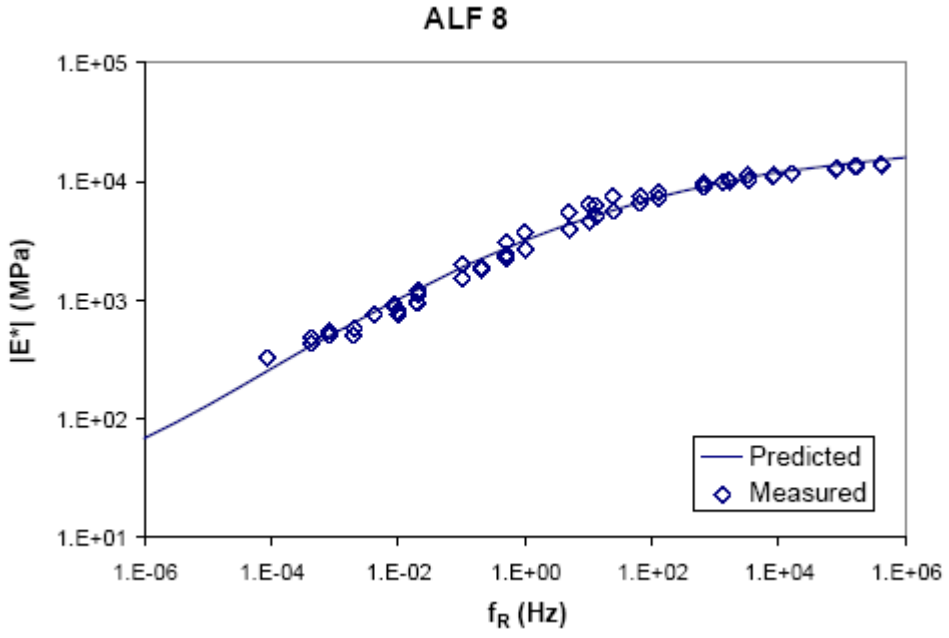

Figure 38. Example of Best Agreement (RMS error=15%) Between Predicted vs. Measured IE*I [Schwartz, 2005]

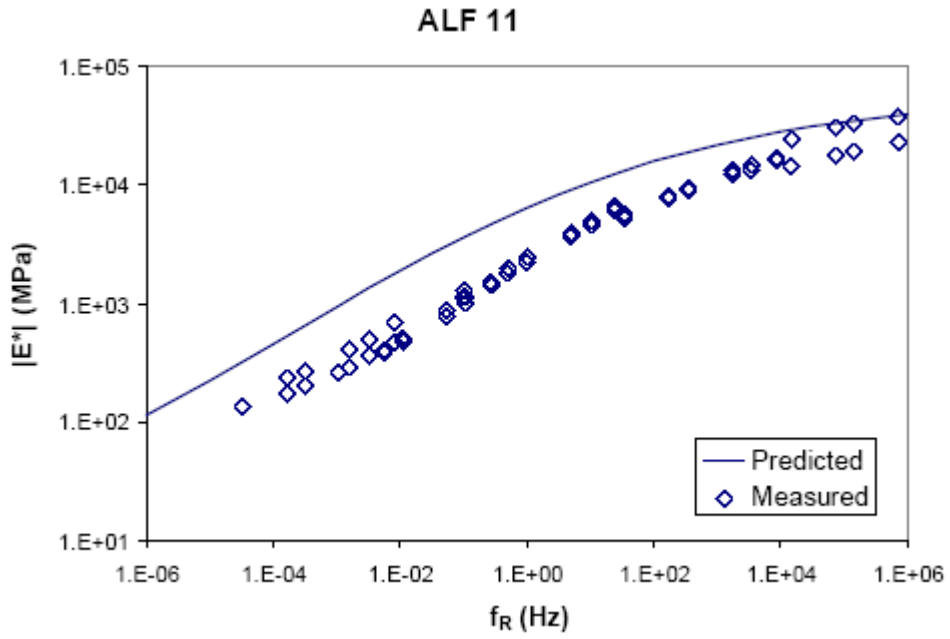

Figure 39. Example of Best Agreement (RMS error=177%) Between Predicted vs. Measured IE*I [Schwartz, 2005]

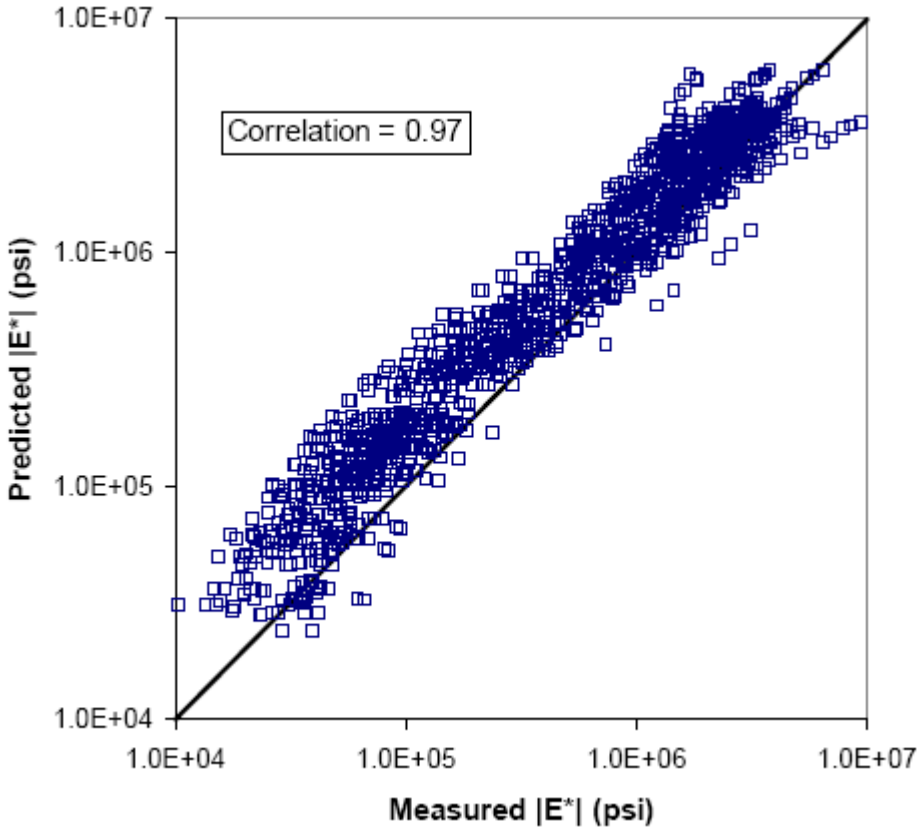

Figure 40. Predicted vs. Measured IE*I for Validation Data in LogIE*I Space [Schwartz, 2005]

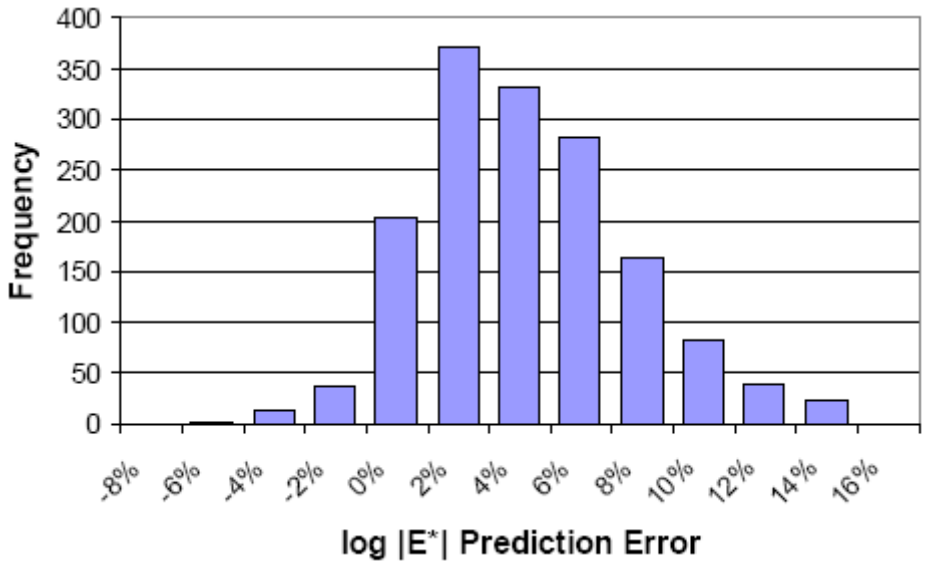

Figure 41. Distribution of Prediction Errors in LogIE*I Space (Mean Error=+3.2%) [Schwartz, 2005]

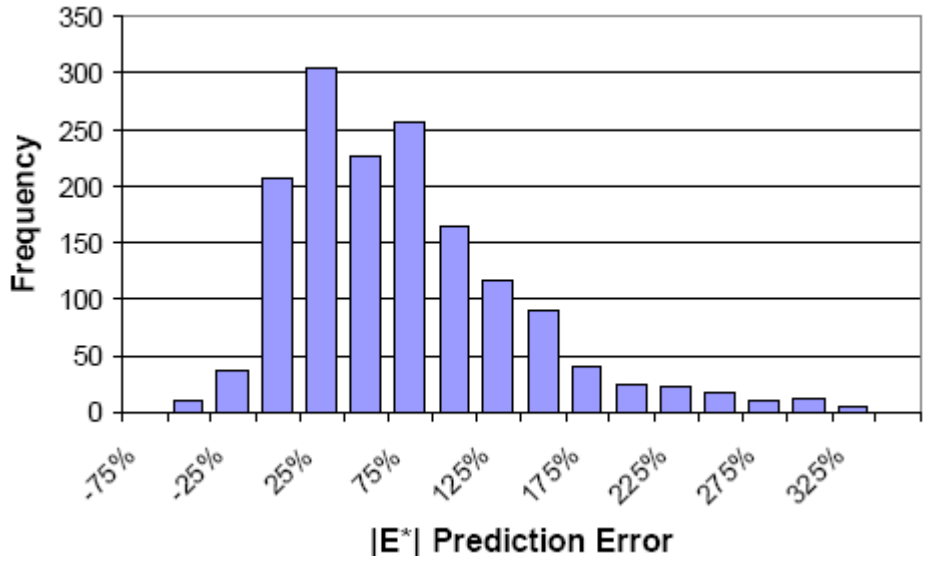

Figure 42. Distribution of Prediction Errors in Arithmetic IE*I Space (Mean Error=+59.4%) [Schwartz, 2005]

The input parameter sensitivity study found that IE*I is at least an order of magnitude more sensitive to temperature than any other input parameter of the Witczak equation. Consequently, the robustness of the model was inspected at a constant temperature to remove the effect of this dominant parameter and highlight the influence of the other parameters. Figures 43 and 44 present the results of this analysis using the Witczak calibration and the Pellinen validation dataset, respectively. As known, temperature and loading rate (frequency) can be interchanged, then only data at 1 Hz were included in order to emphasize the influence of the other input parameters.

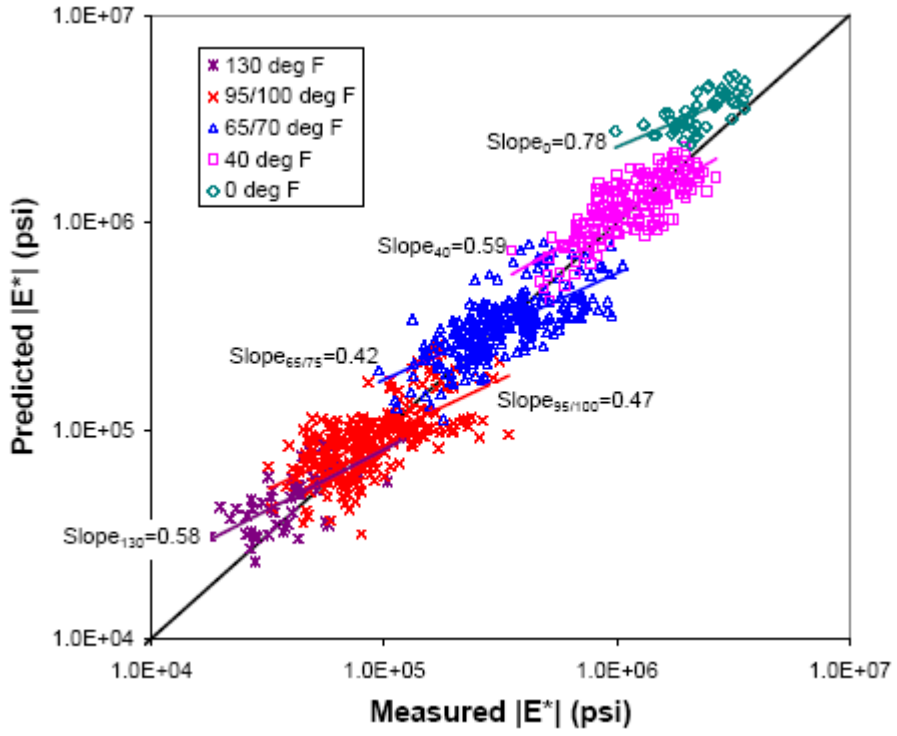

Figure 43. Predicted vs. Measured IE*I at 1Hz for the Witczak Calibration Dataset, Segregated by Temperature [Schwartz, 2005]

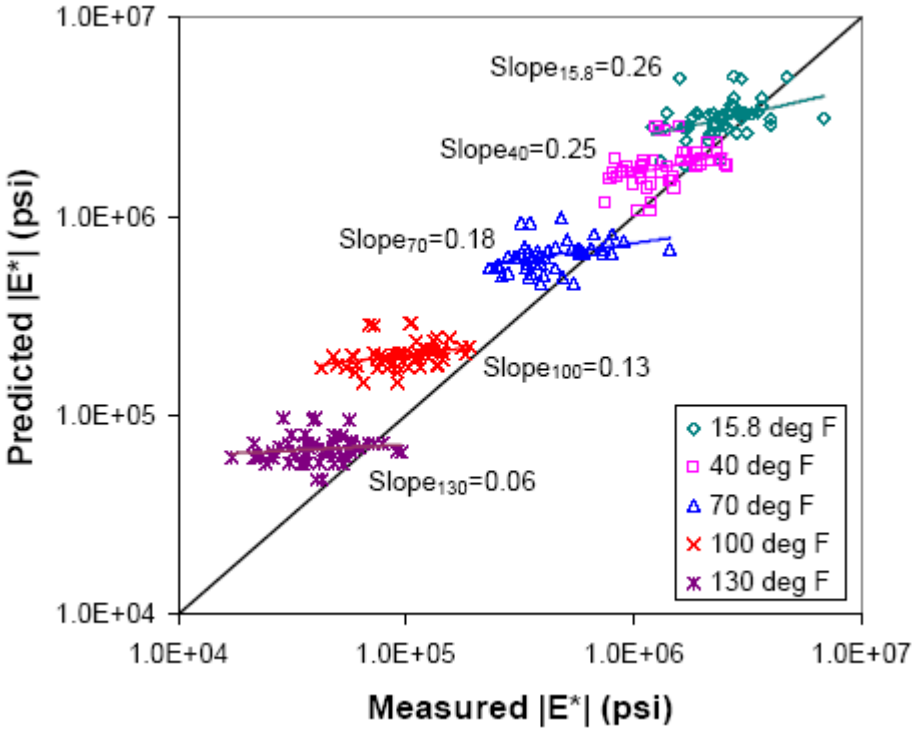

Figure 44. Predicted vs. Measured IE*I at 1Hz for the Pellinen Validation Dataset, Segregated by Temperature [Schwartz, 2005]

In Figure 43 it can be clearly observed that the Witczak predictive model captures very well the temperature effects on logIE*I whereas it appears to understate the effect of the volumetric and gradation parameters. The best-fit slopes shown for each subset of constant temperature suggest that only about 40 to 80% of the influence of the other inputs is captured in the Witczak model. However, though not shown in Figure 43, the strength of the trends at each temperature level was found to be quite low with R^2 ranging from 0.41 to 0.48. Figure 44 shows an even worse capture of the influence of non-temperature inputs. This is especially observed at 100 (37.7) and 130°F (54.4°C), where the slope of the each trend is practically flat and R^2 values are 0.095 and 0.022, respectively.

To better examine the strong influence of temperature in the Witczak model, the simplified model shown in equation (37) was calibrated using the Witczak calibration dataset:

$$\log(|E^*|) = a_1 + \frac{a_2}{1 + e^{a_3 + a_4 \log(f) + a_5 \log(\eta)}} \tag{37}$$

Equation 37 has the same sigmoidal functional form of equation (10), presented earlier, but neglects all mixture gradation and volumetric parameters. The R^2 obtained was 0.91 which is only slightly smaller than R^2 equal to 0.96 for the complete Witczak model (equation (10)) as seen in Table 1. Therefore, the author concludes that the mixture gradation and volumetric terms in the Witczak model add very little to its predictive power. Furthermore, no significant relationship was found between residuals from the simplified model and any of the gradation or volumetric parameters, with the exception of VMA, which is not an input parameter in the Witczak equation.

Schwartz's overall conclusion is that the Witczak predictive equation provides a sufficiently accurate and reasonably robust estimate of IE*I for use in mechanistic-empirical performance prediction and design. Although the model has more limited capability to make fine distinction between the performance of different mixtures at the same temperature and other design conditions, it nevertheless can provide IE*I estimates of acceptable accuracy for overall performance prediction and design.

Even though the modified Hirsch model (Equations (33) and (34)) was beyond the scope of his study, Schwartz mentions that preliminary evaluations suggest that the findings described for the Witczak model generally apply to the modified Hirsch model as well.

[Note 13: In the reference of this study [Schwartz, 2005], the Witczak equation used is based on [2002 Design Guide, 1999].]

[Note 14: It seems that Figure (35) is incorrect. Using the same data supposedly utilized by the author in its development, it was not possible to obtain the same curves.

Besides, what the author mentions in the text is not in agreement with what Figure 35 shows.]

5.6. University of Arkansas Study [Tran and Hall, 2005]

Dynamic modulus tests were performed to evaluate the Witczak predictive equation. Asphalt mixtures were prepared using three replicate test specimens (150 mm diameter and 170 mm height) for the aggregate types, binder grades, nominal maximum aggregate sizes, and air voids levels showed in Table 17. The tests were run on each specimen at temperatures of 14, 111.2, 70, 100, and 130^{o}F (-10, 4.4, 21.1, 37.8 and 54.4^{o}C) and frequencies of 25, 10, 5, 1, 0.5, and 0.1 Hz. Master curves were developed with the lab results, using the sigmoidal function approach. Tables 18 and 19 show the mix properties used in the Witczak predictive equation.

To evaluate the performance of the predictive equation, the correlation of the measured and predicted values was assessed using goodness-of-fit statistics according to the subjective criteria shown in Table 20 (based on Witczak et al., 2002a). The statistics include S_e/S_y (standard error of estimate values/standard deviation of measured values) and correlation coefficient, R^2, according to equations (38), (39), and (40).

$$S_e = \sqrt{\frac{\sum \left(Y - \hat{Y}\right)^2}{(n-k)}} \tag{38}$$

$$S_y = \sqrt{\frac{\sum \left(Y - \overline{Y}\right)^2}{(n-1)}} \tag{39}$$

$$R^2 = 1 - \frac{(n-k)}{(n-1)} \cdot \left(\frac{S_e}{S_y}\right)^2 \tag{40}$$

where

S_e = standard error of estimate
S_y = standard deviation of measured values
R^2 = correlation coefficient
Y = tested dynamic modulus
$\hat{Y}$ = predicted dynamic modulus
$\overline{Y}$ = mean value of tested dynamic modulus
n = sample size
k = number of independent variables in the model

Table 17. Summary of Selected Mixtures [Tran and Hall, 2005]

Source	Aggregate Size (mm)	Binder Grade	Design Gyrations	Design Air Voids (%)
MCA (Limestone)	12.5 25.0 37.5	PG 70-22	100	4.5
		PG 76-22	125	4.0
GMQ (Syenite)	12.5 25.0 37.5	PG 70-22	100	4.5
		PG 76-22	125	4.0

Table 18. Binder and Mix Data for Predictive Equation [Tran and Hall, 2005]

Mix ID	Binder Grade	RTFO Aged		Va (%)	Vbeff (%)
		VTS	A		
MCA_12.5_70_4.5	PG70-22	-3.426	10.299	4.8	10.1
MCA_12.5_70_7.0	PG70-22	-3.426	10.299	7.3	9.8
MCA_12.5_76_4.0	PG76-22	-3.208	9.715	3.7	11.1
MCA_12.5_76_7.0	PG76-22	-3.208	9.715	6.6	10.7
MCA_25_70_4.5	PG70-22	-3.426	10.299	4.2	8.7
MCA_25_70_7.0	PG70-22	-3.426	10.299	7.0	8.5
MCA_25_76_4.0	PG76-22	-3.208	9.715	4.0	9.9
MCA_25_76_7.0	PG76-22	-3.208	9.715	7.2	9.6
MCA_37.5_70_4.5	PG70-22	-3.426	10.299	4.7	7.3
MCA_37.5_70_7.0	PG70-22	-3.426	10.299	7.1	7.1
MCA_37.5_76_4.0	PG76-22	-3.208	9.715	3.6	7.9
MCA_37.5_76_7.0	PG76-22	-3.208	9.715	7.1	7.6
GMQ_12.5_70_4.5	PG70-22	-3.426	10.299	4.9	9.9
GMQ_12.5_70_7.0	PG70-22	-3.426	10.299	7.3	9.6
GMQ_12.5_76_4.0	PG76-22	-3.208	9.715	4.2	11.7
GMQ_12.5_76_7.0	PG76-22	-3.208	9.715	7.1	11.3
GMQ_25_70_4.5	PG70-22	-3.426	10.299	4.2	8.9
GMQ_25_70_7.0	PG70-22	-3.426	10.299	7.0	8.6
GMQ_25_76_4.0	PG76-22	-3.208	9.715	3.8	9.8
GMQ_25_76_7.0	PG76-22	-3.208	9.715	6.8	9.5
GMQ_37.5_70_4.5	PG70-22	-3.426	10.299	4.3	7.7
GMQ_37.5_70_7.0	PG70-22	-3.426	10.299	6.6	7.5
GMQ_37.5_76_4.0	PG76-22	-3.208	9.715	3.8	7.7
GMQ_37.5_76_7.0	PG76-22	-3.208	9.715	6.9	7.4

Table 19. Aggregate Gradation for Predictive Equation [Tran and Hall, 2005]

Mix ID	Aggregate Source	P34 (%)	P38 (%)	P4 (%)	P200 (%)
MCA_12.5_70_4.5	Limestone	0.0	13.0	29.0	4.2
MCA_12.5_70_7.0	Limestone	0.0	13.0	29.0	4.2
MCA_12.5_76_4.0	Limestone	0.0	15.0	32.0	4.0
MCA_12.5_76_7.0	Limestone	0.0	15.0	32.0	4.0
MCA_25_70_4.5	Limestone	9.0	10.0	30.0	3.6
MCA_25_70_7.0	Limestone	9.0	10.0	30.0	3.6
MCA_25_76_4.0	Limestone	9.0	11.0	31.0	3.3
MCA_25_76_7.0	Limestone	9.0	11.0	31.0	3.3
MCA_37.5_70_4.5	Limestone	15.0	6.0	17.0	3.1
MCA_37.5_70_7.0	Limestone	15.0	6.0	17.0	3.1
MCA_37.5_76_4.0	Limestone	16.0	6.0	16.0	3.1
MCA_37.5_76_7.0	Limestone	16.0	6.0	16.0	3.1
GMQ_12.5_70_4.5	Syenite	0.0	12.0	24.0	4.2
GMQ_12.5_70_7.0	Syenite	0.0	12.0	24.0	4.2
GMQ_12.5_76_4.0	Syenite	0.0	10.0	25.0	3.9
GMQ_12.5_76_7.0	Syenite	0.0	10.0	25.0	3.9
GMQ_25_70_4.5	Syenite	12.0	13.0	21.0	3.4
GMQ_25_70_7.0	Syenite	12.0	13.0	21.0	3.4
GMQ_25_76_4.0	Syenite	12.0	14.0	18.0	3.2
GMQ_25_76_7.0	Syenite	12.0	14.0	18.0	3.2
GMQ_37.5_70_4.5	Syenite	10.0	5.0	13.0	3.8
GMQ_37.5_70_7.0	Syenite	10.0	5.0	13.0	3.8
GMQ_37.5_76_4.0	Syenite	10.0	5.0	13.0	3.8
GMQ_37.5_76_7.0	Syenite	10.0	5.0	13.0	3.8

Table 20. Criteria for Goodness of Fit Statistical Parameters [Tran and Hall, 2005]

Criteria	R^2	S_e/S_y
Excellent	≥ 0.90	≤ 0.35
Good	0.70 – 0.89	0.36 – 0.55
Fair	0.40 – 0.69	0.56 – 0.75
Poor	0.20 – 0.39	0.76 – 0.89
Very Poor	≤ 0.19	≥ 0.90

Table 21 presents the predictive equation evaluation for the mixtures of each aggregate type separately and for all the mixtures used in the study.

Figure 45 shows a comparison between the measured and predicted dynamic modulus values obtained in this study.

Table 21. Goodness of Fit Statistics for the Predictive Equation, Modified from [Tran and Hall, 2005]

Mixture Aggregate	R^2	S_e/S_y	Evaluation
Limestone	0.88	0.35	Good / Excellent
Syenite	0.87	0.36	Good / Very Good
All Mixtures	0.88	0.35	Good / Excellent

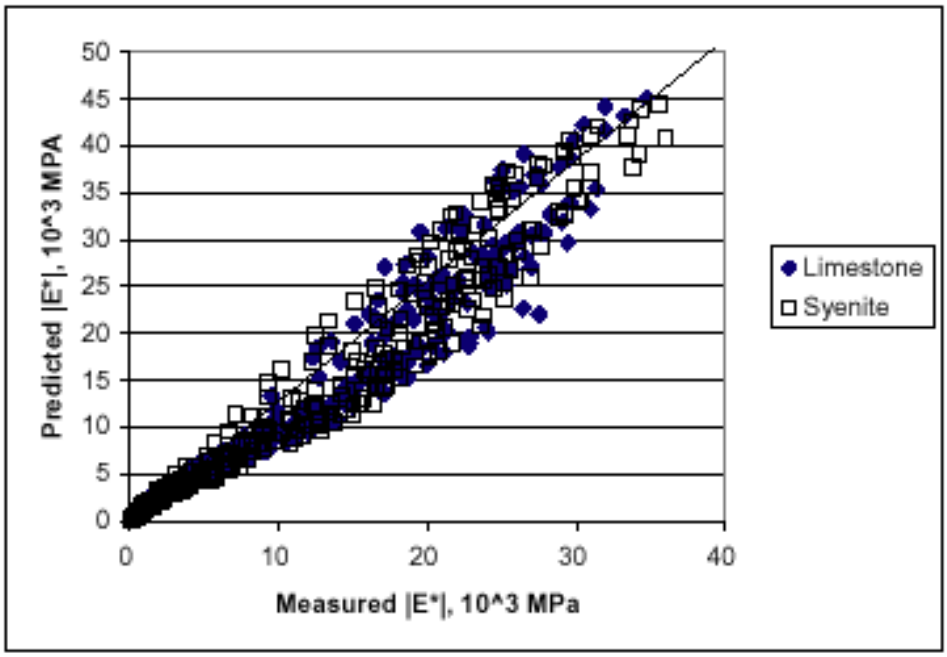

Figure 45. Predicted and Measured IE*I Comparison [Tran and Hall, 2005]

Figure 46 shows an example where the measured and predictive dynamic modulus master curves are compared for a 12.5-mm limestone mixture using PG 70-22 at two levels of air voids, 4% (design) and 7%.

Figure 47 presents the comparison of measured and predictive dynamic modulus master curves for a 37.5-mm syenite mixture using PG 76-22 at 4% (design) and 7% air voids.

The authors conclude that the Witczak predictive equation had a good correlation to the measured dynamic modulus values. They also found that the goodness-of-fit statistics showed that the mixtures used in the study had a very good to excellent performance and that the master curve comparison of the measured and predictive values confirmed that the Witczak predictive equation fits the test data of this study very well. Finally, they

recommend that the Witczak predictive equation be used for Arkansas mixes not specifically tested in the study.

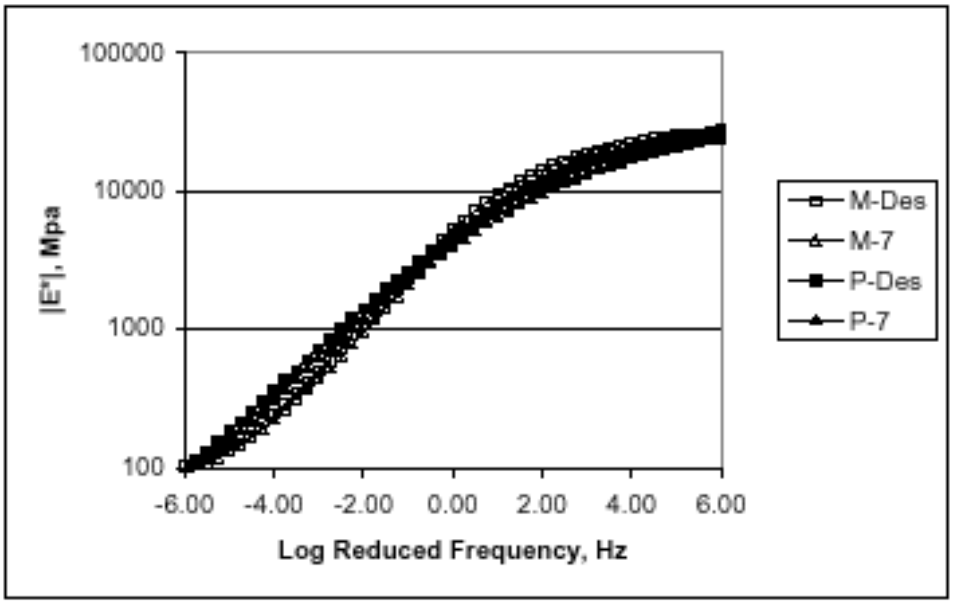

Figure 46. Master Curve Comparison for MCA_12.5_70 Mixture at 4.5 (Design) and 7% Air Voids [Tran and Hall, 2005]

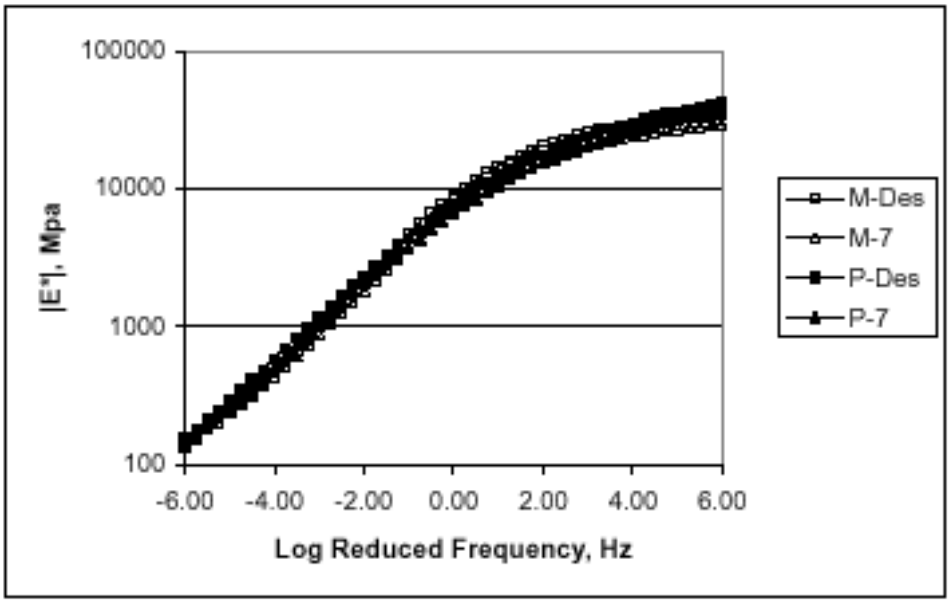

Figure 47. Master Curve Comparison for GMQ_37.5_76 Mixture at 4.5 (Design) and 7% Air Voids [Tran and Hall, 2005]

[Note 15: In the reference of this study [Tran and Hall, 2005], the Witczak equation used is like equation 2.3 in [2002 Design Guide, 2000], except that IE*I is expressed in terms of 10^2 MPa, which means that a constant was introduced in the left side of the original equation (log(IE*I/6.894)).]

[Note 16: In the development of the master curves using the Witczak predictive equation, the authors did not calculate directly (from lab tests) the A and VTS parameters to take into account the temperature viscosity relationship. Instead, they used the recommended default A and VTS values from Table 2.2.10 [2002 Design Guide, 2004], which correspond to the hierarchical Level 3 of the Design Guide. It is thought that this is a drawback of this study because, as shown later in the Dongré et al. study and in a study developed by the University of Illinois during the last year, the default A and VTS values used in Level 3 have been found to be significantly different than those estimated in the cited studies.]

5.7. Louisiana Transportation Research Center (LTRC) Study [Mohammad et al., 2005]

The main objective of this study was to compare two Simple Performance Tests (SPT) (IE*I and flow number test) measured in two laboratories (the FHWA mobile laboratory and the LTRC laboratory). The secondary objective was to evaluate the Witczak and the Hirsch models by comparing the predicted vs. the measured IE*I data.

Two plant-produced Superpave mixtures (one base and one binder course mixture) plus one laboratory mixture which was equivalent to the base course mixture were used in this study. Table 22 shows the job mix formula (JMF) for the two base courses (US190 Base) and for the binder course mixtures (US190 Binder).

Both base and binder course mixtures used about 19% RAP. However, the RAP used in the base course mixtures was different from that used in the binder course mixture. The source of the aggregate material was the same for all of the three mixtures. After deducing the RAP binder content, the actual virgin asphalt content used in both plant-produced mixtures was 3.3 and 2.7 for the base course and the binder course mixture, respectively. On the other hand, the laboratory mixture was produced at three different asphalt contents: 3.3, 3.8, and 4.3%. As seen in Table 22, the base course mixtures used a PG 64-22 conventional asphalt binder; the binder course mixture, however used a PG 76-22 SB polymer modified.

To determine the binder related inputs for the Hirsch model, IG*I values of RTFO aged binder were obtained from an AR 2000 rheometer at six temperatures and six frequencies, as shown by the corresponding isotherms in Figure 48. For the Witczak equation, however, viscosity values of RTFO aged binder were obtained at 140, 275, and 329^{o}F (60, 135 and 165^{o}C), using Absolute viscosity, Kinematic viscosity, and Rotational viscosity tests, respectively. Figure 49 shows the results of the viscosity tests. The equations in Figure 49 correspond to equation (17), so the slope and the

ordinate represent the VTS and A parameters, respectively, for each of the binders tested.

The dynamic moduli were obtained from the average of several 100-mm diameter and 150-mm tall test specimens, cored and cut from gyratory specimens of 150-mm diameter 170-mm tall at the temperatures and frequencies specified in Table 23. The target air voids for the samples was 7.5±0.5%. Each test was performed applying a load level so that the obtained strain was about 100 μstrain for those tested in the FHWA mobile laboratory and between 50 and 95 μstrain for those tested in the LTRC.

Table 22. Job Mix Formula [Mohammad et al., 2005]

Mix Name	US190 Base	US190 Binder
AC %	PG64-22	PG76-22M[1]
	3.8%	3.6%
Aggregates	31.4% No. 5 LS [2] 13.7% No. 67 LS 19.3% No. 78 LS 8.1% Coarse sand 8.1% Fine sand 19.4% RAP	31.6% No. 5 LS 13.8% No. 67 LS 19.4% No. 78 LS 8% Coarse sand 8.1% Fine sand 19.1% RAP
Gradation (% passing)		
11/2" (37.5 mm)	100	100
1" (25 mm)	97	97
3/4" (19 mm)	84	84
1/2" (12.5 mm)	64	65
3/8" (9.5 mm)	49	52
No. 4 (4.75)	29	32
No. 8 (2.36)	22	24
No. 16 (1.18)	18	20
No. 30 (0.60)	14	15
No. 50 (0.30)	7	9
No. 200 (0.075)	3.1	3.6
G_{mb}	2.459	2.459
G_{mm}	2.526	2.534
%VMA @ N_{des}	12.3	11.8
%VFA @N_{des}	67.0	67.0
%Air Voids @ N_{des}	3.8	4.0
%Gmm @N_{ini}	87.7	87.9
%Gmm @N_{final}	97.4	96.0

Note: [1] M refers to polymer modified asphalt cements
[2] LS - Limestone

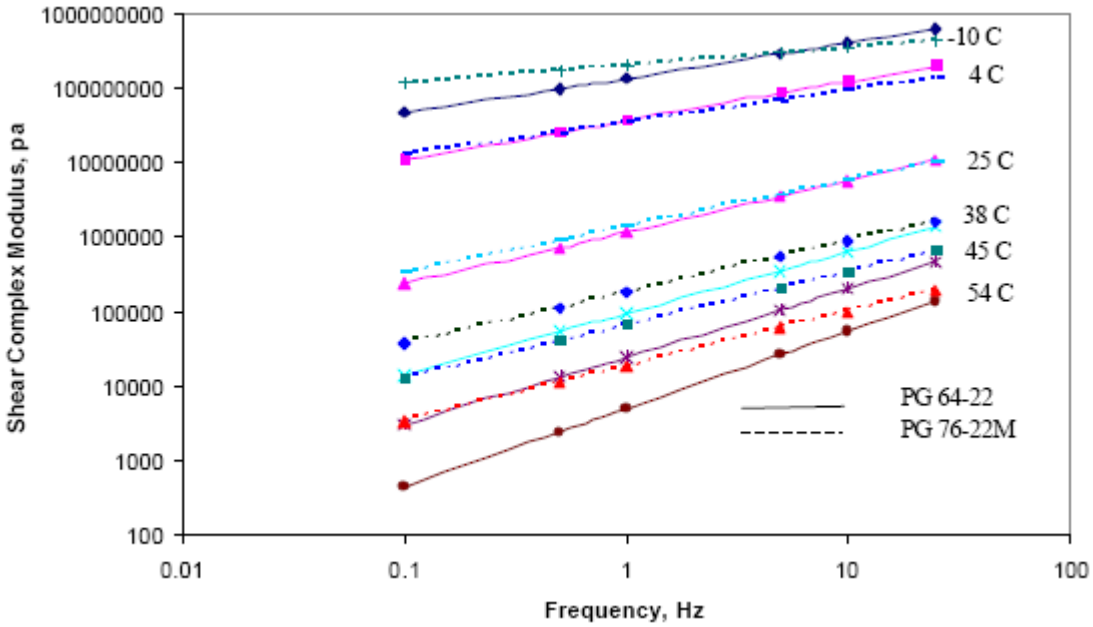

Figure 48. IG*I_{binder} Isotherms [Mohammad et al., 2005]

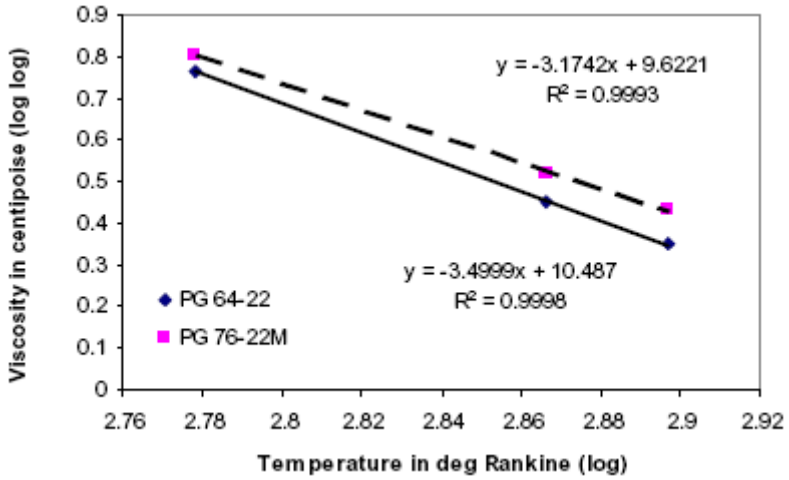

Figure 49. Binder Viscosity Results [Mohammad et al., 2005]

Table 23. IE*I Laboratory Test Factorial [Modified from Mohammad et al., 2005]

Laboratory	Mixture		Samples Tested	Temperature °F (°C)	Frequency Hz
FHWA Mobile	US190 Base Lab Mix	3.3% AC	4	77 (25) 113 (45) 129.2 (54)	25 10 5 1 0.5 0.1
		3.8% AC	4		
		4.3% AC	4		
	US190 Base Plant Mix	Day-1	4		
		Day-2	4		
		Day-3	4		
		Day-4	4		
	US190 Binder Plant		8		
LTRC	US190 Base Plant Mix	Day-1	1	14 (-10) 39.2 (4) 77 (25) 100.4 (38) 129.2 (54)	25 10 5 1 0.5 0.1
		Day-2	1		
		Day-3	1		
	US190 Binder Plant		3		

Tables 24 and 25 present the average IE*I results along with their standard deviation and coefficient of variation for the mixtures tested at the FHWA mobile laboratory and LTRC laboratory, respectively. These results were statistically analyzed by means of the Fisher's Least Significant Difference (LSD) method, at a 95% confidence interval, to detect the influence of production variation, binder content, mixture type, and laboratory testing system on the IE*I values obtained.

The results from the LSD analysis showed that, with only a few exceptions, no significant differences exist among the three plant-produced mixtures. This was expected by the authors, because of the consistent plant production process used in this study. It implies that the IE*I test can provide consistent results for plant-produced mixtures.

On the other hand, it was seen that at all test temperatures there was a significant difference in IE*I results between the lab mixtures with 4.3% of AC and those with 3.3 and 3.8%. Taking into account that the optimum AC content for these mixtures was 3.8%, this indicates that over-asphalting a mixture could result in lower IE*I. In addition, at high temperatures (113 and 129.2°F (45 and 54°C)), the dynamic modulus values for mixtures with 3.8 and 3.3% of AC also exhibit statistically significant differences.

Table 24. Summary of IE*I Results at FHWA Mobile Trailer Laboratory [Mohammad et al., 2005]

Project	Mixture		|E*| - Dynamic Modulus (Mpa)																	
		Temp	25C						45C						54C					
		Freq (Hz)	25	10	5	1	0.5	0.1	25	10	5	1	0.5	0.1	25	10	5	1	0.5	0.1
US190 Base Lab Mixture	3.3% AC	Avg.	8363	6886	5887	3857	3175	1838	2365	1607	1213	593	441	214	1079	674	491	231	165	88
		STD	432	380	336	246	219	154	81	42	32	15	11	6	51	23	17	10	9	8
		% C.V.	5.2	5.5	5.7	6.4	6.9	8.4	3.4	2.6	2.7	2.5	2.5	2.9	4.7	3.5	3.5	4.3	5.3	8.5
	3.8% AC	Avg.	7412	6120	5220	3370	2746	1548	1982	1317	961	483	358	172	953	589	420	205	148	81
		STD	803	624	500	314	241	126	210	167	148	71	55	30	80	55	51	27	22	16
		%C.V.	10.8	10.2	9.6	9.3	8.8	8.2	10.6	12.7	15.4	14.7	15.4	17.6	8.4	9.3	12.2	13.0	14.6	19.5
	4.3% AC	Avg.	5973	4740	3932	2379	1891	1021	1360	870	636	308	237	120	610	358	255	128	97	58
		STD	860	728	629	430	348	181	189	116	74	30	24	15	57	30	27	13	8	9
		%C.V.	14.4	15.4	16.0	18.1	18.4	17.7	13.9	13.4	11.6	9.8	10.1	12.7	9.4	8.4	10.4	10.5	8.5	14.9
US190 Base Plant Mixture	Production Day-1	Avg.	6072	4894	4115	2571	2079	1159	1914	1285	968	472	354	176	878	544	395	210	179	107
		STD	786	697	619	424	363	208	348	256	196	90	63	28	170	116	97	38	63	53
		% C.V.	12.9	14.2	15.0	16.5	17.4	18.0	18.2	19.9	20.2	19.1	17.9	16.0	19.4	21.3	24.5	18.2	35.1	49.9
	Production Day-2	Avg.	7372	5957	5005	3119	2504	1364	2134	1425	1064	513	378	176	1003	622	455	219	160	87
		STD	780	681	647	499	436	292	382	293	242	150	113	60	215	160	128	71	54	27
		%C.V.	10.6	11.4	12.9	16.0	17.4	21.4	17.9	20.6	22.8	29.2	30.0	33.9	21.5	25.8	28.1	32.3	33.9	31.0
	Production Day-3	Avg.	7776	6402	5456	3493	2811	1517	1701	1076	783	357	265	131	729	418	297	145	109	68
		STD	268	249	249	245	228	154	115	86	68	32	26	12	50	30	18	12	12	10
		%C.V.	3.4	3.9	4.6	7.0	8.1	10.2	6.8	8.0	8.7	8.9	9.6	8.9	6.9	7.1	6.1	8.2	11.0	15.3
US190 Binder Plant	Plant Produced	Avg.	9418	7802	6688	4434	3669	2199	2888	2039	1583	867	701	408	1430	949	722	383	296	172
		STD	1554	1367	1222	954	837	581	376	327	288	217	206	176	199	158	127	73	58	36
		%C.V.	16.5	17.5	18.3	21.5	22.8	26.4	13.0	16.0	18.2	25.1	29.3	43.3	13.9	16.7	17.5	18.9	19.7	20.9

Table 25. Summary of IE*I Results at LTRC Laboratory [Mohammad et al., 2005]

US190 Base Course	|E*| - Dynamic Modulus (Mpa)																	
	-10C						4C						25C					
	25 Hz	10 Hz	5 Hz	1 Hz	0.5 Hz	0.1 Hz	25 Hz	10 Hz	5 Hz	1 Hz	0.5 Hz	0.1 Hz	25 Hz	10 Hz	5 Hz	1 Hz	0.5 Hz	0.1 Hz
Average	25903	24932	23354	20595	19060	16250	19303	18054	16516	13165	11635	8449	7620	5974	5121	3361	2680	1613
STD	1880	1850	1672	1544	1262	1551	2022	2517	2246	1973	1722	2066	1676	1286	1147	995	734	597
%C.V.	7.3	7.4	7.2	7.5	6.6	9.5	10.5	13.9	13.6	15.0	14.8	24.5	22.0	21.5	22.4	29.6	27.4	37.0
	38C						54C											
	25 Hz	10 Hz	5 Hz	1 Hz	0.5 Hz	0.1 Hz	25 Hz	10 Hz	5 Hz	1 Hz	0.5 Hz	0.1 Hz						
Average	2503	1775	1393	733	606	400	889	627	508	328	289	233						
STD	354	240	159	40	7	45	146	88	62	21	13	1						
%C.V.	14.1	13.5	11.4	5.4	1.2	11.2	16.5	14.1	12.1	6.4	4.5	0.5						
US190 Binder Course	**|E*| - Dynamic Modulus (Mpa)**																	
	-10C						4C						25C					
	25 Hz	10 Hz	5 Hz	1 Hz	0.5 Hz	0.1 Hz	25 Hz	10 Hz	5 Hz	1 Hz	0.5 Hz	0.1 Hz	25 Hz	10 Hz	5 Hz	1 Hz	0.5 Hz	0.1 Hz
Average	24399	23047	22050	20547	19450	17123	23451	21708	20113	16445	14870	11649	8843	7214	6038	3876	3144	1810
STD	1525	908	773	1166	812	460	45	222	405	192	41	368	290	116	123	36	45	23
%C.V.	6.2	3.9	3.5	5.7	4.2	2.7	0.2	1.0	2.0	1.2	0.3	3.2	3.3	1.6	2.0	0.9	1.4	1.3
	38C						54C											
	25 Hz	10 Hz	5 Hz	1 Hz	0.5 Hz	0.1 Hz	25 Hz	10 Hz	5 Hz	1 Hz	0.5 Hz	0.1 Hz						
Average	3853	2714	2137	1210	985	574	1607	1211	1014	696	625	545						
STD	273	146	84	61	50	47	215	158	96	87	58	48						
%C.V.	7.1	5.4	3.9	5.1	5.1	8.2	13.4	13.0	9.4	12.4	9.3	8.7						

In general, there were no statistical differences in the mean IE*I values between the lab-produced and plant-produced US190 base mixture tested in the FHWA mobile laboratory (the US190 base lab mixture used in the comparison was that one with the optimum asphalt content of 3.8%). However, significant differences in IE*I values were found between the US190 binder mixtures and the US190 base mixtures (lab or plant-produced) at all three temperatures in the FHWA mobile laboratory, and at temperatures greater than 77°F (25°C) in the LTRC laboratory. This indicates that at temperatures higher than 77°F (25°C), the IE*I test seems to be sensitive to different mixture types with a different binder type, but not sensitive to the difference between the lab-produced and plant-produced mixtures.

The LSD analysis finally showed that at 77°F (25°C) there were no significant differences in IE*I results between both laboratories. However, at 129.2°F (54°C) the LTRC results showed higher IE*I values for both US190 base and binder plant mixtures than those from the FHWA mobile laboratory, especially at frequencies lower than 1Hz. Since the major difference in the tests performed at both laboratories was the strain level selected for the test, it is thought by the author, that the significant differences found at 129.2°F (54°C) could be attributed to this factor.

Dynamic modulus master curves were developed fitting a polynomial function on log-log coordinates. The temperature shift factors were determined based on the Arrhenius equation. Figures 50 and 51 show a typical master curve for the IE*I tests conducted at the LTRC and FHWA mobile laboratory, respectively.

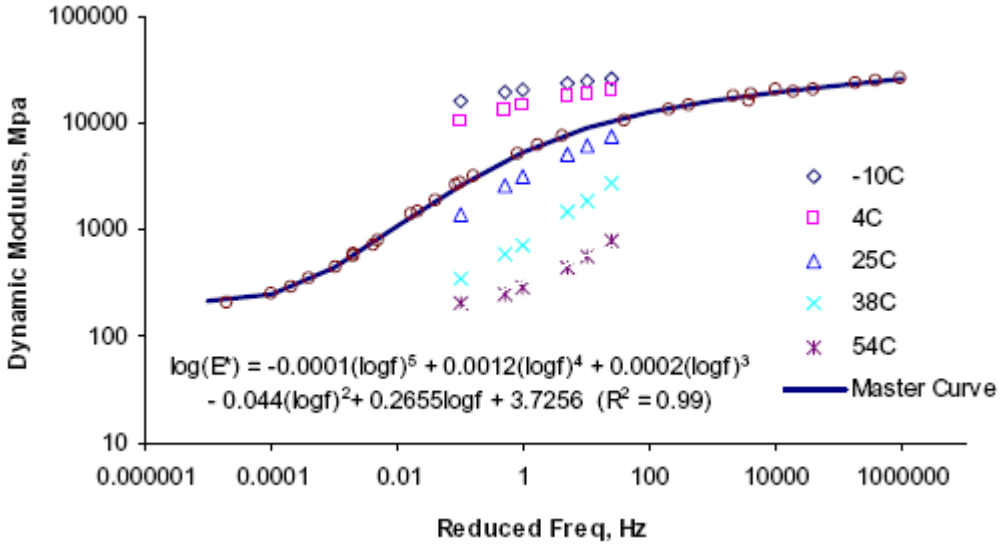

Figure 50. Typical IE*I Isotherms and Master Curve of LTRC Laboratory Results at 68°F (20°C) Reference Temperature [Mohammad et al., 2005]

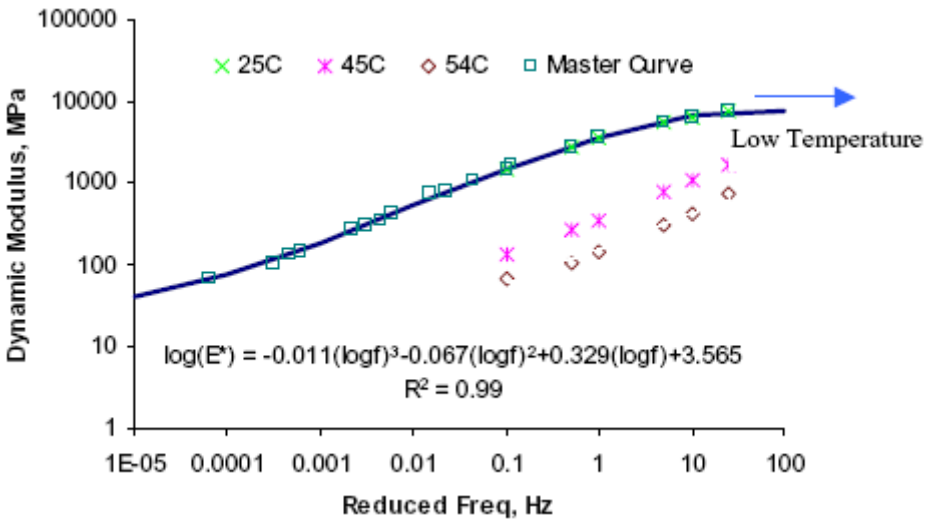

Figure 51. Typical IE*I Isotherms and Master Curve of FHWA Mobile Laboratory Results at 77°F (25°C) Reference Temperature [Mohammad et al., 2005]

[Note 17: It should be noted in Figure 50, that when checking the polynomial function appearing there in an Excel spreadsheet, the shape of the master curve obtained was different than that shown in Figure 50. It is thought that there is some typo in the function written by the authors.]

Figures 52 and 53 present a comparison of the measured and predicted IE*I values using the Witczak and the Hirsch model, respectively.

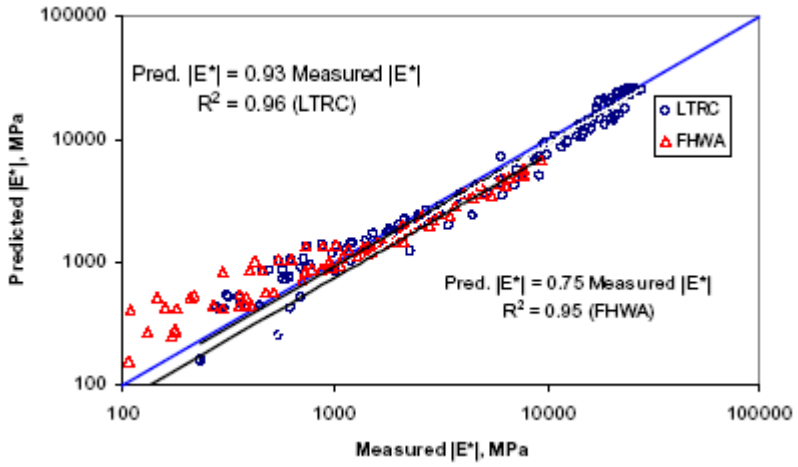

Figure 52. Comparison of Measured and Predicted IE*I (Witczak's Model) [Mohammad et al., 2005]

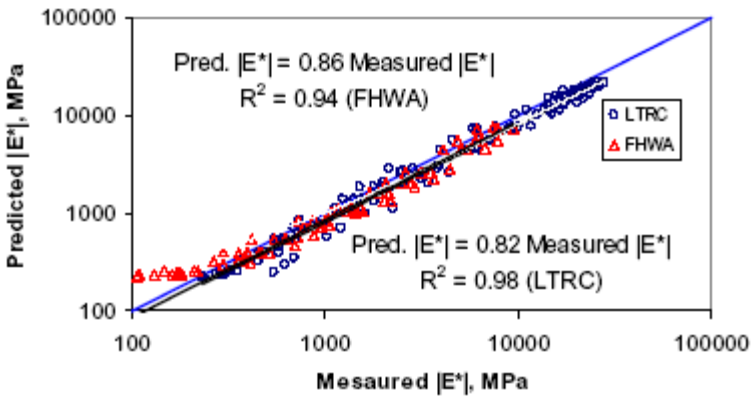

Figure 53. Comparison of Measured and Predicted IE*I (Hirsch Model) [Mohammad et al., 2005]

In general, a good agreement was found between the measured and predicted IE*I values with both the Witczak and the Hirsch models.

As seen in Figure 52 the Witczak model, in total, predicted IE*I values were equal to 0.93 and 0.75 times the measured IE*I values for the LTRC and FHWA laboratories, with R^2 of 0.96 and 0.95, respectively. In general, predicted IE*I values at high temperature and low frequency were higher than the measured ones. However, the opposite occurred at intermediate temperature and high frequency. The authors remark that, although the overall predicted IE*I values were lower than those measured in the FHWA laboratory, the most important difference between predicted and measured values was found at the highest test temperature of 129.2°F (54°C). On the other hand, a large difference also was found at this high temperature between the LTRC and the FHWA mobile laboratory results. This indicates that the strain level of 100 μstrain used in the FHWA mobile laboratory might be too high for this temperature and the mixtures tested. They suggest that a lower strain level (50~75 μstrain) may be used at high temperature IE*I testing.

The Hirsch model predicted IE*I values, as shown in Figure 53, were equal to 0.86 and 0.82 times the measured IE*I values for the FHWA and the LTRC laboratories, with R^2 of 0.94 and 0.98, respectively. At the high temperature of 129.2°F (54°C), the predictions were slightly better than with the Witczak model. The overall Hirsch model prediction appears fairly consistent with most of data points equally distributed along the predicted lines.

Finally, the authors conclude that both the Witczak and Hirsch models can predict the IE*I values from mixture properties within a reasonable reliability.

[Note 18: In the reference of this study [Mohammad et al., 2005], the Witczak equation used is based on [2002 Design Guide, 1999]]

5.8. Dongré, Myers, D'Angelo, Paugh and Gudimettla Study [Dongré et al., 2005]

In this study, dynamic modulus was measured for asphalt mixtures from five pavement construction sites across the United States and compared with the corresponding IE*I predicted using the Witczak and the Hirsch models. Table 26 presents a summary with the properties of the mixtures evaluated. A minimum of four replicate specimens were prepared per laboratory-blended and plant-produced sample for each of the project mixes. Specimens 100-mm in diameter and 150-mm tall were cored and cut from typical gyratory specimens 180-mm high by 150-mm in diameter.

Dynamic modulus values for mixes from each site were obtained using the new Superpave Simple Performance Tester (SPT) in unconfined compression. The axial stress was maintained at a level such that the corresponding strains were in the range of 75 to 125 μstrain. The tests were performed at frequencies of 25, 10, 5, 1, 0.5, and 0.1 Hz at the specific test temperatures shown in Table 27. Predicted and measured values were then compared to evaluate the predictive capability of both models.

Master curves were also generated. In addition, the GAS (explained earlier) was investigated using the measured and predicted dynamic modulus. Only the original to mix/laydown correction was used in this study.

Master curves were generated using a new procedure developed by Bonaquist in NCHRP 9-29. According to the authors, this procedure does not require IE*I data to be collected at temperatures below 77^{o}F (25^{o}C) and has an added advantage that it only needs data at a total of three different temperatures to generate accurate master curves. In fact, the asphalt binder glassy modulus of 1 GPa is used in the Modified Hirsch Model to determine the low temperature asymptote of the sigmoidal master curve function. Thus, determination of IE*I at 10^{o}F (-12.2^{o}C) is not required.

Three methods of calculating shift factors were used in this study, the Arrhenius function, the VTS method proposed by Witczak (as in equation (24) earlier) and the third method consisted of generating shift factors by shifting the asphalt binder rheological data and directly using them to shift the HMA IE*I data.

[Note 19: Dongré et al. determined IE*I based on part of the NCHRP 9-29 project by Bonaquist in which, according to the authors, the procedure does not require data collected at temperatures below 77^{o}F (25^{o}C). It must be noted, however, that in the paper submitted to the 2005 TRB Conference by Bonaquist and Christensen (2005) they mention that the recommended testing temperatures for the proposed alternative approach to determine IE*I, equation (9), are 40, 70, and 115^{o}F (4.4, 21.1, and 46.6^{o}C)].

Table 26. Mixture Properties at Each Site Evaluated [Dongré et al., 2005]

	Project ID				
Properties	0357	0358	0359	0360	0462
Binder Grade	PG 64-22	PG 58-28	PG 64-28	PG 70-22	PG 64-22
Air Voids	4.0	4.7	4.5	2.6	4.5
Binder Content	5.5	5.4	5.8	5.0	3.8
VMA	15.1	14.8	14.3	12.0	12.4
VFA	72.4	68.2	68.5	78.3	63.7
Sieve Size	**Gradation (% passing)**				
37.5 mm	100	100	100	100	100
25mm	100	100	100	100	95
19mm	98	100	100	100	82
12.5mm	88	96	100	99	62
9.5mm	79	87	98	94	49
4.75mm	63	73	60	66	29
2.36mm	43	53	39	50	23
1.18mm	27	36	25	41	18
0.6mm	17	23	15	29	14
0.3mm	9	11	9	16	7
0.15mm	5	7	6	10	4
0.075mm	4	5	4	6	3

Table 27. Project Specimen Test Temperatures [Dongré et al., 2005]

Project ID	Test Temperatures, ^{o}C
0357	15.6, 19.6, 23.6, 31.2
0358	17.0, 23.0, 40.0
0359	17.9, 23.9, 37.5
0360	20.8, 25.0, 45.0
0462	25.0, 45.0, 54.0

*Witczak Model IE*I Predictions*

Figure 54 compares measured vs. predicted IE*I values using the Witczak equation for three binder aging conditions (original, RTFO and PAV).

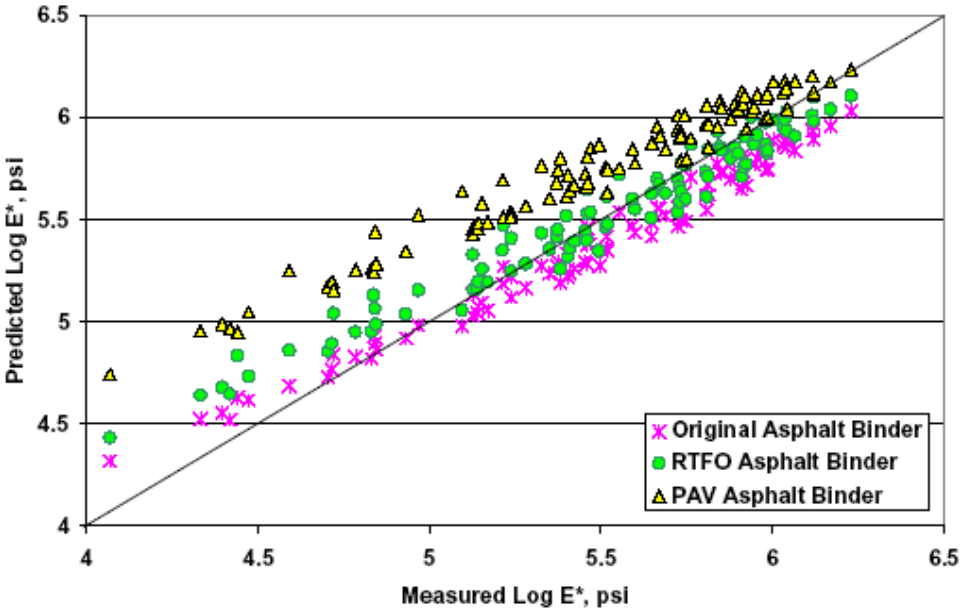

Figure 54. Measured and Predicted IE*I Data Using the Witczak Model, Plotted for All Sites [Dongré et al., 2005]

Table 28 shows the results of statistical analysis performed on the data shown in Figure 54 for each site, as well as all of the data combined.

Table 28. Results of Statistical Analysis of the IE*I Predictions Using the Witczak Model [Dongré et al., 2005]

Statistic	Site ID	ORG	RTFO	PAV
R^2	0357	0.52	0.81	0.49
S_e/S_y	0357	0.787	0.495	0.805
R^2	0358	0.93	0.98	0.67
S_e/S_y	0358	0.305	0.183	0.679
R^2	0359	0.94	0.94	0.33
S_e/S_y	0359	0.288	0.286	0.974
R^2	0360	0.96	0.89	0.81
S_e/S_y	0360	0.225	0.389	0.520
R^2	0462	0.96	0.94	0.66
S_e/S_y	0462	0.250	0.290	0.693
R^2	Combined	0.90	0.92	0.61
S_e/S_y	Combined	0.311	0.284	0.631

The statistics S_e/S_y and R^2 are defined as in equations (38), (39), and (40). The same criteria shown earlier in Table 20 were applied in this study.

The general trend found from Figure 54 and Table 28 indicates that binder data from RTFO aging condition appears to predict IE*I values relatively close to the measured data.

Figure 55 shows the error (defined as the log difference) between measured and predicted values vs. measured IE*I values.

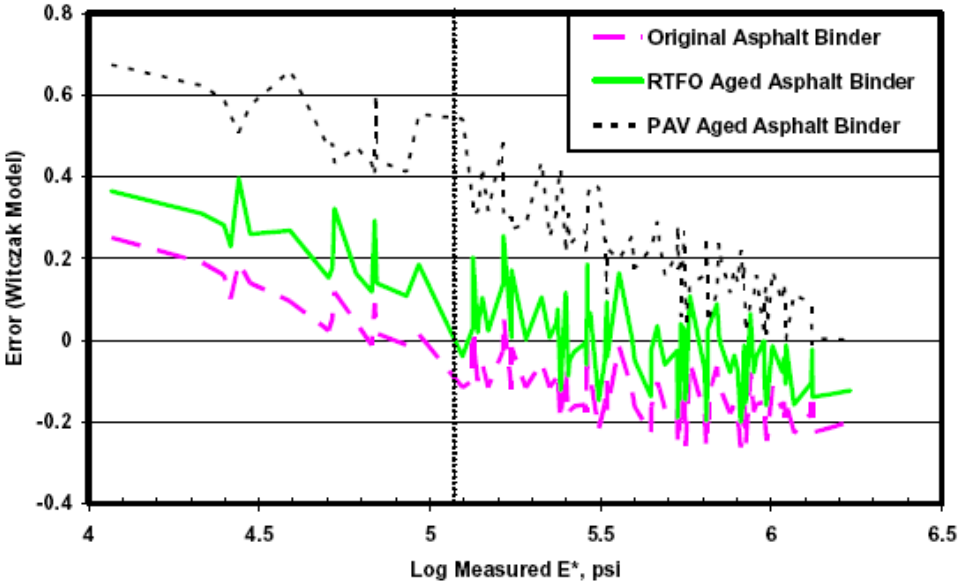

Figure 55. Plot of Error in Prediction of IE*I for Data Using the Witczak Model for All Sites [Dongré et al., 2005]

From this plot it can be inferred that the Witczak model begins to converge beyond an IE*I value of approximately 125,000 psi (log(IE*I) ≈ 5.1 psi). There also seems to be a bias in the error values as they seem to converge below zero error. According to the authors, this could be attributed to the fact that the A and VTS parameters used in the Witczak model were developed based on traditional viscosity and penetration test data, whereas IG*I and phase angle values were used in this study to calculate viscosity and the A and VTS parameters. Therefore, from Figures 54 and 55 it seems that below IE*I values of 125,000 psi, the Witczak model over-predicts the dynamic modulus. It also appears that the amount of over-prediction is dependent on the decrease in modulus below 125,000 psi. Thus, they recommend that the IE*I should be measured if the anticipated value is below 125,000 psi.

Figure 56 shows a plot of predicted vs. measured IE*I values for HMA plant produced specimens (specimens made using HMA sampled from haul trucks) for site 0357. Table 29 shows the gradation and volumetric properties for all the production days shown in

Figure 56. In that Figure, it seems that the agreement between the predicted and measured values depends on the production day. This may be attributed to differences in production and mix-design asphalt content and air voids for each day in which the production was sampled and tested. This was not expected by the authors since the Witczak equation is supposed to account for changes in volumetrics, asphalt content, and air voids and therefore the prediction should agree with the measured data even if the inputs values are different. According to them, this implies that the Witczak model loses accuracy if the volumetrics and binder content deviate from the mix design levels.

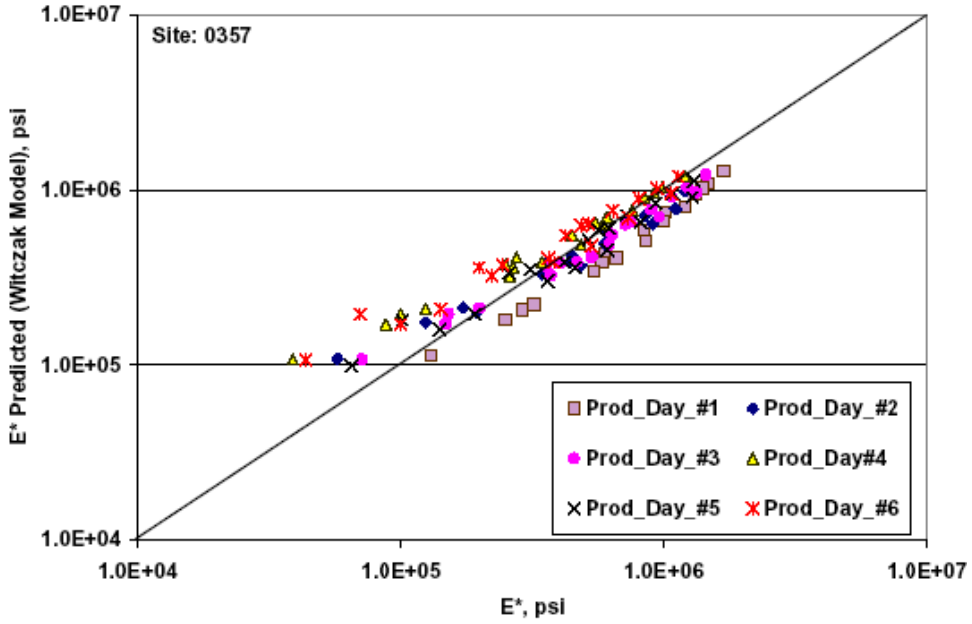

Figure 56. Measured Versus Predicted IE*I Values from the Witczak Model for Production Specimens at Site No. 0357. RTFO Aged Binder Data Was Used [Dongré et al., 2005]

Table 29. Volumetrics Input Values for Witczak Model IE*I Prediction Used at Site 0357 and Plotted in Figure 56 [Dongré et al., 2005]

Site No. 0357	% Retained			% Pass		
	19 mm	9.5 mm	4.75 mm	0.075 mm	V_{beff}, %	Va
Production Day No. 1	1.6	22.9	38.7	5.1	8.344	8.2
Production Day No. 2	2.4	22.1	37.1	4.7	9.351	8.1
Production Day No. 3	2.7	24.5	38.8	4.5	9.592	8.0
Production Day No. 4	3.8	28.2	43.9	5.5	10.021	7.9
Production Day No. 5	3.4	29.6	45	4.4	10.214	8.2
Production Day No. 6	2.3	19.4	33.8	4.7	9.761	8.4
FHWA Mix Design	1.9	21.5	36.9	4.0	9.556	7.0

Overall, the authors found that the Witczak model provided reasonable predictions of IE*I using HMA volumetric properties and the Superpave RTFO binder data (IG*I and δ at 10 rad/s).

[Note 20: The Witczak equation used in this study is that appearing in Appendix CC-4 of the Design Guide [2002 Design Guide, 1999]. It must be noted, however, that after reviewing the files with the original database used in the first version of the paper of this study, it was found that in the spreadsheets used to make the calculations, three of the factors of the right side of the original equation were truncated just before the last decimal. Comparing the predicted dynamic modulus values obtained in some of the files of this study and those calculated with the Witczak equation appearing in [2002 Design Guide, 2004] and without truncating any factor, the differences ranged from 462 to 3454 psi. This situation was reported to the authors and supposedly corrected in the final version of the paper.]

Figure 57 shows IE*I predictions using the GAS vs. the measured data for site 0357. The IE*I predictions using original, RTFO, and PAV aged binder data are also shown with unfilled symbols. As seen in the Figure, the amount of aging predicted by the GAS exceeds the RTFO aging and comes close to the PAV IE*I data, which was observed in data from all sites in this study. The authors conclude that the GAS over estimates the hardening of the binder as the hardening rate (HR) becomes poorer and only the IE*I values predicted for excellent HR agree with the RTFO data. As the Superpave system does not account for hardening rates, the authors mention that this may be indicated by the ratio of G*/sinδ values of original and RTFO binder. On the other hand, in this study, asphalt binders were not extracted from the plant produced mixes in order to avoid any variation in the physical properties of the extracted binders. They also determined an estimate hardening rate to be used in the GAS, based on the ratio of IE*I values measured for the plant produced mix and IE*I values predicted using the Witczak model and the original (unaged) asphalt binder properties. Table 30 shows the comparison of the Superpave hardening ratio indicators and those estimated as explained.

They found that the binders from all sites showed poor estimated hardening rates; whereas, the Superpave indicators show that there are differences in hardening rate for the binders included in this study. Comparing the estimated hardening rate and the Superpave ratio obtained, they do not appear to be related. However, when the GAS equation and hardening rate codes are applied to the original asphalt viscosity, the predicted IE*I values always show the hardening rate of excellent to be equivalent to RTFO based IE*I predictions. They mention that the GAS was based on extracted binders which may have affected the model and thus, over-predicting the amount of hardening. They did not conclude which hardening rate, if any, actually represents field aging.

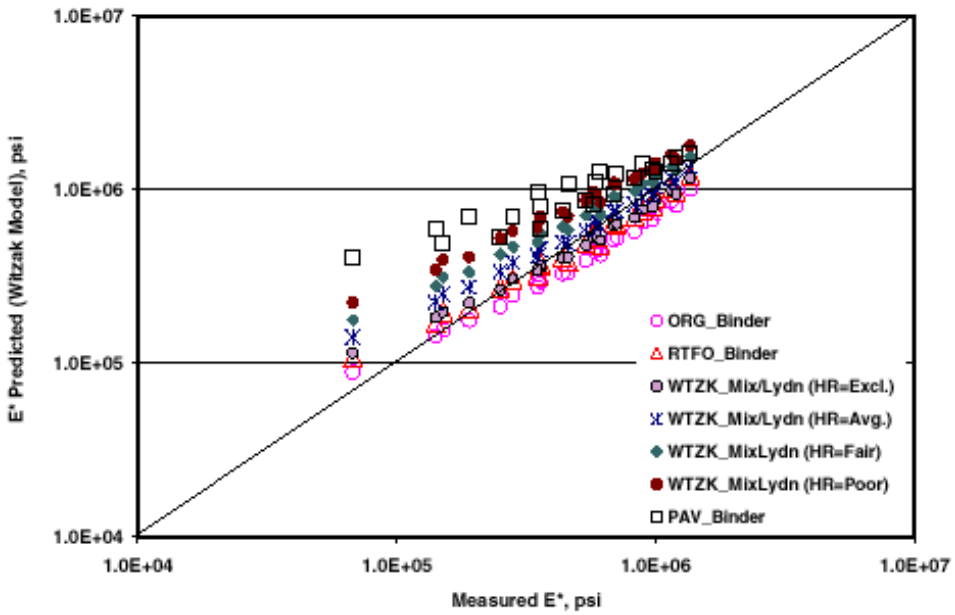

Figure 57. Effect of GAS on IE*I Predictions from the Witczak Model for Site No. 0357. HR Denotes Hardening Rate in the GAS [Dongré et al., 2005]

Table 30. Superpave Hardening Ratio (Indicators) [Dongré et al., 2005]

Project Site No.	PG Grade	ORG G*/sin d	RTFO G*/sin d	G*/sin d Ratio	Estimated Hardening Rate
0357	PG67-22	1.44	3.42	2.38	1.213
0358	PG59.4-28	1.19	2.6	2.18	1.232
0359	PG66.4-28	1.29	3.58	2.78	1.252
0360	PG72.1-22	1.23	2.78	2.26	1.317
0462	PG64-22	1.96	3.63	1.85	1.303

Figure 58 presents a master curve for predicted and measured IE*I data from site 0357. In the master curves developed for every other case, it was also found that the curve was easily generated using the Bonaquist approach for the sigmoidal function. Both the Arrhenius and the VTS methods to determine shift factors produced nearly identical results.

Figure 59 shows a master curve for site 0357, in which the curve was developed using asphalt binder shift factors, plotted along with IE*I master curves generated using the VTS shift factors as shown in Figure 58. RTFO Binder Shift denotes that the HMA IE*I data were shifted using RTFO binder shift factors and likewise for Original and PAV shift factors. They conclude from this Figure that clearly, the binder shift factors may be successfully used to shift HMA data. Figure 60 further confirms that binder and HMA shift factors are well correlated and may be used as surrogates.

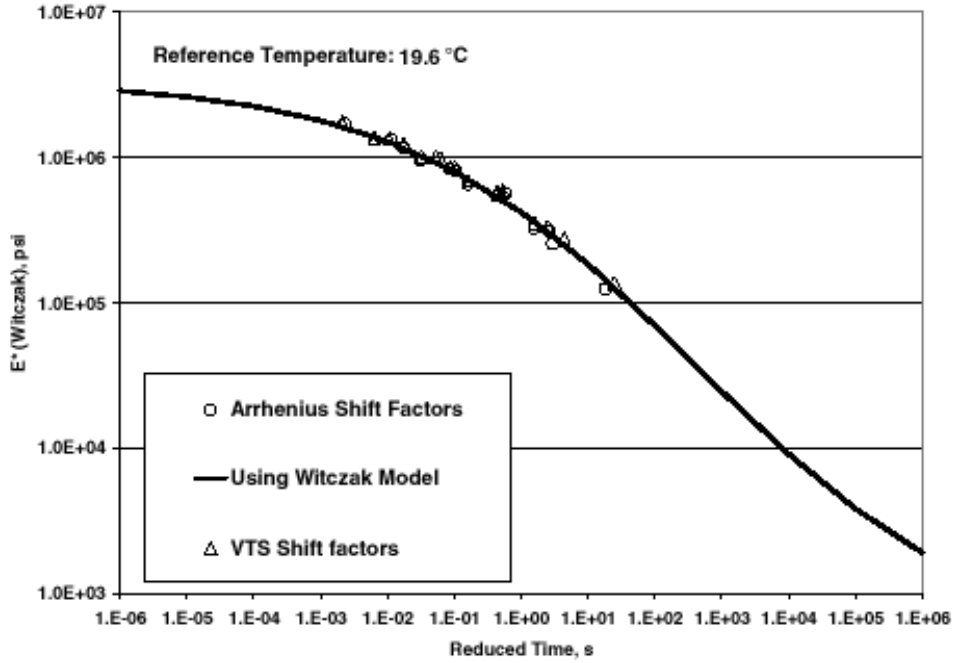

Figure 58. IE*I Master Curve Generated Using the Modified Bonaquist Procedure and VTS and Arrhenius Shift Factors for Site No. 0357 [Dongré et al., 2005]

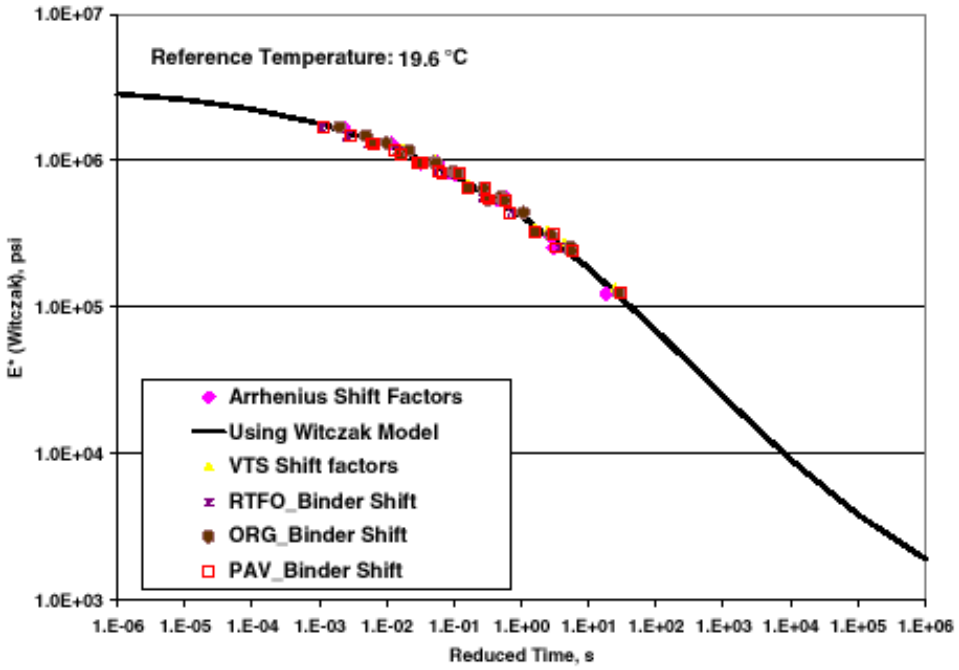

Figure 59. IE*I Master Curve Generated Using Binder Shift Factors for Site No. 0357. Also Shown is Master Curve Generated Using the Modified Bonaquist Procedure and VTS Shift Factors [Dongré et al., 2005]

[Note 21: In Figures 58 and 59, it is not clear from the report of this study, if what there is named “Using Witczak Model” refers to the Witczak model or the Modified Bonaquist Procedure using the sigmoidal function].

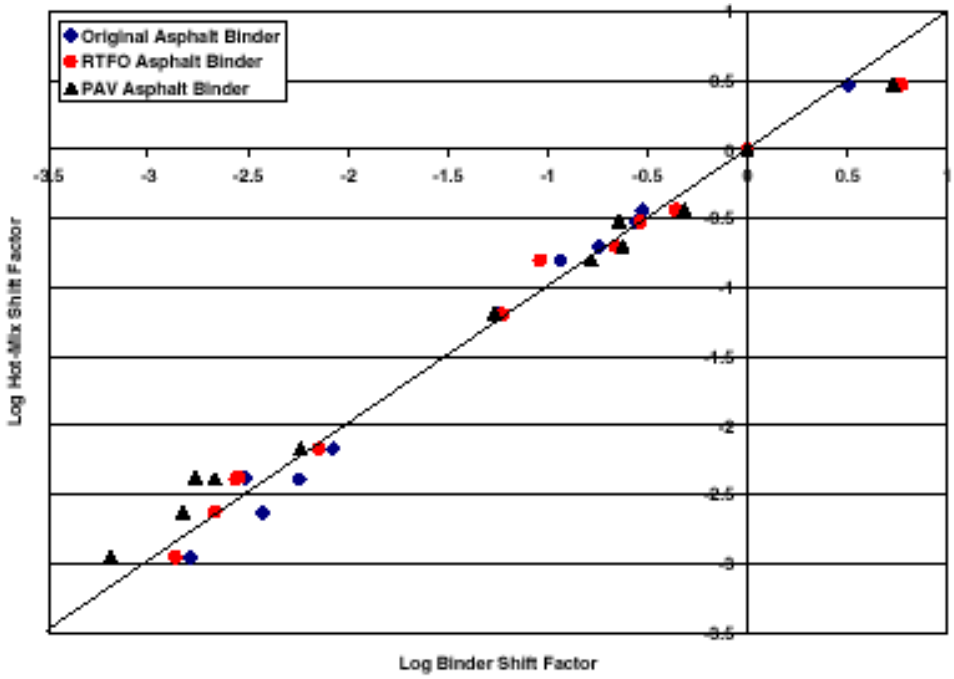

Figure 60. Binder Shift Factors Plotted Versus VTS and Arrhenius Shift Factors from Hot-Mix IE*I Data for All Sites [Dongré et al., 2005]

An interesting finding of this study was that the activation energy, E_A, used in the Arrhenius shift factor equation (equation (41) [Pellinen et al., 2002]), is highly correlated (R^2 = 0.90) to the Useful Temperature Range (UTR) of the asphalt binders studied. The UTR is calculated by taking the algebraic sum of the high and the low continuous PG grade of asphalt binders. For example, if the continuous PG grade of a given binder is PG 64.6-23.5, the UTR will be, 64.6+23.5=88.1.

$$\log(a(T)) = \frac{\Delta E_A}{2.303 \cdot R}\left(\frac{1}{T} - \frac{1}{T_0}\right) \qquad (41)$$

where

a(T) = shift factor for $T<T_g$
T_g = glass transition temperature
ΔE_A = apparent activation energy, J/mol
R = universal gas constant = 8.314 J/^{o}K-mol
T = temperature, ^{o}K
T_0 = reference temperature, ^{o}K

Equation (42) presents the correlation between E_A and UTR which allows the estimation of E_A without the need of testing asphalt binders at various times and temperatures. The E_A determined in this way can be used to shift HMA master curves. Figure 61 shows the corresponding plot:

$$E_A = 2484.7 \cdot UTR - 43168.0 \quad (42)$$

where

E_A = activation energy, J/mol
UTR = Useful Temperature Range, ^oC

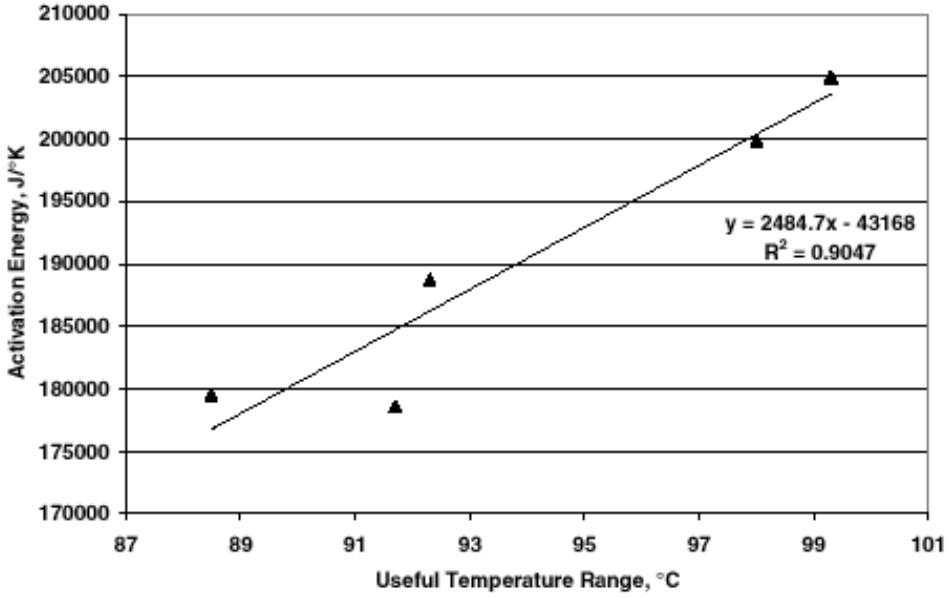

Figure 61. Correlation Between Activation Energy (E_A) and Useful Temperature Range (UTR) for Asphalt Binders from All Sites in This Study [Dongré et al., 2005]

The validation of this finding was performed predicting E_A values using equation (42) for asphalt binders and mixtures from the Accelerated Loading Facility (ALF) research project. IE*I data from those mixtures were shifted using the predicted E_A values and Arrhenius equation for all ALF asphalt binders to produce master curves. Similar master curves and E_A values were also calculated using the modified Bonaquist procedure. Figure 62 shows those master curves for asphalt AC-5.

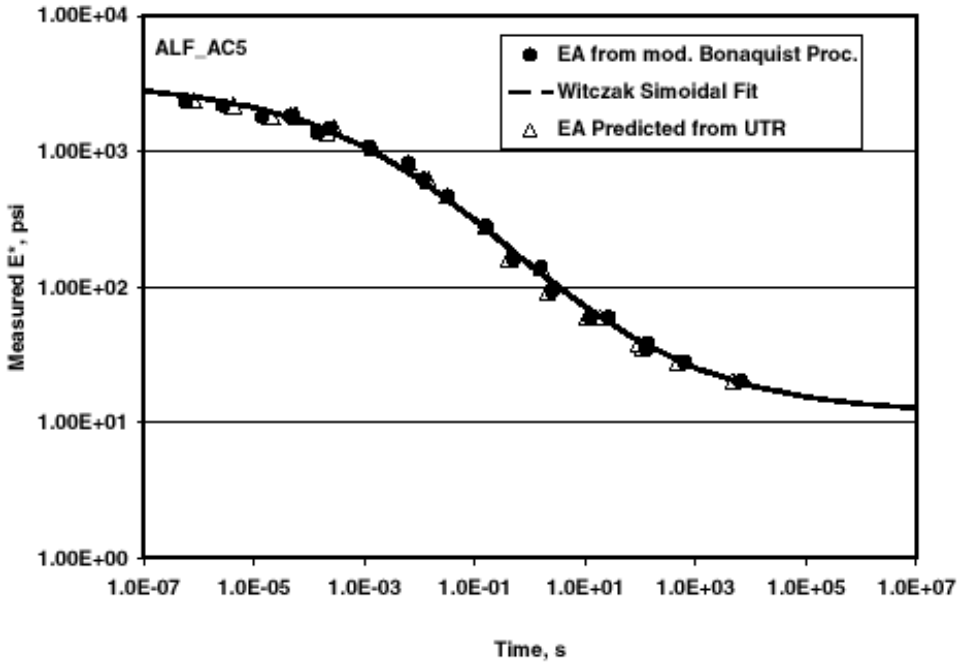

Figure 62. Typical Effect of E_A Predicted From Equation 39 and E_A Determined from Modified Bonaquist Procedure on the HMA IE*I Master Curve for Asphalt Binder ALF_AC5 [Dongré et al., 2005]

Table 31 shows the correlations and goodness of fit statistic (S_e/S_y) values obtained for both procedures using different asphalt cements.

Table 31. Effect of Prediction of Activation Energy (E_A) on HMA IE*I Master Curves Generation [Dongré et al., 2005]

Project ID	PG Grade	Shift Factor (E_A) Determined Using	Activation Energy kJ/mol	R^2	S_e/S_y
ALF_AC5	PG63.3-34.7	mod. Bonaquist proc.	200245	0.99	0.069
		E_A Predicted from UTR	191885	0.99	0.077
ALF_AC10	PG62.6-31.4	mod. Bonaquist proc.	202861	0.99	0.093
		E_A Predicted from UTR	193624	0.99	0.100
ALF_AC20	PG70-22	mod. Bonaquist proc.	210304	0.99	0.089
		E_A Predicted from UTR	198593	0.99	0.102
ALF_Novophalt	PG74.7-21.4	mod. Bonaquist proc.	174961	0.99	0.083
		E_A Predicted from UTR	205798	0.96	0.186
ALF_Styrelf	PG77.8-30.9	mod. Bonaquist proc.	208681	0.99	0.074
		E_A Predicted from UTR	243566	0.97	0.154
Average		**mod. Bonaquist proc.**	**199410**	**0.99**	**0.082**
		E_A Predicted from UTR	**206693**	**0.98**	**0.124**

[Note 22: It must be noted in Table 31 that the units of the activation energy should be J/mol instead of kJ/mol.]

From the results shown in Table 31, the authors estimate that master curves determined using E_A predicted from equation (42) are not significantly different than those using the modified Bonaquist procedure. However, they recommend that more research is needed to further confirm this finding. They also suggest, comparing the values in Table 31 and others proposed by other researchers, that a single value of E_A = 210 kJ/mol may be used as a reasonable approximation for E_A where high degree of accuracy is not required as is the case in the Level 3 in the new AASHTO Design Guide.

In Tables 32 and 33, the authors make a comparison between the binder viscosity parameters A and VTS as calculated in this study and those proposed in the new AASHTO Design Guide (Table 2.2.10 [2002 Design Guide, 2004]). In this study, A and VTS values were determined from Superpave IG*I and phase angle measurements. In both tables, the parameters proposed in the new AASHTO Design Guide are named as default 1-37A. As can be seen, the default values appear to be significantly different from the values obtained in this study for the original, RTFO, and PAV aged binders for each site.

It must be noted that the Design Guide [2002 Design Guide, 2004] recommends the use of IG*I and phase angle at 10 rad/sec in equation (19) above. However, equation (19) is based on the general form of the Superpave Models Study, which applies a phase angle correction factor to the empirical Cox-Merz rule relating complex modulus and steady state viscosity, equation (43) below [2002 Design Guide, 2000]:

$$\eta = \frac{|G^*|}{\omega}\left(\frac{1}{\sin\delta}\right)^{a_0+a_1\cdot\omega+a_2\cdot\omega^2} \tag{43}$$

where

η = viscosity, Pa·sec
IG*I = binder complex shear modulus, Pa
ω = angular frequency, rad/sec
δ = phase angle
a_0, a_1, a_2 = fitting parameters

In the development of the Design Guide, values for each fitting parameter (a_0 = 3.639216, a_1 = 0.131373 and a_2 = -0.000901) were proposed after a study with different binder types and aging conditions [2002 Design Guide, 2000]. When these proposed fitting parameters are used and an angular frequency of 10 rad/sec is selected, equation (43) transforms into equation (19).

In this study, on the other hand, two approaches were used to determine viscosity from binder IG*I values. The first one, used ω = 10 rad/sec, then A and VTS were obtained as in Table 32. However, as many data were collected at frequencies other than 10 rad/sec, another approach was used, applying those frequencies in equation (43) along

with the proposed fitting parameters. In this case, A and VTS were obtained as in Table 33.

Table 32. Comparison Between Default A and VTS Parameters Used in NCHRP 1-37A Design Guide Software and Those Calculated in This Study at 10 rad/s [Dongré et al., 2005]

Site ID	Field PG Grade	Parameter A_i				Parameter VTS			
		Binder Aging Condition			NCHRP 1-37a	Binder Aging Condition			NCHRP 1-37a
		Original	RTFO	PAV	Default	Original	RTFO	PAV	Default
0357	PG64-22	9.65	10.26	3.81	10.98	-3.201	-3.417	#N/A	-3.680
0358	PG58-28	10.74	10.48	9.46	11.01	-3.611	-3.508	-3.119	-3.701
0359	PG64-28	9.98	9.35	7.64	10.31	-3.326	-3.086	-2.444	-3.440
0360	PG70-22	10.42	10.02	8.88	10.30	-3.477	-3.320	-2.897	-3.426
0462	PG64-22	11.08	10.73	9.46	10.98	-3.724	-3.587	-3.109	-3.680

Table 33. Comparison Between Default A and VTS Parameters Used in NCHRP 1-37A Design Guide Software and Those Calculated at Various Frequencies in This Study [Dongré et al., 2005]

Site ID	Field PG Grade	Parameter A_i				Parameter VTS			
		RTFO Aged Binder tested at Frequency			NCHRP 1-37a	RTFO Aged Binder tested at Frequency			NCHRP 1-37a
		0.1 rad/s	10 rad/s	all Freq.	Default	0.1 rad/s	10 rad/s	all Freq.	Default
0357	PG64-22	10.59	10.26	9.24	10.98	-3.534	-3.417	-3.042	-3.680
0358	PG58-28	10.75	10.48	10.65	11.01	-3.602	-3.508	-3.571	-3.701
0359	PG64-28	9.38	9.35	9.35	10.31	-3.093	-3.086	-3.086	-3.440
0360	PG70-22	9.74	10.02	10.08	10.30	-3.217	-3.320	-3.338	-3.426
0462	PG64-22	10.64	10.73	10.93	10.98	-3.553	-3.587	-3.661	-3.680

The difference between A and VTS found in this study and those proposed in the AASHTO Design Guide, is attributed by the authors to the fact that Superpave IG*I and phase angle data were used in this study instead of traditional viscosity values from which the default values used in the guide were determined. They recommend that the default values must be reevaluated and based on routinely available Superpave binder data.

They also conclude from Table 33 that A and VTS parameters depend on the frequency at which IG*I and phase angle were determined.

*Hirsch Model IE*I predictions*

Figure 63 shows measured vs. predicted IE*I using the Hirsch model from HMA samples representing each site and three binder aging conditions. As also seen in the Witczak model application, the line of equality lies near the RTFO based predictions. Table 34 shows the results of statistical analysis corresponding to the data in Figure 63. The R^2 and S_e/S_y values are slightly improved compared with those obtained for the Witczak model (Table 28). Both Figure 63 and Table 34 show clearly that data from

RTFO aging condition generally appear to predict IE*I values relatively close to the measured data, as the Witczak model also does.

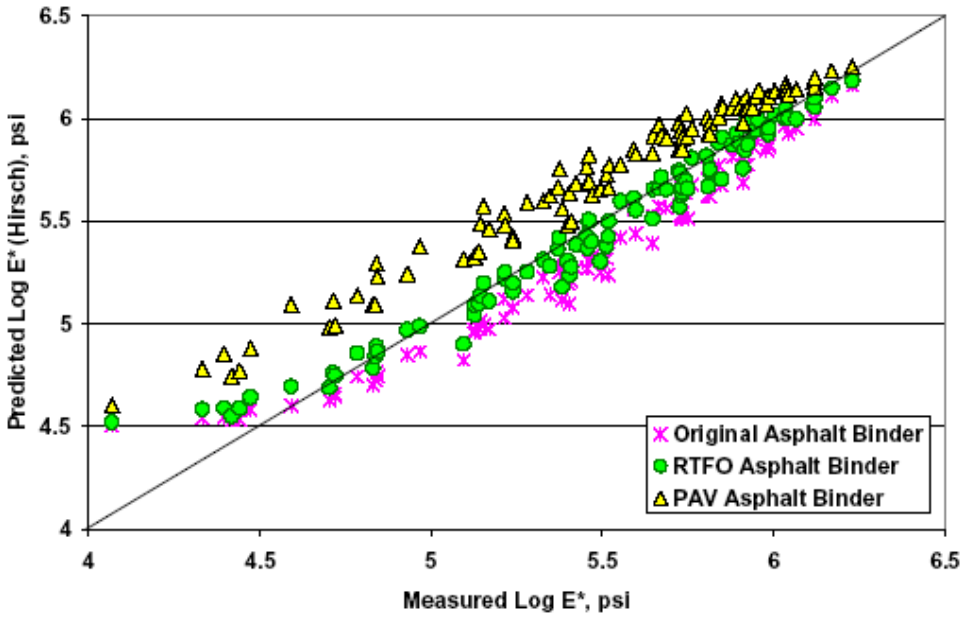

Figure 63. Measured and Predicted IE*I Data Plotted for All Sites. Data Predicted Using the Hirsch Model [Dongré et al., 2005]

Table 34. Results of Statistical Analysis of IE*I Predictions Using Hirsch Model [Dongré et al., 2005]

Statistic	Site ID	Original	RTFO	PAV
R^2	0357	0.67	0.87	0.79
S_e/S_y	0357	0.646	0.410	0.519
R^2	0358	0.95	0.99	0.80
S_e/S_y	0358	0.261	0.139	0.533
R^2	0359	0.94	0.99	0.53
S_e/S_y	0359	0.285	0.137	0.819
R^2	0360	0.92	0.99	0.89
S_e/S_y	0360	0.329	0.132	0.403
R^2	0462	0.94	0.96	0.77
S_e/S_y	0462	0.287	0.248	0.574
R^2	Combined	0.91	0.96	0.75
S_e/S_y	Combined	0.303	0.192	0.503

[Note 23: The Hirsch model presented in this study is the same one that was proposed by [Christensen et al., 2003] and presented in equations (33) and (34) earlier. However, after reviewing the files with the original database used in the study, it was found that in the spreadsheets used to make the calculations, the parenthesis was erroneously omitted in the factor ($3IG^*I_{binder}$·VFA) in the second term in the right side of the equation (which is the denominator of VMA). This situation was reported to the authors who

informed that: “In fact the agreement between the E* values predicted using the RTFO aged binder properties and the measured data actually improves because of the correction”. It is assumed that the correction was included in the final version of the paper.]

Figure 64 shows the error between measured and predicted IE*I values for the Hirsch model. As can be seen, the model begins to converge beyond IE*I value of 50,000 psi (logIE*I=4.7 psi). Unlike the Witczak model, there is no significant bias in the error as they seem to converge around the zero error line. It is thought that this is due to the fact that the model is based directly on binder IG*I values and accuracy is not lost for further conversion to viscosity as in the case of the Witczak equation.

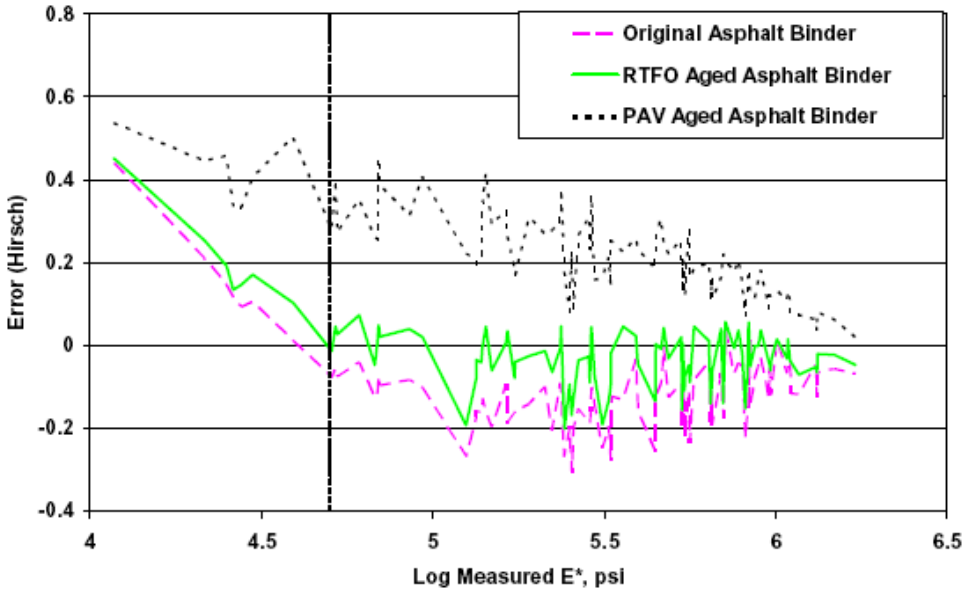

Figure 64. Plot of Error in Prediction of IE*I for Mix Design Data Using Hirsch Model for All Sites [Dongré et al., 2005]

Figure 65 shows a plot of predicted vs. measured IE*I values for HMA plant produced specimens for site 0357. Table 35 shows the VMA and VFA for all the production days shown in Figure 65. In that figure, it seems that the agreement between the predicted and measured values depends on the production day as was the case with the Witczak model. This was not expected by the authors because the Hirsch model is supposed to account for changes in volumetric, asphalt content, and air voids through VMA and VFA like the Witczak model. This means that the Hirsch model also loses accuracy if the volumetrics and binder content deviate from the mix design levels. According to the authors, a future refinement of the model would need to consider this factor.

Figure 66 presents the master curves obtained using the Hirsch model IE*I predictions for site 0360. The Hirsch model does not recommend any particular method to develop master curves. Binder shift factors were used in this study, based on the previous findings with the Witczak model. In the same figure, IE*I master curves developed using

Original, RTFO and PAV binder IG*I data are also shown, as well as the Witczak sigmoidal master curve, as a reference. The IE*I data measured at 69.4°F (20.8°C) are also plotted in the same figure.

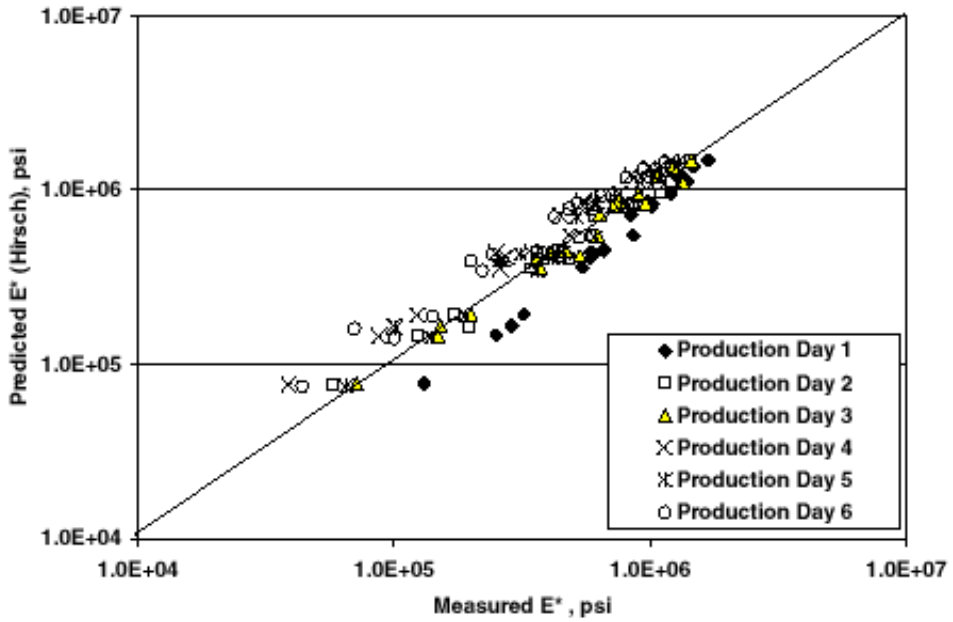

Figure 65. Measured Versus Predicted IE*I Values from the Hirsch Model for Production Specimen at Site No. 0357. RTFO Aged Binder Data Were Used [Dongré et al., 2005]

Table 35. Volumetrics Input Values for Hirsch Model IE*I Prediction Used at Site 0357 and Plotted in Figure 65 [Dongré et al., 2005]

Site No. 0357	VMA	VFA
Production Day No. 1	16.50	50.58
Production Day No. 2	17.42	53.68
Production Day No. 3	17.64	54.40
Production Day No. 4	17.93	55.91
Production Day No. 5	18.37	55.60
Production Day No. 6	18.18	53.70
FHWA Mix Design	16.55	57.74

As seen in Figure 66, the measured data agree well and fall in between the original and RTFO master curves. This agreement between the measured data and the master curves using binder shift factors further validate the use of this approach, as noted with the Witczak model. The authors noted that similar results were obtained from other sites.

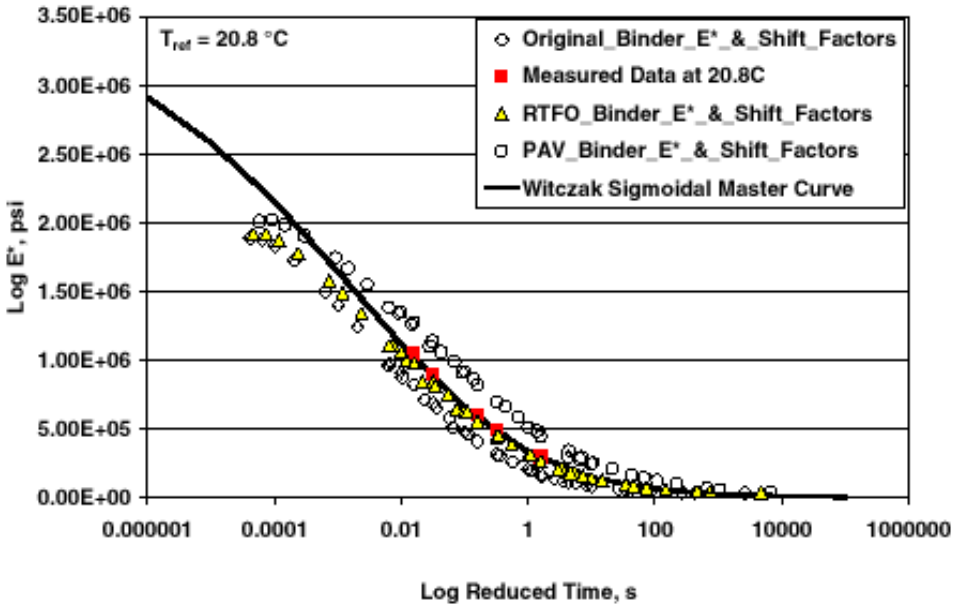

Figure 66. Master Curve Generated Using IE*I Predicted from the Hirsch Model and Binder Shift Factors for Site No. 0360 [Dongré et al., 2005]

6. SUMMARY AND CONCLUSIONS

The most important hot-mix asphalt (HMA) property influencing the structural response of a flexible pavement is the HMA modulus (E_{HMA}). Temperature and rate of loading significantly influence E_{HMA}, given a specific HMA, as well as the effect of aging.

The main dynamic modulus concepts have been reviewed. The construction of master curves for HMA mixtures following the AASHTO 2002 Design Guide has been presented, which is based on the fitting of a sigmoidal function. A new approach proposed by Bonaquist and Christensen (which is based on the Hirsch model and the sigmoidal function) is presented. It eliminates the need to perform tests at temperatures less than 40°F (4.4°C). Thus, the cost of the equipment, the complexity of the procedure, and the overall time to generate a master curve can be reduced.

Two IE*I predictive equations have been presented, the Witczak, proposed in the new AASHTO 2002 Design Guide, and the Hirsch model proposed by Christensen et al. In general, both appear to be in good agreement and have similar accuracy.

Even though the Hirsch model needs only three input parameters, which are known from routine Superpave mix design process, to build the IE*I master curve, a master curve for IG^*I_{binder} has to be developed in order to take into account the effect of temperature and frequency. This can be done easily with data obtained from a Dynamic Shear Rheometer test. The Witczak predictive equation, on the other hand, needs eight input parameters. This information is normally available from material specifications or

volumetric design of the mixture, and the master curve for IE*I can be developed directly introducing the binder A and VTS parameters in the viscosity components of the equation.

Perhaps the main disadvantage of the Witczak predictive equation when compared with the Hirsch model is that viscosity is used in the predictive equation to describe the temperature effects and to express the shift factors. Consequently, it needs the application of the VTS method (to determine A and VTS parameters) which is considered only applicable for conventional (non modified) type “S” (Shell Oil / Heukelom category) asphalt cements. The Hirsch model only needs the master curve for IG^*I_{binder}, which does not have that limitation.

Several studies, where the dynamic modulus predictive models are evaluated, were presented.

The study by the University of Minnesota (on mixtures from four cells at Mn/ROAD) found that the Witczak predictive equation fitted the data relatively well in some locations at intermediate and low temperatures, but for other locations the differences were significant. This study concluded that the Witczak equation should be used with caution and that further research is needed to validate the Witczak equation for mixtures typically used in Minnesota.

In another study by Christensen et al., where they proposed the Hirsch model, several verifications of the model were performed. They concluded that the Hirsch model is simpler and more rational than existing models for predicting modulus. They also found that the model was in good agreement with the Witczak predictive equation, and was of similar accuracy. Finally, they said that moduli predicted using the Hirsch model were potentially nearly as accurate as measured modulus values.

A study by Birgisson at the University of Florida, evaluated the Witczak predictive equation for 28 mixtures typical to Florida. Overall, it was found that the Witczak predictive equation resulted in a slight bias for the mixtures investigated. However, the results also allow for a correction of the bias between predicted and measured IE*I, using the regression relationships found in the study. Another finding was that predictions based on the viscosity obtained from Brookfield viscometer test were statistically better than the results based on the viscosity obtained from DSR measurements. However, the last procedure was the only one to give IE*I predictions lower than those measured. It was also found that IE*I predictions at higher temperatures generally were closer to measured values than predictions at lower temperatures, suggesting that the database used to develop the Witczak model could be biased toward mixtures tested at higher temperatures, or that, for the mixtures studied, the sigmoidal function used may produce slightly biased IE*I values at lower temperatures. Finally, it was concluded that when testing results are not available, reliable first order estimates of IE*I for mixtures typical to Florida can be obtained with the Witczak predictive equation, by applying a correction factor obtained from the testing of local mixtures.

In a study by North Carolina State University, 41 mixtures commonly used in North Carolina were used to evaluate the prediction accuracy of both the Witczak and the Hirsch models and the influence of some mixture variables in the prediction of IE*I. One of the findings was that the aggregate source and gradation, within the same NCDOT Superpave classification, seem to have no significant effect on IE*I. Binder source, PG grade, and asphalt content seem to affect the IE*I of the mixtures studied. The study showed that Witczak's prediction at cooler temperatures was better than at warmer temperatures. The Hirsch model performed very poorly at 50^{o}F (10^{o}C) and approximately the same as the Witczak model at the others temperatures. However, the poorer prediction of the Hirsch model was attributed to the fact that the binder data at 50^{o}F (10^{o}C) were extrapolated instead of directly measured.

A study by Schwartz at the University of Maryland, evaluated the accuracy and robustness of the Witczak predictive equation through a set of sensitivity and validation analyses, using the same database with which the Witczak model was calibrated plus an independent set of laboratory IE*I test data for 26 other mixtures. Temperature showed, by far, the strongest normalized influence on predicted IE*I, followed by the mixture volumetric parameters. Gradation, in turn, showed a very small influence for all gradation parameters other than the percent retained on the No.4 sieve. It was also found that the normalized sensitivity of IE*I to viscosity is greater at warmer temperatures. It was noted, however, that it is the combination of normalized sensitivity and the expected variation of the input parameters that must be considered. On the other hand, the validation of the Witczak model against the independent set of data showed an agreement between predicted and measured IE*I values that was nearly as good as for the calibration data set, but with a slight positive bias (predicted values generally higher than the measured data) which was higher for lower stiffness/higher temperature conditions. The overall conclusion of this study is that the Witczak model provides sufficiently accurate and reasonably robust estimation of IE*I to be used in mechanistic-empirical performance prediction and design. However, it is admitted that the model has more limited ability to make fine distinctions between the performance of different mixtures at the same temperature and other design conditions. Although beyond the scope of this study, limited preliminary evaluations suggest that the findings described for the Witczak model generally apply to the Hirsch model as well.

The University of Arkansas study on 12 different mixtures showed a good correlation between the Witczak predicted IE*I values and those measured. The goodness-of-fit statistics showed that the prediction of IE*I for the mixtures used in the study was very good to excellent, according to the subjective criteria used. However, as noted earlier, the A and VTS parameters used in the Witczak predictive equation were the default values proposed in the new AASHTO 2000 Design Guide and not directly calculated. They finally recommend the use of the Witczak equation for Arkansas mixes not specifically tested in the study.

The Louisiana Transportation Research Center conducted a study on two 25-mm Superpave mixtures with two different binder types to compare two Simple Performance

Tests performed in two laboratories. The prediction capability of the Witczak and the Hirsch models was also evaluated. It was found that the dynamic modulus values of the mixture using a PG 76-22 polymer modified binder were generally higher than those of the mixture using a PG 64-22 conventional binder. It was also found that the IE*I can provide consistent results for plant-produced mixtures. Another finding was that the IE*I was sensitive to different binder contents in the mixture. They conclude that the Witczak and the Hirsch models can predict IE*I values with a reasonable reliability.

Finally, the study developed by Dongré et al. showed that the Witczak and the modified Hirsch model were able to produce reasonable predictions of dynamic modulus when compared to data from mixtures tested in laboratory. However, they found that the Hirsch model is valid over a wider range of IE*I values, and uses Superpave IG*I directly in the calculations, thus avoiding a source of errors compared with the Witczak equation. They also found that both models need to be corrected or refined to more accurately predict IE*I values from production samples. Currently, both models under-predict IE*I values when higher binder content or air voids than the mix design are used in production samples. The Global Aging System over-predicted the increase in IE*I due to aging during the mixing/placement process, compared to the RTFO aging. They successfully generated master curves using the modified Bonaquist procedure and accurately shifted the IE*I data using binder shift factors. An interesting finding of this study was that the Useful Temperature Range (UTR) of the binder may be used to accurately predict the activation energy (E_A), which is needed to apply the Arrhenius shift factor equation. Values of A and VTS found in this study were significantly different from the default values proposed in the new AASHTO Design Guide. Their study also found that below a IE*I of 100,000 psi for the Witczak model and 50,000 psi for the Hirsch model, the predictive equations may not predict reasonable IE*I. There exists a need to test the mixtures in the laboratory below those values.

7. REFERENCES

Alavi, S.H., and Monismith, C.L. (1994). “Time and Temperature Dependent Properties of Asphalt Concrete Mixes Tested as Hollow Cylinders and Subjected to Dynamic Axial and Shear Loads.” Journal of the Association of Asphalt Paving Technologists, Volume 63, St. Louis, MO.

Birgisson, B., Sholar, G., and Roque, R. (2005). “Evaluation of Predicted Dynamic Modulus for Florida Mixtures.” 84th Annual Meeting of the Transportation Research Board, Paper No. 05-1309, Washington D.C.

Bonaquist, R., Cristensen, D.W., and Stump, W. (2003). “Simple Performance Tester for Superpave Mix Design: First-Article Development and Evaluation.” NCHRP Report 513, Transportation Research Board, Washington, D.C., 2003.

Boaquist, R., and Christensen, D.W. (2005). “A Practical Procedure for Developing Dynamic Modulus Master Curves for Pavement Structural Design.” 84th Annual Meeting of the Transportation Research Board, Paper No. 05-0389, Washington D.C.

Christensen, D.W., and Anderson, D.A. (1992). “Interpretation of Dynamic Mechanical Test Data for Paving Grade Asphalt Cements.” Journal of the Association of Asphalt Paving Technologists, Volume 61, Charleston, SC.

Christensen, D.W., Pellinen, T.K., and Bonaquist, R.F. (2003). “Hirsch Model for Estimating the Modulus of Asphalt Concrete.” Journal of the Association of Asphalt Paving Technologists, Volume 72, Lexington, KY.

Clyne, T.R., Li, X., Marastenau, M.O., and Skok, E.L. (2003). “Dynamic and Resilient Modulus of Mn/DOT Asphalt Mixtures.“ Final Report MN/RC – 2003-09. University of Minnesota, Minneapolis, MN.

Dongré, R., Myers, L., D’Angelo, J., Paugh, C., and Gudimettla, J. (2004). “Field Evaluation of Witczak and Hirsch Models for Predicting Dynamic Modulus of Hot-Mix Asphalt.” Pre-Print of the Journal of the Association of Asphalt Paving Technologists, Volume 74, 2005. (in press)

Dougan, C.E., Stephens, J. E., Mahoney, J., and Hansen, G. (2003). “E* - Dynamic Modulus. Test Protocol – Problems and Solutions.” Report No. CT-SPR-0003084-F-03-3. University of Connecticut, Storrs, CT.

Harman, T. (2001). “Using the Dynamic Modulus Test to Assess the Mix Strength of HMA.” Public Roads, Volume 64, No. 6, May/June 2001, <http://www.tfhrc.gov/pubrds/mayjun01/dynamicmodulus.htm>.

Kim, Y.R., King, M., and Momen, M. (2005). “Typical Dynamic Moduli Values of Hot Mix Asphalt in North Carolina and Their Prediction.” 84th Annual Meeting of the Transportation Research Board, Paper No. 05-2568, Washington D.C.

Mirza, M.W., and Witczak, M.W. (1995). “Development of a Global Aging System for Short and Long Term Aging of Asphalt Cements.” Journal of the Association of Asphalt Paving Technologists, Volume 64, Portland, OR.

Mohammad, L.N., Wu, Z., Myers, L., Cooper, S., and Abadie, C. (2005). “A Practical Look at Simple Performance Tests: Louisiana’s Experience.” Journal of the Association of Asphalt Paving Technologists, Volume 74, 2005 (in press).

Painter, P.C., and Coleman, M.M. (1997). “Fundamentals of Polymer Science – An Introductory Text.” Technomic Publishing Co. Inc., ISBN 1-56676-559-5, Lancaster, PA.

Pellinen, T.K., and Witczak, M.W. (2002). “Stress Dependent Master Curve Construction for Dynamic (Complex) Modulus.” Journal of the Association of Asphalt Paving Technologists, Volume 71. Colorado Spring, CO.

Pellinen, T.K., Witczak, M.W., and Bonaquist, R.F. (2002). “Asphalt Mix Master Curve Construction Using Sigmoidal Fitting Function with Non-Linear Least Squares Optimization.” Proceedings of the Pavement Mechanics Symposium at the 15th ASCE Engineering Mechanics Conference (EM2002). Columbia University, New York, NY.

Schwartz, C. W. (2005). “Evaluation of the Witczak Dynamic Modulus Prediction Model.” 84th Annual Meeting of the Transportation Research Board, Paper No. 05-2112, Washington D.C.

Tran, N.H., and Hall, K.D. (2005). “Evaluating the Predictive Equation in Determining Dynamic Moduli of Typical Asphalt Mixtures Used in Arkansas.” Pre-Print of the Journal of the Association of Asphalt Paving Technologists, Volume 74, 2005. (in press)

Witczak, M.W., Fonseca, O.A. (1996). “Revised Predictive Model for Dynamic (Complex) Modulus of Asphalt Mixtures. Transportation Research Record 1540. Transportation Research Board, Washington, D.C., 1996.

Witczak, M.W., Pellinen, T., and El-Basyouny, M. (2002a). “Pursuit of the Simple Performance Test for Asphalt Concrete Fracture/Cracking.” Journal of the Association of Asphalt Paving Technologists, Volume 71, 2002.

Witczak, M.W., Kaloush, K., Pellinen, T., El-Basyouny, M., and Von Quintus, H. (2002b). “Simple Performance Test for Superpave Mix Design.” NCHRP Report 465, Transportation Research Board, Washington, D.C., 2002.

Yoder, E.J., and Witczak, M.W. (1975). “Principles of Pavement Design .” J. Wiley and Sons, Inc., Second Edition.

2002 Design Guide for New & Rehabilitated Pavements (Draft) (2000). “2.4 Modulus of Elasticity for Major Material Groups”, NCHRP Project 1-37A, October 2000.

2002 Design Guide for New & Rehabilitated Pavements (Final Report) (2004). “Part 2-Design Inputs, Chapter 2 Material Characterization, 2.2.2 Input Characterization for the Asphalt Material Group”, NCHRP Project 1-37A, March 2004. <http://www.trb.org/mepdg/guide.htm>.

2002 Design Guide for New & Rehabilitated Pavements (Final Document) (1999). “Appendix CC-4: Development of a Revised Predictive Model for the Dynamic (Complex) Modulus of Asphalt Mixtures”, NCHRP Project 1-37A, March 1999. <http://www.trb.org/mepdg/guide.htm>.

2002 Design Guide for New & Rehabilitated Pavements (Final Document) (2003). “Appendix CC-3: “Updated Traffic Frequency Calculation for Asphalt Layers”, NCHRP Project 1-37A, December 2003. <http://www.trb.org/mepdg/guide.htm>.


Illinois Department
of Transportation


ILLINOIS
UNIVERSITY OF ILLINOIS AT URBANA-CHAMPAIGN